The Institute of Paper Chemistry

Appleton, Wisconsin

Doctor's Dissertation

Study of Changes in Cellulose Fine Structure in the Wet State During Tracheid Wall Component Removal by Sodium Chlorite Pulping

Veli Veikko M. Lapinoja

January, 1972

STUDY OF CHANGES IN CELLULOSE FINE STRUCTURE IN THE WET STATE DURING TRACHEID WALL COMPONENT REMOVAL BY SODIUM CHLORITE PULPING

A thesis submitted by

Veli Veikko M. Lapinoja

B.S. 1966, Michigan Technological University

M.S. 1968, Lawrence University

in partial fulfillment of the requirements
of The Institute of Paper Chemistry
for the degree of Doctor of Philosophy
from Lawrence University,
Appleton, Wisconsin

January, 1972

TABLE OF CONTENTS

SUMMARY

The objective of this investigation was to determine whether the cellulose fine structure of wood tracheids undergoes changes while in the wet state, during the tracheid wall component removal. The further goal was to obtain understanding of the factors influencing the cellulose fine structure in the wet state.

Noble fir, Abies procera Rehd., wood was delignified with sodium chlorite-acetic acid buffered liquor at room temperature. This technique was selected since it does not involve temperature cycles, the solubilizing action is fairly specific on lignin, and the holowood retains the natural tracheid alignment.

Never-dried sapwood was brought through the following treatment sequence: waterlogging, hygrothermal treatment, delignification to various degrees (up to 120 days, 57% yield), distilled water washing, and hygrothermal treatment. The changes in the wood block and holowood block dimensions were measured throughout this sequence and the swollen specific volume of the pulps obtained by the centrifugal water retention technique. The changes in the cellulose fine structure were determined by the x-ray diffraction analysis on the wood- and holowood sections in the wet state. Measures of crystallinity index, degree of order of the highly ordered regions, and crystallite orientation were obtained.

The hygrothermal treatment and the reaction liquor penetration result in a tangential expansion (1.6 to 2.0%) and a radial shrinkage (0.5%) of the wood block. The first is accompanied by a small increase in the crystallinity index while the reaction liquor penetration has an opposite effect on the cellulose fine structure.

Expansion during water washing becomes more severe with time in the reaction liquor. Holowood blocks (57% yield) expand 20% tangentially, 8% radially, and only 0.6% longitudinally. These changes are accompanied by a 74% increase in the swollen specific volume of pulp. Throughout the reaction range, on water washing, the crystallinity index increases and the angle which the crystallites make with the fiber axis becomes wider.

During the hygrothermal treatment, the holowood continues to expand up to 15.5% tangentially, 4% radially, and 0.4% longitudinally. This, however is accompanied by about a 24% decrease in the tracheid water-holding capacity. The crystallinity index continues to increase during the hygrothermal treatment, and the increase in the degree of order of the highly ordered regions is strong.

The expansion of the holowood along the three structural axes was thought to result in stretching of the microfibrils within the tracheid wall lamellae. This results in a better alignment of cellulose molecules within the microfibrils, and in a better alignment of microfibrils within the lamellae.

In order to elucidate the factors causing the increase in the degree of order of cellulose, the reaction liquor was considered as an electrolyte solution. The washed pulp was submerged in the original reaction liquor and its swollen specific volume was found to decrease. Similar observation was made in the 0.1N univalent cationic electrolyte solutions. This behavior can be qualitatively explained in terms of the Donnan potential and the electrostatic repulsion effects. As the electrolyte concentration in the bulk solution decreases, the electrical double layers of two neighboring lamellae expand and repel each other. Simultaneously, the Donnan potential increases resulting in an osmotic

movement of water into the swellable cellulose and into the amorphous hemicellulose. The tracheid walls appear to swell, but the actual swelling takes place in the amorphous regions of the tracheid walls, while the load-carrying, highly ordered framework constituents become more highly ordered due to the stretching caused by swelling.

INTRODUCTION AND OBJECTIVES

Wood fibers are subjected to many physical and chemical processes on their route from the growing tree to the finished sheet of paper. Each of these processes can modify the structure of the fiber and therefore influences its properties.

The structure of the fiber wall as it exists in the living tree is not fully understood. Even less is known of the changes in the structure of the tracheid wall cellulose during delignification. Furthermore, the changes in the structure of the delignified tracheid wall in the wet state during the papermaking process are not fully known.

Most of the knowledge about tracheid walls is obtained on the dried delignified fibers. This information, of course, is very useful in characterizing the pulp types but does not reveal the changes that have occurred in the fiber wall structure. Knowledge in these areas could be of considerable help in efforts to maximize the desired characteristics of the wood fiber.

A controversy exists whether the delignification of woody plants results in a decrease in the crystallinity (1, 2) or in an increase in the crystallinity of cellulose (3, 4, 5). The recent work of Nelson (6) and that of Marton and McGovern (7) favors the increase in the degree of order of cellulose in the fiber wall due to pulping. However, these studies have been made on dry fibers. The drying process results in some complications, since the effect of drying on the fiber wall structure is not fully understood, and furthermore appears to be large and variable (8). It is entirely possible that the drying process masks the changes that have taken place in the wet state. For this reason, the observations made in the dry state may be erroneous. The studies of the water-

saturated fiber wall (9, 10, 11) indicate an increase in the fiber wall volume during the component removal. This, of course, implies a swelling of the remaining fiber wall constituents.

The objective of the present study is to determine whether the degree of order of cellulose in the tracheid walls changes during delignification, during the subsequent room temperature water washing, and during the first hygrothermal treatment of the delignified tracheid walls. The understanding of the factors causing the changes is also sought.

The natural orientation of tracheids as they exist in the tree is preserved throughout the testing sequence, and the observations are made on samples in the water-saturated condition.

REVIEW OF THE PRESENT CONCEPTS IN THE TRACHEID WALL ARCHITECTURE

ANATOMY OF CONIFEROUS WOODS

Excellent reviews of coniferous wood anatomy are given by Esau (12), Panshin (13), and Isenberg (14). The noble fir (Abies procera Rehd.) has only two types of cells: the tracheids and the ray parenchyma, and hence is one of the least complex test materials available.

The tracheids can be considered as elongated, four-sided, hollow, prismatic structural elements. The average length of the noble fir tracheid is about 3.6 ± 0.6 mm., the tangential diameter is about 35 to 45 μm., and the radial diameter is more variable (13). The tracheids are uniformly bonded along the tangential walls of the neighboring tracheids through a thin middle lamella. The bonding along the radial walls is through thicker middle lamella which has been shown to include remnants of the parent cell wall (15, 16). The tracheid to tracheid bonding along the radial walls is further interrupted by the presence of pits and ray cells.

In the noble fir the rays are uniseriate and occupy only about 6.5% of the total wood volume (13).

TRACHEID WALL CONSTITUENTS AND THEIR RELATIONSHIP TO PHYSICAL PROPERTIES

The variability in chemical composition of wood within species depends on the genetic factors, the environmental conditions of growth, and the location of the tracheid in the given tree (17, 18). Furthermore, the distribution of constituents is variable even within the layers of the tracheid walls (19, 20).

In coniferous woods, the cellulose content is about 43 ± 2%, the hemicelluloses 20%, and the lignin 28-35% (ovendry basis) (18, 21). These high-molecular weight substances form an interpenetrating system of which degree of interpenetration is not known (17). About 70% of wood lignin is distributed throughout the secondary wall (22).

Delignification modifies the relative distribution of tracheid wall constituents within layers of the tracheid walls and affects the physical structure of the remaining constituents. Consequently, it is an oversimplification to correlate the physical properties of tracheids solely with the chemical composition of the sample, as is frequently done in literature (23-27). The distribution and the structural state of the tracheid wall components are important and need further study before the strength properties of the tracheids are more fully understood.

The tracheid wall is considered to be a fiber-reinforced plastic where lignin represents the plastic binder and cellulose the reinforcing fibers (22, 23). The cellulose is the framework constituent (27, 28). The hemicelluloses are the matrix constituent and are an integral part of the tracheid wall (29). The lignin is the encrusting constituent (28). Several investigators further believe that some relatively unbranched glucomannan also functions as a framework constituent, since it is found in close association with the cellulose fraction (30, 31).

FINE STRUCTURE OF CELLULOSE WITHIN THE TRACHEID WALL LAMELLAE

CELLULOSE MOLECULE AND ITS PACKING CHARACTERISTICS

The cellulose macromolecule consists of glucose residues linked together in a linear polymer by β-1,4 glucosidic bonds. The degree of polymerization is

reported to be as high as 14,000 in the native cellulose (32). This corresponds to a molecule with length of 70,000 A.

According to Hermans (33) the C_1-O-C_4 bond is bent so that intramolecular hydrogen bonding between the O_5 of one glucose ring and the O_3 of the next glucose ring becomes possible. This feature stabilizes the flat ribbonlike shape of the cellulose molecule. This characteristic, along with the polar hydroxyl groups of glucose residue, results in a high polymer with a strong tendency to crystallize.

The cellulose I crystallite has a monoclinic unit cell. Meyer and Misch (34) on the basis of x-ray data, calculated the following dimensions for the unit cell: 8.35 A. in the plane of the glucose ring (a), 10.3 A. along the molecular axis (b), and 7.9 A. perpendicular to the plane of the glucose ring (c). The angle between a and c axis is 84 degrees. Ellefsen, et al. (35) have modified a to equal 8.2 A., and the angle between a and c to 83.3 degrees on the basis of more recent x-ray data on cellulose I. According to Hermans (33), the cellulose molecules in the crystal lattice possesses both intrachain as well as lateral interchain hydrogen bonds. On the basis of infrared spectral studies of hydrogen bonds in the native cellulose I, Liang and Marchessault (36) refined the unit cell by modifying the interchain hydrogen bonding (Fig. 1).

Not all the cellulose molecules are packed into highly ordered crystalline regions. The cellulose molecule packing can vary from perfectly crystalline to completely amorphous. Howsmon and Sisson (37) gave the following four classifications of cellulose molecule packing in the sequence of decreasing degree of order: perfectly crystalline, paracrystalline, amorphous with correlation, and wholly amorphous, shown in Fig. 2A. The important point is that there cannot be a sharp distinction between crystalline and noncrystalline regions.

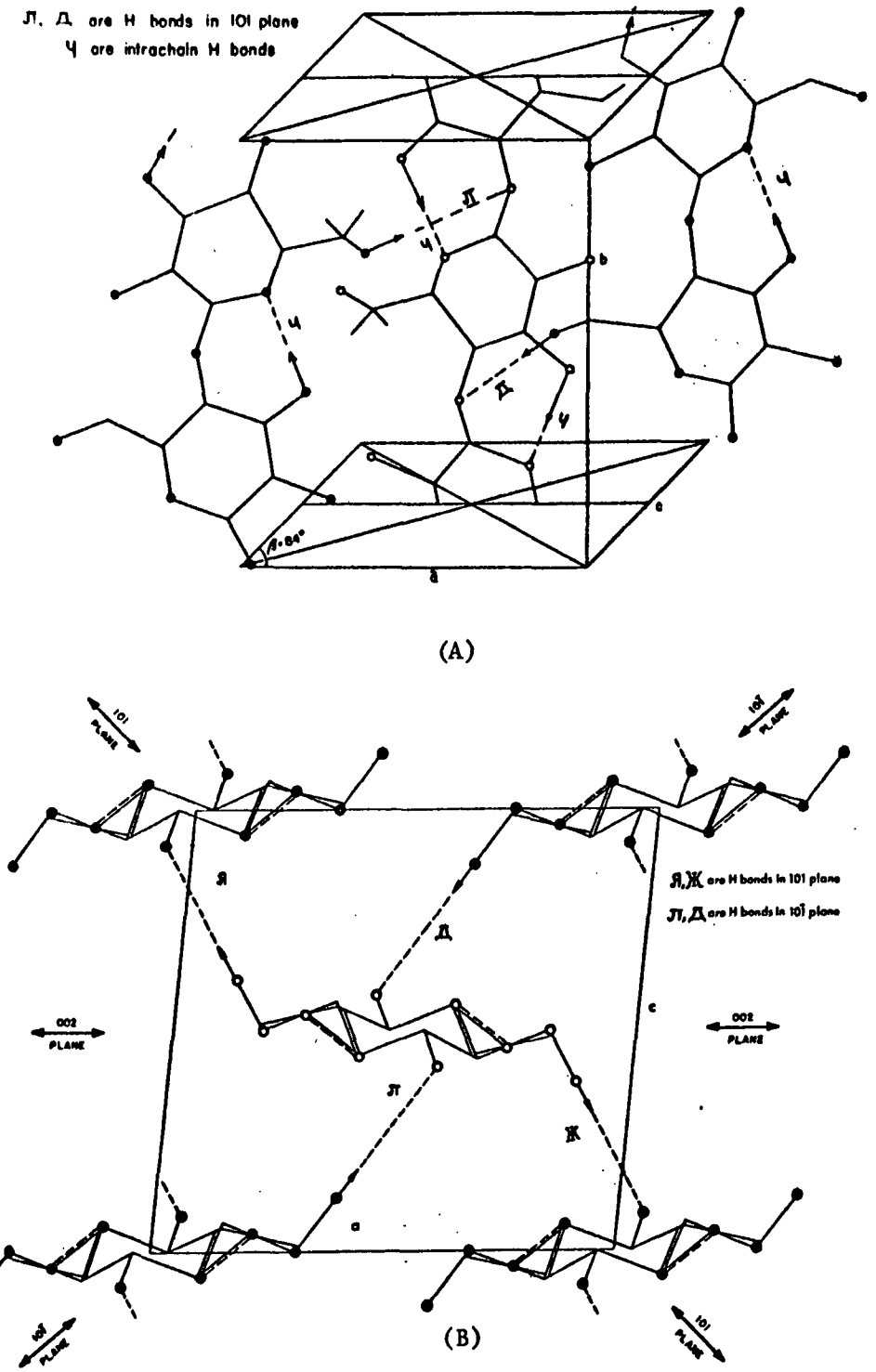

Figure 1. Side View of Chain Segments in a Cellulose I Crystal (A); End View of Cellulose Chains in a Unit Cell (B). From Liang and Marchessault (36)

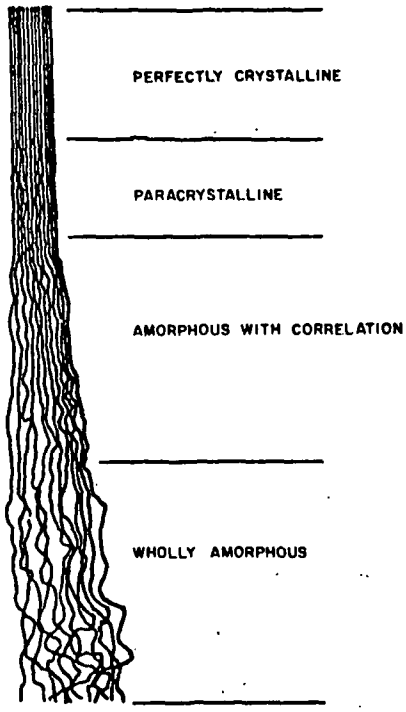

(A)

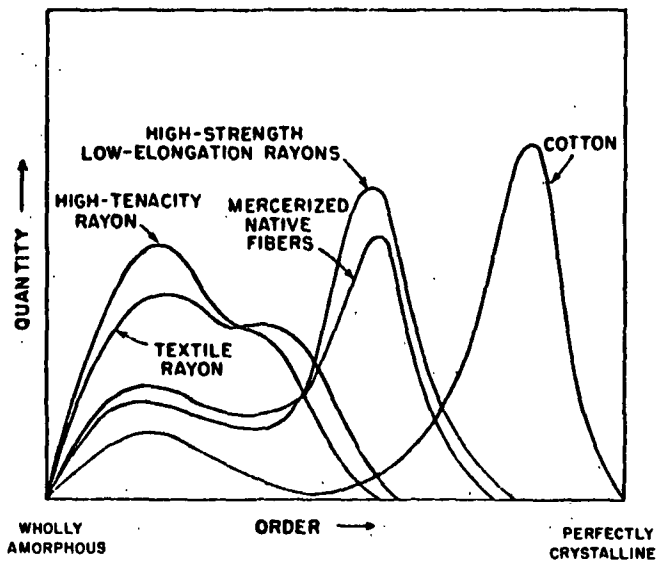

(B)

Figure 2. Range of Molecular Order from Perfectly Crystalline to Amorphous for Cellulose Substances (A); Representative Mass-Order Distribution Curves for Cellulosic Fibers (B). From Howsmon and Sisson (37)

The mass order curve of Fig. 2B illustrates the difficulty of classifying a cellulosic material according to its degree or order. The transition from one classification to another according to order is not abrupt and is therefore dependent on the method of determination. Furthermore, the mass order distribution curve of cellulosic material is not unique and depends strongly on the treatment history of the specimen.

ELEMENTARY FIBRILS

The elementary fibril is often considered to be the basic morphological structural element of native cellulose fiber (38-41). Unfortunately, the arrangement of cellulose molecules within the elementary fibril has defied definition. More than 30 models have been reviewed by Hearle (42). It is generally accepted that the elementary fibril consists of alternating regions of highly ordered crystalline regions and less-ordered amorphous regions. The two main concepts of the mutual arrangement and of the dimensions of these regions are (1) the fringed micelle model and (2) the fringed fibril model. The first model implies that the boundaries of the crystalline region are fairly uniform (41, 43). The fringed fibril model implies that the crystalline region is much longer along the molecular axis than in the two perpendicular directions, and that the boundaries are not as uniform as in the fringed-micelle model (42, 44).

For the present purpose it is not necessary to distinguish between these models. The essential concept is that the cellulose macromolecules are packed in regions of high order and regions of low order, and that the boundary between these regions is not rigorously defined.

The diameter of the elementary fibril is reported to be between 20 and 60 A. units; but the most commonly reported width is from 35 to 40 A. (7, 40-46). Heyn (40) proposes that the 35 A. elementary fibril is the universally occurring morphological unit in all cellulosic fibers. He came to this conclusion on the basis of electron micrographs of various negatively stained cellulosic materials. By relating the radial width of the 002 crystallite plane diffraction peak to the crystallite size, Marton and McGovern (7) have observed variations in the crystallite width between wood species. Also, the crystallites in earlywood were found to be wider than in latewood. However, relating the diffraction peak width to the crystallite transverse dimensions can be criticized since the crystallite imperfections have similar broadening effects on the diffraction peak width as small crystallites.

The length of the crystalline region in the elementary fibril is reported to vary from 100 to 600 A. units (40-46). Heyn (40) observed a beaded appearance in the negatively stained elementary fibril with periodicity of about 100 to 150 A. According to Fengel (45) the crystalline region is about 300 A. long. The crystalline regions are separated with 50 A. long amorphous regions (46). Fengel (45) observed an increase in the length of the disordered region on acid hydrolysis. Mühlethaler (47), on the other hand, considers the elementary fibrils as highly crystalline along their entire length and the disordered areas very short, if present.

Frey-Wyssling and Mühlethaler (38, 41) have presented a model of the elementary fibril as shown in Fig. 3. According to this model the 35 A. elementary fibril is made up of 36 cellulose macromolecules. The cellulose molecules are aligned in 18 antiparallel cellulose macromolecule pairs of which 16 have at least one of the cellulose molecules on the surface of the elementary fibril.

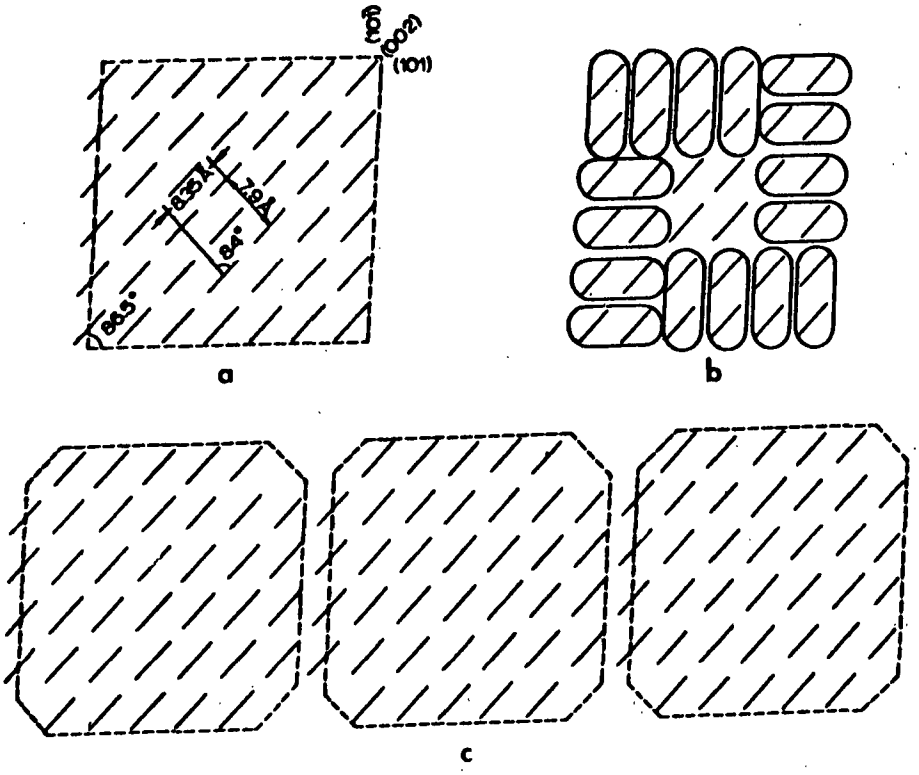

Figure 3. Cross Section of Cellulose I Elementary Fibril Made Up of 36 Cellulose Molecules, a; the Elementary Fibril Made Up of 18 Units Consisting of Pairs of Antiparallel Cellulose Molecules, b; Consolidation of the 35° A. Elementary Fibrils Along the $10\bar{1}$ Crystallite Plane to Form a Microfibril, c. From Frey-Wyssling and Mühlethaler (38, 41)

MICROFIBRILS

The generally accepted view is that elementary fibrils consolidate to form microfibrils which have a diameter ranging from 50 to 500 A. (41-48). According to Frey-Wyssling (42) the crystalline region of the elementary fibril is embedded in a cortex of paracrystalline cellulose. The aggregation of elementary fibrils occurs along these paracrystalline regions, which have a greater tendency for lateral association along the $10\bar{1}$ plane than perpendicular to it (38, 41). According to Mühlethaler (47) this consolidation of elementary fibrils to microfibrils occurs in the direction of the 101 plane because free hydroxyl groups are abundant on those surfaces.

According to Fengel's (45) electron microscope data, the microfibrils in the delignified wood have a diameter of about 250 A. However, the microfibrils are rather unstable and easily split into 120 A. diameter fibrils on acid hydrolysis. The 120 A. fibrils are made up of 16 elementary fibrils bonded together through a thin amorphous layer of polyoses. The aggregation of elementary fibrils to microfibrils and their subsequent aggregation to larger units are at least partly caused by the specimen preparation procedure (45).

Asunmaa and Schwab (49) have observed splitting of the 100 A. microfibrils of aspen holocellulose on ultrasonic treatment into 50 A. elementary fibrils.

MACROFIBRILS

The macrofibrils, some of which can be seen by light microscope, are aggregates of several microfibrils. Their diameters vary from 600 to 3600 A. (44, 46). These fibrillar aggregates are found in delignified samples where the neighboring microfibrils have an opportunity to consolidate.

LAMELLAE

Ritter (50) and Bailey and Kerr (51) were among the first to find that the tracheid walls consist of cellulosic lamellae separated by ligneous and hemicellulosic materials. According to Stone and Scallan (52) the lignin, being a three-dimensional, cross-linked high polymer, functions as a "network of tie-rods" locking the tracheid wall cellulose-rich lamellae together. According to Wardrop (53), all the layers of the wood fiber exhibit lamellation. In mature tracheids it is not readily apparent due to incrustation by lignin and other substances, but lamellae can be seen in developing cells before lignification begins in the thickened secondary wall. The lamellae are again apparent in the mature delignified tracheids (Fig. 4).

Stone and Scallan (10) have calculated that the fully delignified tracheid wall is composed of several hundred lamellae separated by water-filled spaces ranging from 25 to 300 A. with an average of 35 A. According to this model, the thickness of the cellulose-rich lamella is about 63 A. in the water-swollen condition, and about 50 A. in the dry condition. In the swollen condition, the cellulose-rich lamella has small pores with a diameter of less than 20 A.

The lamellae in this model are thin in comparison with the lamellae observed in the electron micrographs, whereas in the delignified tracheid walls they appear to vary from a few hundred Angstrom units to several thousand in thickness (54-57). Apparently, the observed lamellae are actually aggregates of several elementary lamellae.

Wardrop (53) has proposed a model for the tracheid wall lamellae aggregating to form compound lamellae. He states that the 101 crystallite planes lie parallel to the tracheid surfaces. These planes are apparently exposed

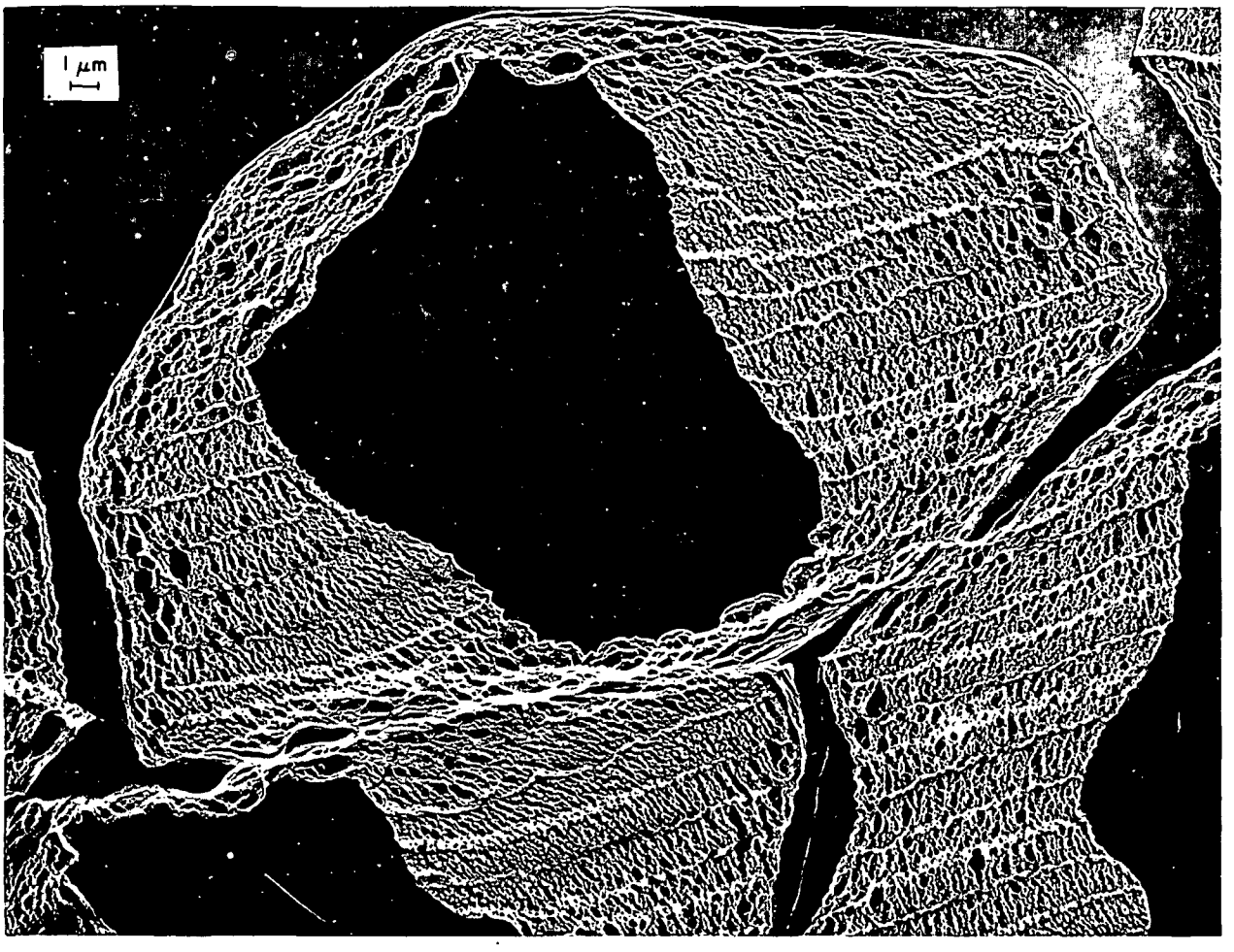

Figure 4. Palladium-Shadowed, Ultrathin Cross Section of Slash Pine Holowood Tracheids Illustrating the Lamellar Structure of the Delignified Tracheid Walls as Observed After Butyl Methacrylate Embedding. Magnification: 2750. From Kaustinen (57)

when the lignin and hemicelluloses are removed. Frey-Wyssling and Mühlethaler (38, 41, 47) also consider the 101 plane to be the plane of lamellation in the tracheid walls. Wardrop (53) believes this to be a very significant structural feature, since these surfaces are likely to enter into cellulose to cellulose hydrogen bonding causing consolidation of the cellulosic lamellae when the lamellae are brought into close association. This can occur, for example, when the moisture content of the specimen is lowered.

It is unlikely that the aggregation of the lamellae is perfect resulting in interconnected and irregular lamellae consolidation. Jayme and Fengel (58) have found the secondary wall of the delignified spruce tracheids to consist of irregular lamellar structure. The neighboring lamellae often touch laterally and sometimes converge to form rather broad lamellae. McIntosh (54) has also observed that the thin lamellae of the secondary wall are interconnected laterally. Norberg (59) observed a decrease in the number of lamellae that could be observed by electron microscopy as the sample moisture content is lowered before final low-temperature freeze drying. In the extreme case of air-dried tracheids, the tracheid wall is essentially nonporous (60), indicating consolidation of all the cell wall lamellae.

Further support for the concept of the thin (63 to 200 A.) elementary lamellae structure of the tracheid wall is found in the works of Preston, Wardrop, and Dunning. Preston (61) observed that the seaweed Valonia cell wall can be stripped into individual lamellae made up of parallel sheets of microfibrils, one microfibril thick. In conifers, according to Wardrop (62), the concentric lamellae of the S_2 layer in the intact tracheids appear to be 100 to 200 A. in thickness and, hence, must consist of only one or two sheets of microfibrils. Dunning (16) found that he could peel about twelve individual lamellae

in the S_3 layer. If this layer is assumed to be 0.6 μm. thick, then the individual layers have an average thickness of about 500 A.

LATERAL STRUCTURE OF THE LAMELLAE

Peterlin and Ingram (63) have presented a model of a sheet of elementary fibrils in a water-swollen and a cuene swollen cotton secondary wall lamellae based on electron microscopy. According to their model, the adjacent elementary fibrils have both crystalline and amorphous "bridges" connecting them laterally. In the unswollen condition the crystalline region of the elementary fibril is about 50 to 60 A. in width, corresponding to five to seven unit cells. In the cuene swollen state the crystalline region of the microfibril is about 35 to 40 A. and contains about four and five unit cells, respectively, in one direction. Most of the crystalline regions are surrounded by the swollen, less-ordered surface layer of cellulose but are bonded laterally by crystalline regions appearing in random along the elementary fibril. The thickness of the swollen surface layer on the elementary fibril is about one or two unit cells thick, corresponding to two or four cellulose molecules. The outermost molecules in the swellable surface layer are not perfectly in register with the crystalline lattice. However, in some places where the interelementary fibril "crystalline bridges" occur, the crystallographic order is largely maintained. These "crystalline bridges" give the coherence to the neighboring elementary fibrils so that they become bundled into a single microfibril. In a similar manner, the outermost elementary fibrils of the neighboring microfibrils get bonded together laterally forming the sheetlike structure of the lamellae.

STRUCTURAL CHANGES IN THE CELLULOSE OF THE TRACHEID WALLS

CRYSTALLINITY IN IMMATURE AND MATURE TRACHEID WALLS

The differences in the cellulose of immature and mature tracheids are not completely elucidated, and the information on cellulose in the developing fibers has been obtained mainly on cotton.

Berkley and Kerr (64) suggested that the cellulose in the immature cellulosic fibers may not be laid down in the crystalline form, since they did not find any evidence of crystalline cellulose structure in immature, undried cotton fibers fresh from the boll. On drying, the cellulose pattern appeared and remained on rewetting. Also, if the undried immature cotton fibers are stretched while wet, the cellulose pattern appears. Dehydration of fresh cotton in ethyl alcohol also causes the appearance of the crystalline pattern. From these observations Berkley and Kerr (64) concluded that the cellulose in the fresh cotton tissue is not associated into crystalline regions during deposition. In a living boll, hydroxyl groups on adjacent chains are separated by water molecules. The crystalline regions form during the initial dehydration period when water is lost, and cellulose-to-cellulose bonding becomes possible.

Preston (65) has criticized this interpretation on the grounds that the absence of an x-ray diffraction diagram of crystalline cellulose does not necessarily mean the absence of crystalline regions, but merely that the crystalline regions are too small in size to be seen as crystalline by the x-ray beam. However, it is clear that some changes in the packing of cellulose occur during maturation.

Rånby and Katzmire (66), in a study of cotton, could not find definite evidence of crystalline cellulose in the solvent exchange dried immature cotton fibers, while the mature cotton (35 days and older) always showed a crystalline pattern. Similarly, for undried flax fibers, Berkley and Kerr (64) did not observe any x-ray crystallinity in the specimen taken from near the top of the growing tip, while a sample from the base of the stem showed a clear crystalline pattern of cellulose I. A sample taken from the midregion showed an intermediate degree of crystallinity. These observations indicate that the amount of material capable of exhibiting crystalline x-ray diagram increases during the maturation and aging.

Preston, et al. (67) demonstrated that major changes occur in the cellulose fine structure in the wet state. The fresh softwood immature tracheids submerged in water exhibit only a halo characteristic of the x-ray diffraction by water, while the same tissue exposed to x-rays after equilibrium at 98% relative humidity gives a diffraction ring typical of cellulose I.

Preston (68) further reports that in the air-dried condition, the immature tracheids exhibit a crystalline pattern, but that the arcs are much more diffuse radially than in the mature tracheid cellulose patterns. Preston interprets this to mean that the cellulose crystallites in the dried immature tissue are much smaller than in the mature secondary wall. He calculates the crystallite size in the immature tissue to be 20 to 30 A. in width, while in the mature tracheids the average width is 35 to 40 A. These values, however, can be considered only as approximations since crystallite imperfections can also have a broadening effect on the diffraction peaks. Preston further calculates that the crystallites are separated by 90 to 120 A. spaces in the growing wall. These

observations are clear evidence that the degree of order of cellulose in the tracheid walls undergoes changes during maturation.

ORIENTATION OF CRYSTALLITES DURING MATURATION

In the air-dried condition, the immature cotton (25 days) has a diffraction pattern characteristic of small crystallites oriented in a random manner. As the cotton hair develops, the diffraction pattern shifts from the Debye ring type to one of preferred crystallite orientation. The first signs of preferred orientation appear in the 35-day-old cotton fibers and reach maximum in 50 days (69, 70). In the case of air-dried white fir wood, the maximum preferred orientation occurs in ten day old tracheids (71). If all the cellulosic materials laid down in the fiber walls are highly crystalline, that is, if the degree of cellulose-to-cellulose bonding is high, then it is unlikely that such large changes in the crystallite orientation could take place during tracheid wall maturation.

It must be concluded that the cellulose in the never-dried condition (immature and mature) exists in an amorphous phase, a paracrystalline state, and small crystalline regions. The border line between these conditions is not sharp and can be readily modified by changes in the sample environment.

CRYSTALLINITY DURING DRYING AND LOADING

Even though the concept of Berkley and Kerr (64) suggesting that immature cellulosic fibers do not possess crystalline order, is severely criticized, their reasoning merits further consideration. They postulated that the individual cellulose molecules are held apart by water molecules. If Preston's (65) concept of small crystalline regions (too small to be seen by x-rays) is

accepted, it is possible to argue that these small crystallites are held apart by water layers. On dehydration, the small crystallites can consolidate to form larger crystallites which are seen as crystalline by x-ray techniques.

Heyn (8) found that water-submerged, undried mature cotton shows definite evidence of crystallinity even though the crystallite peak is very faint. Equilibrating the cotton moisture content at 100% R.H. nearly doubled the intensity of the crystallite peak. The compression of the wet sample at 25,000 p.s.i. tripled the intensity. Air drying greatly increased the intensity, and prolonged exposure to the ambient condition further increased the intensity of the crystallite peak. The stretching of the wet sample resulted in a higher crystallinity than that in the unstretched sample, when examined in the dried state. Murphey (72) has found for wood that tensile loading results in an increase in the crystallinity and that most of this increase is irreversible on unloading.

The recent study by Fahmy and Mobarak (39) on density of cotton cellulose in water and on its water-holding capacity supports the conclusions made from the x-ray data. They conclude that, in the never-dried condition, cotton cellulose is far from entirely crystalline, and the cellulose can be considered to have an excessive amount of lattice defects or to contain an amorphous phase in the presence of a crystalline phase. They observed an increase in the water density of cellulose after air drying and concluded that air drying results in almost complete crystallization of cellulose. Since, on resubmersion in water, the fiber water-holding capacity is only one-half of that in the biological swollen state, Fahmy and Mobarak conclude that the airdry fiber does not have the same basic morphological structural elements as the undried fiber. The original biological elementary fibrils aggregate, forming microfibrils during drying.

Apparently, the crystallinity of cellulosic substances is a variable quantity and depends not only on the maturity of the tracheids but also on the environmental history of the specimen. A process that brings aligned cellulose molecules or crystalline regions into close contact can result in an irreversible increase in the cellulose-to-cellulose bonding.

LAMELLAR STRUCTURE DURING DRYING

The lamellar wall structure in the delignified tracheids is strongly dependent on the moisture content. In the water-swollen, never-dried condition the pore volume is about 1.4 ml./g. for 60%-yield kraft, about 1.8 ml./g. for 60%-yield sulfite, and about 1.8 ml./g. for 80%-yield holocellulose (52, 73). In the airdry state, the wood tracheid wall, as well as the delignified tracheid wall, is essentially nonporous (74, 75).

According to the multilamellar model (10) of the tracheid walls in the air-dry state, the interlamellar macropores are essentially collapsed, and the adjacent lamellae have consolidated into aggregates of lamellae along the amorphous mantle surfaces (Fig. 5). The amorphous mantle which accomodated the micropores in the water-swollen state, shrinks about 60% on air drying, becoming essentially nonporous.

The loss in lamellae surface area is considerable even at very high moisture content. Drying of the pulp pad to 40% moisture content at room temperature from waterlogged condition before solvent exchange drying reduces the B.E.T. surface area by about 80% (75). Apparently, the collapse of pores begins at relatively high moisture contents.

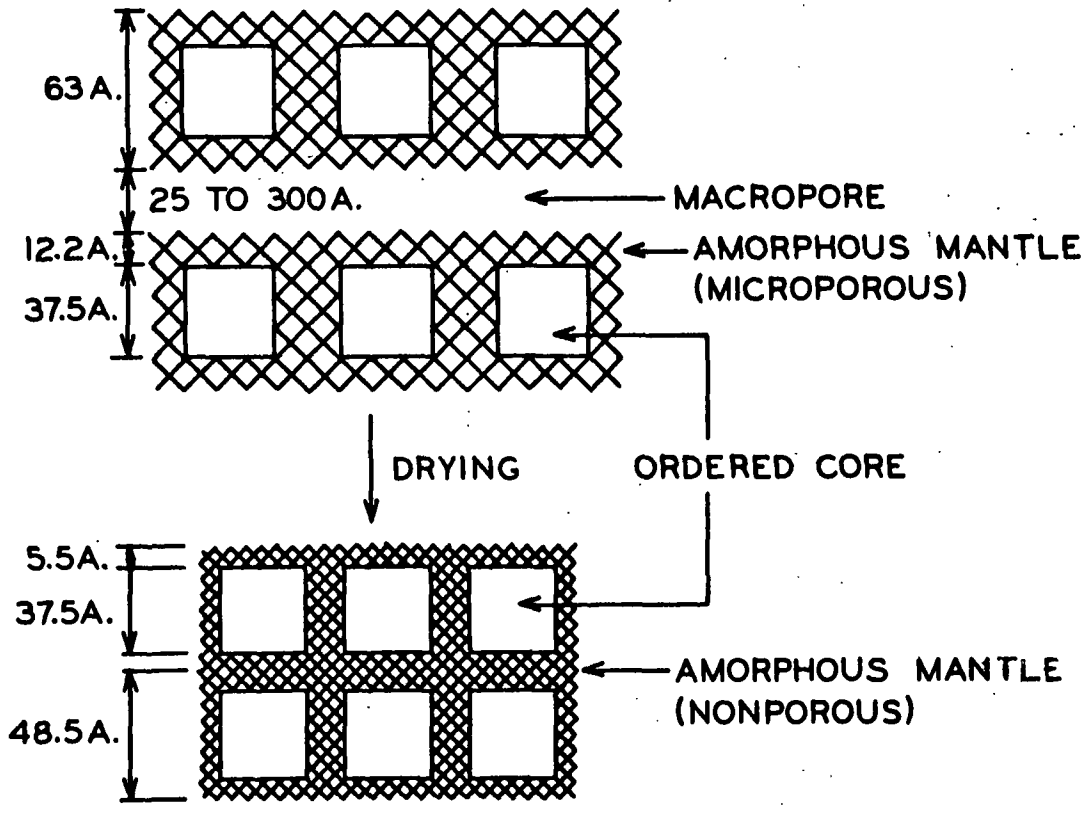

Figure 5. Fine Structure of Lamellae in the Wet and in the Dry States. From Stone and Scallan (10)

These observations imply that the tracheid wall structure defies any simple definition, and that the structural state of the cell wall is highly dependent on the previous conditions and the present environment of the sample. Each change in the sample environment modifies the structure of the tracheid wall.

This point is significant, since most of the knowledge about the tracheid wall structure is obtained in the samples which have been converted to the dry state by air drying, freeze drying, or solvent exchange drying. None of these techniques leaves the tracheid wall structure in the water-swollen condition (10, 16, 59).

LAMELLAR STRUCTURE DURING DELIGNIFICATION

In harmony with their multilamellar tracheid wall model, Stone and Scallan (52) claim that, during commercial pulping, the lignin-hemicellulose rich lamellae are solubilized and in effect removed. In the case of kraft, the tracheid walls swell only slightly during pulping to about 60% yield, and then begin to shrink. They attributed the dimensional stability of the cell wall during kraft pulping to the "tie-rod" function of the remaining lignin. The three-dimensional lignin network prohibits the swelling of hemicellulose and of the amorphous cellulose. In the case of sulfite pulp, the tracheid wall expands 20%. The hydrophilic hemicellulose act as compressed springs causing this swelling when the "tie-rod" function of the lignin is destroyed by sulfite liquor before the solubilization of the lignin. According to this model, the tracheid walls in the delignified condition consist of concentric, cellulose-rich lamellae.

CELLULOSE FINE STRUCTURE DURING DELIGNIFICATION

The knowledge of the changes in the cellulose-rich lamellae during delignification is sparse, especially for tracheids in the water-swollen condition. The present knowledge originates from data collected on air-dried samples. Preston (5) observed that the delignification of coir has at least three effects on the x-ray crystallinity of air-dried specimens. (1) The background is less intense, corresponding to the reduction in scattering due to the lignin fraction. (2) The cellulose crystallite arcs are narrower tangentially, indicating a better alignment of the crystallites with the fiber axis. (3) The arcs are also slightly narrower radially, suggesting a slight increase in crystallinity, possibly an increase in the crystallite size.

Nelson (6) has observed different pulping conditions to lead to different cellulose fine structures. Kraft pulping results in smaller crystallite transverse dimensions than sulfite pulping, while the chlorite holocellulose has considerably wider crystallite transverse dimensions than the other two pulps investigated. Furthermore, he reports an increase in the crystallite width as the yield of the holocellulose decreases. This is accompanied by an increase in the crystallinity index. These results were confirmed by Alexander, et al., on Norway spruce (76). These results are very interesting since they imply that the boundary between the crystalline region and the amorphous region is not fixed and/or that two crystalline regions can approach each other laterally, becoming so closely associated as to appear as a single crystallite to the x-ray beam. However, whether these changes in the cellulose fine structure occur in the wet state is still unknown, since these results were obtained on dried samples.

CRYSTALLINITY DURING ACID HYDROLYSIS

Acid hydrolysis by 0.1N HCl of immature tracheid walls of Pinus sylvestris appears to result in cellulose crystallization (77). In the unextracted, airdry immature tissue only a broad 002 plane diffraction ring is present while the diffraction from 101 and $10\bar{1}$ planes is very faint or absent. Acid hydrolysis results in a considerable sharpening of the 002 plane diffraction ring, and the 101 and $10\bar{1}$ plane diffraction appear distinctly. Calculations based on the 002 plane diffraction indicate an increase in the average crystallite width from 18 A. in unextracted immature tissue to 26 A. in the acid-hydrolyzed tissue. Wardrop interpreted the above results to indicate an increase in the crystallite width by crystallization of the paracrystalline region and an increase in the length of the crystallites by ordering of the cellulose molecules at the ends of the crystallites. In a later study, Wardrop (62) observed a decrease in the

002 plane diffraction ring radial width on hydrolysis and interpreted it as crystallization of the paracrystalline phase onto the pre-existing crystallites. Vogel (78) and Wardrop (77) believe that acid hydrolysis of delignified wood results in a crystallization of the paracrystalline phase between the neighboring microfibrils resulting in a lateral bonding of the microfibrils into macrofibrils. In a recent study Jayme and Roeffael (79) observed that heterogeneous hydrolysis of cellulose with H_2SO_4 leads to a pronounced increase in x-ray crystallinity. The amount of increase in the crystallinity is dependent on the acid concentration, temperature of hydrolysis, and the subsequent drying conditions.

It is clear that acid hydrolysis has a considerable effect on the cellulose-to-cellulose bonding. However, again the question remains, how much of these structural changes took place in the wet state, and how influential the drying conditions were on the observed results.

CRYSTALLITE ORIENTATION DURING BLEACHING

Bleaching has also been found to modify the microfibrillar orientation angle with respect to fiber axis. Clark (80) observed that bleaching generally lowers the degree of preferred orientation. The effect is very small in jack pine, while in western hemlock the apparent amount of crystallites parallel to the fiber axis in the bleached condition is only one-half that in the unbleached condition. Understanding the effect of bleaching is complicated by Clark's observation that the bleached poplar kraft is better oriented than unbleached, while in the bleached poplar sulfite, the crystallite orientation is more random than in the unbleached condition.

CRYSTALLINITY DURING HEMICELLULOSE EXTRACTION

Nelson (6) has observed that removal of hemicellulose from the slash pine chlorite holocellulose by 6% NaOH at 60°C. results in an increase in the crystallinity index and in a marked decrease in the width of the diffraction peak, indicating an increase in the average crystallite size. Spiegelberg (81) has made the similar observation on longleaf pine holocellulose except he found that as mild an alkali treatment as the 0.1N NaOH is effective in increasing crystallinity. An interesting complication is that the 0.1N alkali treatment of cotton results in a decrease in the crystallinity index and in a widening of the diffraction peak (81). The holocellulose appears to crystallize while cotton cellulose appears to swell on comparable treatments. The situation is further complicated by the fact that removal of xylan-rich hemicellulose from hardwood and of mannan-rich hemicellulose from softwood results in a decrease in the crystallinity (5) while progressive removal of xylan-rich hemicellulose from high-xylan (19.8%) manila hemp renders the cellulose more crystalline (3). The explanation of these observations cannot be based on chemical composition changes alone, and an additional explanation is needed. This possibly involves an understanding of the mechanism by which cellulosic fibrils and lamellae are brought close together or are forced further apart.

LAMELLAR STRUCTURE DURING REFINING

It is well known that the tracheid in the delignified condition is susceptible to structural damage on mechanical action. Emerton (82) has stated that the coaxial delamination of the cell wall during beating is a general phenomenon causing increased flexibility of the fibers. Others (54-56, 83) have also observed the delamination of the holocellulose tracheid walls into

numerous, concentric lamellae on refining. For example, Page and DeGrace (55) have found that any mechanical action examined promotes delamination of the delignified tracheid walls, but that the interlamellar planes are not all equally weak. Presumably, those planes which are originally rich in lignin and hemicellulose are especially weak and are the first to delaminate. They also found that sulfite tracheids split more readily than kraft tracheids.

The packing of cellulose crystallites within lamellae is modified during refining. Marton, et al. (7, 76) observed that refining invariably causes a decrease in the fibril angle at any yield as observed in gelatin-mounted samples. They also detected an increase in the average crystallite width in the air-dried tracheids as a result of refining. It was further observed that wet pressing of unrefined and refined tracheids causes a shift in the fibril angle toward the tracheid axis.

Apparently, the mechanical action on the delignified tracheid walls causes a loosening of the lamellae and of the fibrils within the lamellae. The increased mobility of the cellulose structural units results in their better packing during drying. But it also may be conjectured that aggregation may already occur during the mechanical action. Certain fibrils may be brought into close enough contact with neighboring cellulosic elements to cause their aggregation in the wet state.

CRYSTALLINITY DURING HYGROTHERMAL TREATMENT

Hermans and Weidinger (84) have made the interesting observation that heating of dry-ground, amorphous cellulose powder in water results in a considerable recovery of the crystalline cellulose I x-ray diffraction pattern. They have made a similar observation on cellulose II powder (85, 86). The

crystalline lattice of the freshly spun fiber is still incomplete. The diffraction maxima corresponding to $10\bar{1}$ and 002 planes are so broad that they merge into one peak. The 101 plane diffraction maximum is particularly indistinct and has shifted inward indicating wider 101 plane spacing. During boiling the crystallization of freshly spun fiber continues. The 101 plane diffraction becomes more distinct, and the $10\bar{1}$ and 002 plane diffractions separate into two distinct peaks. In this process the cellulose II hydrate loses one water molecule.

Wardrop (77) observed somewhat similar sharpening of the cellulose I x-ray diffraction pattern of immature tissue on acid hydrolysis (page 26). It will be recalled that the major objection to the Berkley and Kerr (64) hypothesis of noncrystalline cellulose in the immature cotton is that the purified (chemically treated and boiled) immature cotton does show cellulose crystallite pattern. It is entirely possible that during the purification process the cellulose packing is sufficiently perfected to result in a clear crystalline pattern. If this is the case, then the Berkley and Kerr hypothesis may be correct.

The effect of hygrothermal treatment on cellulose structure is further demonstrated by the following observations. Vigo, et al. (87) have found that boiling the washed, benzyltrimethyammonium hydroxide decrystallized cotton cellulose in water results in a considerable recovery of the crystalline order and a decrease in the accessibility. Risch (88) observed a 50% decrease in the water sorption capacity of rayon filaments after water vapor heating. Hermans (85) has noted that the steamed fibers have a higher density then unsteamed.

Clearly the water heating of cellulosic substances has a profound effect on the structure of cellulose.

APPROACH TO THE PROBLEM

The review of literature indicates that the manner in which the removal of tracheid wall components influences the packing of the remaining constituents is not yet well established. The investigations performed on samples maintained in the wet state indicate that the tracheid wall swells during the component removal. The extent of swelling depends on the manner of pulping and on the extent of delignification achieved. The x-ray data, on the other hand, indicate that the degree of crystallinity of cellulose increases. The conclusions drawn from the x-ray data, however, are not entirely consistent, since both an increase and a decrease in the packing density of cellulose has been reported. Furthermore, the meaning of x-ray results is not clear, since the observations were not made directly after the treatment under investigation. A drying process takes place before the x-ray diffraction experiment is performed, which may affect the x-ray results.

The hypothesis for the present study is that the conversion of the green wood to pulp results in changes in the cellulose fine structure in the wet state.

It is assumed in this investigation that any change in specimen environment is likely to result in some changes in the fine structure of the tracheid wall components. Whenever the test specimen is subjected to a chemical or a physical process, the properties of interest are determined during that process, rather than after some intermediate step.

One half of the wood specimens are brought through the treatment sequence of waterlogging, delignification to various yields, water washing of holowood, and hygrothermal treatment of washed holowood. The other half of the test

specimens, in addition, are hygrothermally treated after waterlogging before delignification. The wood, reacted for 120 days to give 57% yield holowood, is defibered and treated with uni- and multivalent ionic media.

The dimensional changes of green wood blocks (5 cm. by 1 cm. by 1 cm.) and of the holowood blocks are followed during the above treatments. The swollen specific volume of the defibered holotracheids is determined by the centrifugal water retention technique.

The changes in the fine structure of cellulose are determined by x-ray diffraction analysis. The arrangement of the tracheids in the wood is preserved throughout the test sequence. This allows viewing of the specimen perpendicular to the radial and to the tangential tracheid walls. The same population of tracheids in the test section is viewed throughout the experimental sequence. This eliminates the variation between samples, and enables the detection of relatively small changes in the fine structure of cellulose. The x-ray diffraction work is performed on samples in the wet, never-dried condition.

The factors causing changes in the tracheid wall volume or cellulose fine structure are studied by determining the swollen specific volume of the washed pulp in various ionic media other than the pulping liquor.

EXPERIMENTAL

SELECTION OF TEST MATERIALS

WOOD SPECIES

The wood of noble fir, Abies procera Rehd., was selected on the basis of morphological and chemical composition considerations. Abies procera is one of the structurally simplest conifers. It has only two types of cells: the tracheids, and the ray parenchyma cells. The transition from the earlywood to latewood is gradual. These factors are expected to result in a better correlation between the holowood block dimensions and the dimensional behavior of the holowood tracheid. The cold and hot water extractives are low in the noble fir wood. This is a desirable characteristic, since the solubilization of a large amount of material from the tracheid walls may significantly influence their structural behavior.

The total test specimen was a 600-pound disk, out from a 265-year old noble fir tree grown at 3100 feet elevation southeast of Molalla, Oregon. The disk was taken 10 meters above the stump and wax sealed the day of cutting. The first 15 cm. of wood from the cut surfaces were discarded. This left a 46-cm. thick disk. All the data reported in this investigation were obtained on the sapwood of one of the quarters of this disk. The width of the sapwood is about 15 cm. The quarter was sawed into blocks (6.5 cm. by 1.6 cm. by 1.6 cm.) with the long axis in either the tangential, radial, or longitudinal direction. In each case, the tracheid walls were parallel to the block faces. The surfaces were finished with the paper trimmer so that the final block dimensions were 5 cm. by 1 cm. by 1 cm. in the green condition [46.9% moisture content (M.C.); ovendry basis (o.d.)]. The blocks were stored at 5°C., submerged in distilled water. A minute quantity of phenyl mercuric acetate was added.

HOLOWOOD

Delignification at room temperature with sodium chlorite has obvious advantages over conventional pulping techniques (89). This procedure does not involve temperature cycles which are suspected to affect the structure of cellulose. The above delignification leaves the holowood largely with the same morphological details as the green wood. This permits the determination of the dimensional behavior of the holowood block over a wide range of lignin contents. In addition, the crystallinity of the test sample can be determined throughout the test sequence on samples that have preserved the native arrangement of tracheids. Hence, the differentiation between tangentially and radially viewed samples can be made on the same population of tracheids. Also, the solubilizing action of the sodium chlorite in the acetic acid-buffered medium is specific on lignin over a wide range of reaction times, and only at the later stages of delignification a small quantity of hemicelluloses is solubilized. Since the swollen specific volume of pulp is high (90), large structural changes are expected during the conversion of green wood to pulp. These pulps are characteristically strong and possess a high-hemicellulose content (90, 91). This combination provides an interesting material for future studies involving correlations between chemical composition, tracheid wall structure, and tracheid strength properties.

TREATMENT SEQUENCES

HYGROTHERMAL TREATMENT OF WOOD

In the present study, the hygrothermal treatment consisted of a twelve-hour heating in distilled water at 95°C. Review of the literature (92-97) as well as the exploratory work (Appendix I) indicated that when green wood is

brought through the first hygrothermal treatment, it expands tangentially and shrinks radially. During the subsequent hygrothermal treatments, the block shrinks in both radial and tangential directions. The dimensional changes during the first hygrothermal treatment are irreversible and about five times larger in magnitude than the dimensional changes in the subsequent cooling and heating cycles which appeared to be reversible. These observations led the author to believe that irreversible changes in the fine structure of the wood tracheid walls take place during the first hygrothermal treatment. For this reason, both hygrothermally treated and nonheated green wood blocks were studied during the subsequent treatment sequence.

DELIGNIFICATION OF WOOD AND DEFIBERING OF HOLOWOOD

The wood blocks were delignified directly from the green, waterlogged condition without extraction, since the dehydration which occurs during the methanol and chloroform-methanol extraction may result in some changes in the cellulose fine structure.

The waterlogged, hygrothermally treated and the waterlogged, nonheated Abies procera blocks were delignified by the room temperature sodium chlorite-acetic acid buffered reaction process, as described by Thompson and Kaustinen (91). The reaction liquor consisted of 100 g. of reagent-grade sodium chlorite per 1000 ml. of distilled water. The liquor was adjusted to pH 4.5 with acetic acid. The liquor-to-wood ratio was 10:1. The reaction liquor was replaced by fresh solution at two-week intervals. Holowood blocks were removed about every 10 days. The maximum reaction time was 127 days, which is 2 or 3 times the length of time necessary to solubilize all but a trace of lignin.

To determine the swollen specific volume of the tracheid walls, the holowood blocks in reaction liquor were defibered in the British disintegrator for 300 counts. The swollen specific volume of the pulps were determined in unwashed, water washed, and water washed-hygrothermally treated condition. Samples were removed after each treatment to determine the ovendry weight of pulp at each condition.

WATER WASHING OF HOLOWOOD

The holowood blocks were removed from the reaction liquor and placed in distilled water. The washing was done in the test chamber fitted with a linear variable differential transformer to measure the block dimensions (Appendix II). During the 50-hour wash period at 24°C., the holowood block weighing from 3 to 4.5 g. o.d. was exposed to about 20 liters of water. Volume of the chamber was 6.5 liters.

HYGROTHERMAL TREATMENT OF HOLOWOOD

The final wash water was replaced with fresh distilled water. The temperature of water in the test chamber was raised to 95°C. in about 45 minutes with 500-watt and 250-watt knife heaters. The water circulation was aided by bubbling heated air through the test chamber. The hygrothermal treatment lasted 800 minutes.

IONIC TREATMENTS OF PULPS

The holowood blocks, reacted for 120 days to give 57% yield pulp, were defibered in the British disintegrator for 300 counts in the water washed-hygrothermally treated condition. The pulps were centrifuged to remove excess water and immediately placed in 0.1N ionic media. Solutions of sodium chloride,

potassium chloride, calcium chloride, barium chloride, ferric chloride, hydrochloric acid, acetic acid, sodium hydroxide, potassium hydroxide, and 1.1N sodium chlorite reaction liquor were used. After treatment the pulp suspension was centrifuged at 1000 g for 30 minutes, and the centrifugal water retention value determined. This was followed by soakings in 500 ml. of distilled water. The wash water was exchanged four times during the 48-hour wash period, after which the centrifugal water retention value was again determined.

EXPERIMENTAL APPARATUS AND TECHNIQUES

DIMENSIONAL CHANGE MEASUREMENT APPARATUS

A jig was built to measure the dimensional changes of wood and holowood blocks in the water-saturated condition. A schematic diagram of the apparatus is shown in Fig. 6. The test chamber (A) was constructed of Lexan[1]. The test block (B) was placed on the aluminum stage (C), which was connected to the linear variable differential transformer (LVDT) mounting base (D) by nillvar rods (E). The core (F) of the LVDT (G) was connected to the detection probe (H) made of nillvar. The position of the core inside the body of the LVDT determined the magnitude of the electrical output signal, which was the measure of the block dimension. The test chamber was maintained full of distilled water during dimension change measurements. The temperature of the chamber was controlled to within $\pm$ 0.4°C.

A more comprehensive discussion of the construction, calibration, and operation of this apparatus is given in Appendix II.

---

[1]Lexan is a transparent polycarbonate sheet manufactured by General Electric Co., Chemical Materials Department.

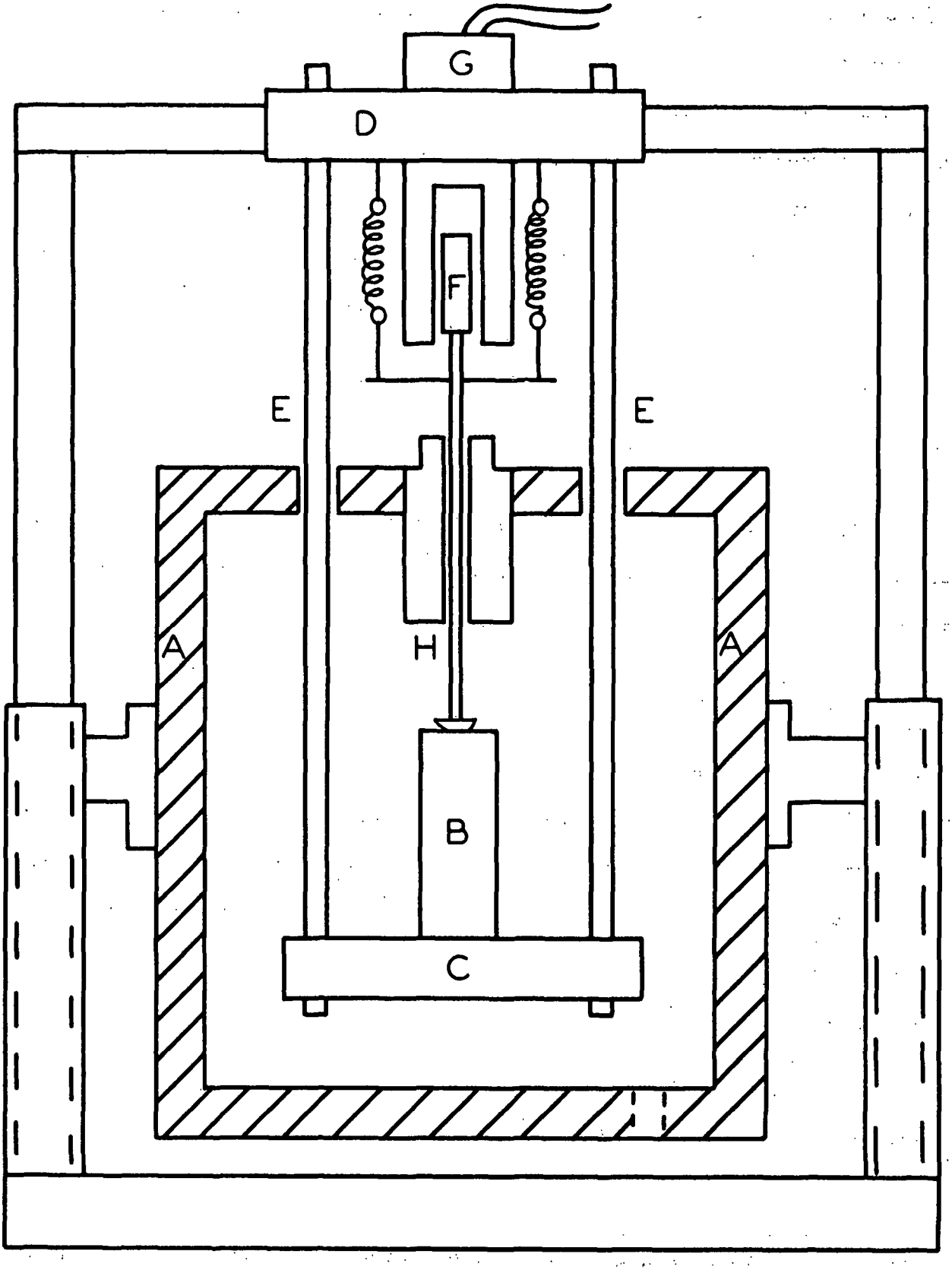

Figure 6. A Simplified Schematic Representation of the Apparatus Built to Measure the Dimensional Changes of Wood and Holowood Blocks During Water Washing and Hygrothermal Treatment

SWOLLEN SPECIFIC VOLUME DETERMINATION

The centrifugal water retention technique was applied to determine the swollen specific volume of pulps in various aqueous media. The centrifuging technique was first developed by Coward and Spencer (98) to determine the water-holding capacity of cotton. Jayme, et al. (99) have modified the centrifugal technique by designing various specimen holding cups. Thode, et al. (100) further modified the technique and adopted it for pulp evaluation.

The basic problem with the centrifugation technique is that it measures both imbibed and capillary water retained by the fibers (101). The capillary water held in interstices between fibers and in lumens is estimated to be between 5 to 13% depending on the pulp, sample cup and centrifugal field (98, 101, 102).

The problem of capillary water has led to the use of different speeds of centrifugation by various investigators. Centrifugal speeds corresponding to centrifugal forces of 100 to 5000 times the gravitational field, g, have been used (98-103). The German Standard Method specifices 3000 g for 10 minutes (103). Thode used 3000 g for 15 minutes (100).

Increasing the speed of centrifugation results in a compaction of the sample against the porous plate of the sample cup. This results in a loss of imbibed water along with the reduction in the amount of water held in the interstices between the fibers. Aggebrant and Samuelson (104) maintain that even 100 g is effective in compressing the fiber wall.

The primary purpose of applying the centrifugal technique in the present study was to compare the observed trends in the swelling behavior of holowood blocks to the swelling of pulp fibers. The success depended on whether

significant differences could be detected in the swollen specific volume of unwashed and washed pulps, and between washed and hygrothermally treated pulps. The average number of interstices between the fibers and their size distribution does not appreciably change between runs, since the number of fibers remains constant and fines are not produced. However, if the tracheid walls are compressed, a problem arises since the amount of imbibed water is reduced.

For the above reason, a preliminary study of the centrifugal technique was carried out. The results are summarized in Appendix III. On the basis of this preliminary study, the centrifugal speed corresponding to 1000 g and centrifugal time of 30 minutes was adopted.

The centrifugal water retention value is calculated from the expression: CWR = (wet weight - dry weight)/(dry weight), and is given in grams of water per gram of ovendry pulp. The CWR is converted to the swollen specific volume by adding a constant 0.62, which corrects for the volume of cellulose.

X-RAY DIFFRACTION ANALYSES

Crystallinity Index

A Laue x-ray diffraction diagram obtained on the air-dried pulp pad is shown in Fig. 7. A typical Debye-Scherrer ring pattern characteristic of randomly oriented cellulose I crystallites is apparent. The equatorial scan from A to B is reproduced to demonstrate the intensity distribution of scatter originating from the various crystallite planes (Fig. 7b).

Ordinarily in the Laue x-ray diffraction camera, the cellulosic substances are exposed to the x-ray beam in the oven-dried condition and under vacuum. This procedure minimizes the background scatter from the air and water vapor. This incoherent scattering is significant when long exposure times are necessary.

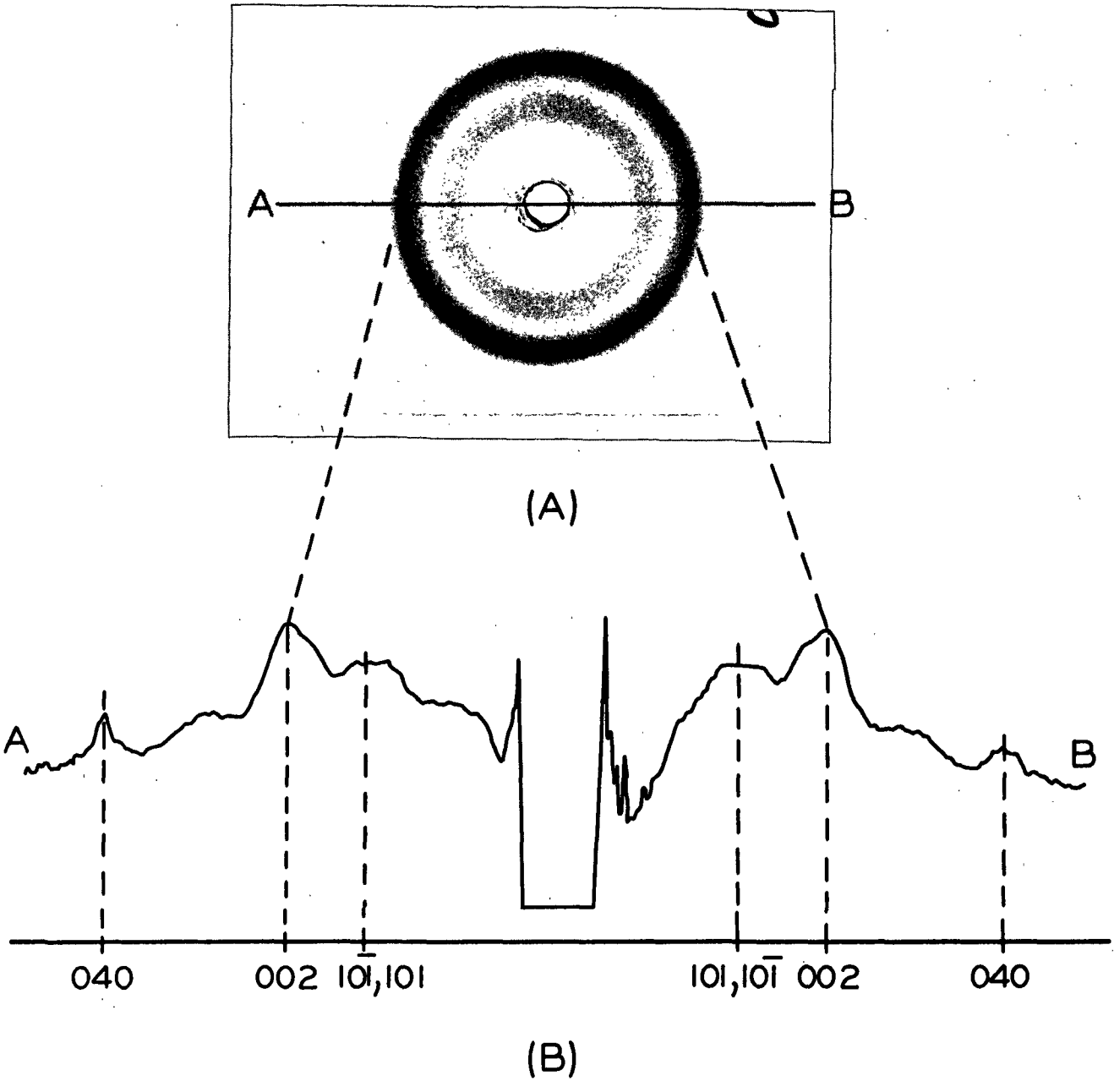

Figure 7. The Laue X-ray Diffraction Pattern of Pulp Pad Air Dried to 9.7% M.C. (A); the Radial Transmittance Trace from A to B (B)

Generally, if the crystallinity information is of prime consideration, the cellulosic fibers are compressed into pellets (105, 106) or are formed into sheets (107). These procedures insure a uniform Debye-Scherrer ring due to the diffraction from the randomly oriented crystallites.

The basic assumption in determining the degree of crystallinity of high molecular weight polymers is that the x-ray scattering from the amorphous fraction and from the crystalline fraction is additive. In the case of cellulose, which has a rather broad intensity maxima, the separation of the scattering due to crystalline and amorphous fractions is ambiguous, since the intensity maxima overlap.

Two techniques have been developed which can be used to rank cellulosic materials according to their degree of order. In the Hermans and Weidinger technique (108, 109) the area under the intensity curve attributed to the diffraction by crystalline regions is compared to the area of amorphous background diffraction. The technique of Ellefsen, et al. (107) differs in that the dividing line between the diffraction due to crystalline and amorphous regions is drawn in a somewhat different manner. However, the physical significance of the numbers in each technique is not well defined, since dividing the cellulose into crystalline and amorphous fractions by x-ray techniques is not justified. These techniques, however, are reliable for ranking the samples within an investigation according to the degree of order of the cellulose.

The technique of Segal, et al. (110) accomplishes the ranking of samples with equal reliability. Here, the height of the intensity maxima corresponding to the 002 plane scattering is compared to the height of the intensity of the amorphous background (Fig. 8). The amorphous background scattering is

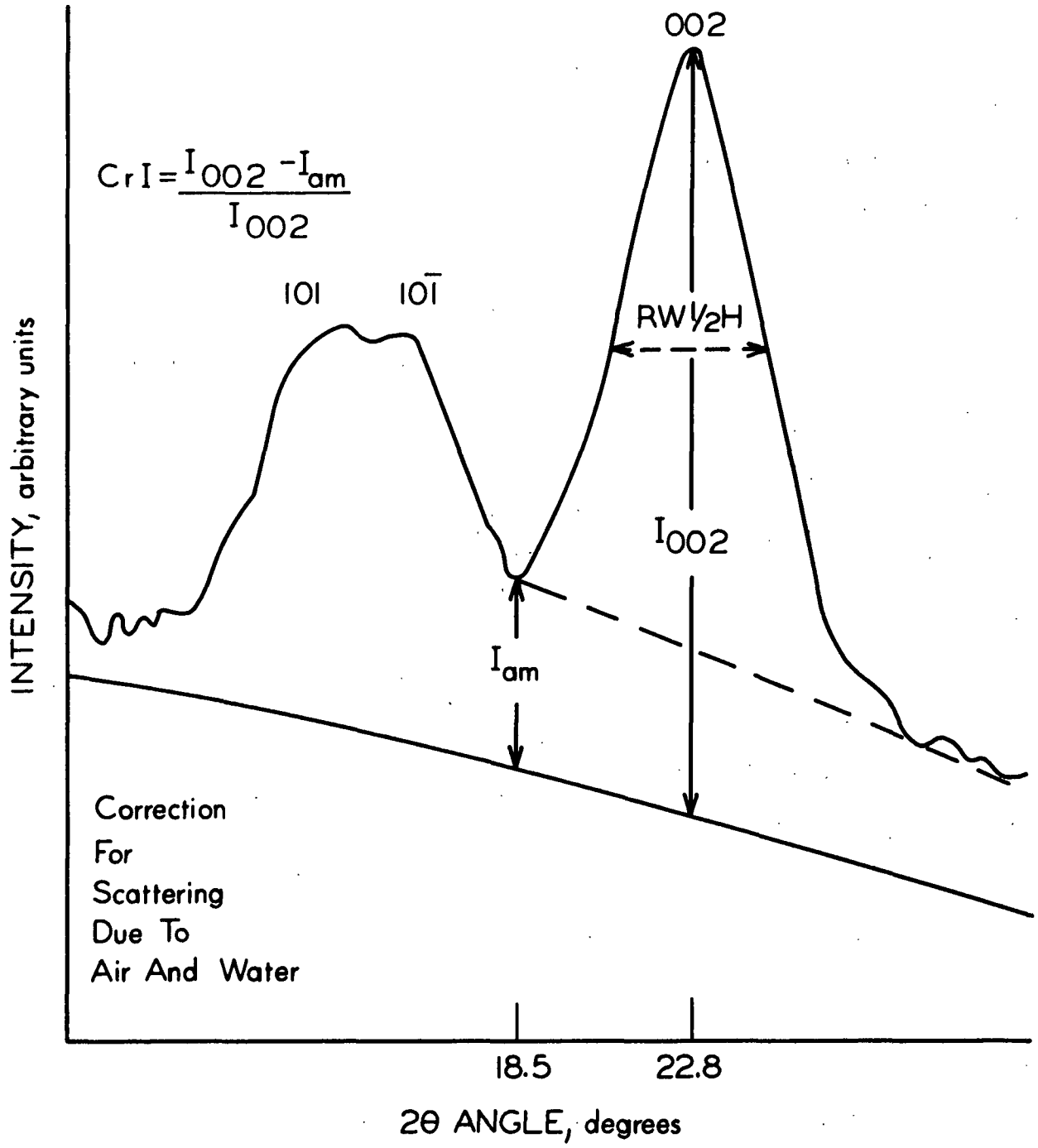

Figure 8. Determination of the Crystallinity Parameters, the Crystallinity Index, and the Radial Width at Half-Height ($RW_{\frac{1}{2}H}$), from the Radial Intensity Trace

arbitrarily chosen to be equal to the minimum, between the 101 and 002 peaks. This selection corresponds well with that defined by Ellefsen, et al. (107).

The Segal, et al. (110) crystallinity index is defined by the equation:

$$CrI = \left[\frac{I_{002} - I_{am}}{I_{002}}\right] \times 100$$

CrI is the crystallinity index. I_{002} is the maximum intensity of diffraction originating from the 002 crystallite planes plus the amorphous scatter at $2\theta = 22.8°$. I_{am} is the intensity attributed to the amorphous scatter and is determined at $2\theta = 18.5°$, which is the minimum intensity between $10\bar{1}$ and 002 maxima. Ant-Wuorinen and Visapää (111) have developed a similar relative index. The Segal, et al., index is used in the present study to establish the direction of change in the degree of order of cellulose.

The present study, unlike the conventional x-ray diffraction analyses, is carried out on samples maintained waterlogged throughout the exposure. The choice of waterlogged samples does, however, present several problems. The x-ray diffraction analysis of Heyn (8) indicates that in the water-swollen condition, cotton exhibits an 002 peak of 10 arbitrary units, while the control in the dry state exhibits a peak of 71 arbitrary units. Heyn suggested this difference to be due to the masking effect of water halo, the dissipation effect of water, and the crystallization during drying. However, he did not draw conclusions about the relative amounts of amorphous and crystalline cellulose in the wet and dry states.

Support for the concept of a lower amount of crystalline material in the wet state is provided by Ray (112). He found that the degree of crystallinity of raw jute and mesta fibers decreases as the moisture content of the sample

increases. He obtained his data on fibers which were equilibrated at given relative humidities (0, 65, and 100%) and maintained at those relative humidities during the exposure. Later, Ray (113) made the same observation for jute and mesta holo- and α-celluloses. The masking effect of the increased quantity of sorbed moisture was found to have a negligible dissipative effect on the intensity of the cellulose pattern. Caulfield and Steffes (114) observed a higher degree of crystallinity for ball-milled cellulose I held at 90% relative humidity than for the dry samples. Changes in the cellulose fine structure apparently were larger than the masking or dissipative effects of the additional water.

A comprehensive study of the diffraction characteristics of water was made by Narten (115). For the purposes of x-ray diffraction analyses of cellulosic substances, the water diffraction pattern can be considered to be a broad halo and is assumed to be superimposed on the cellulose pattern, so that it can be subtracted from the total pattern (8, 33, 116). The intensity of diffraction by water was determined from independent exposures on a 1-mm. thick water layer (Appendix V). In the present study, the exposed area of the waterlogged holowood sections was not covered, eliminating the additional correction for the encapsulating plastic.

In Fig. 9, the difference between the x-ray diffraction diagrams of wet and dry samples is obvious. Diagram A is obtained on a 1.5-mm. thick pulp pad centrifuged to 460% moisture content (o.d. basis). Only a faint diffraction ring originating from the 002 planes is visible. It is impossible to get structural information from this diagram. Diagram B is for the same pulp pad after equilibration in a constant temperature and humidity room for three days to 9.7% M.C. (o.d. basis) and exposing essentially at that M.C. Various diffraction

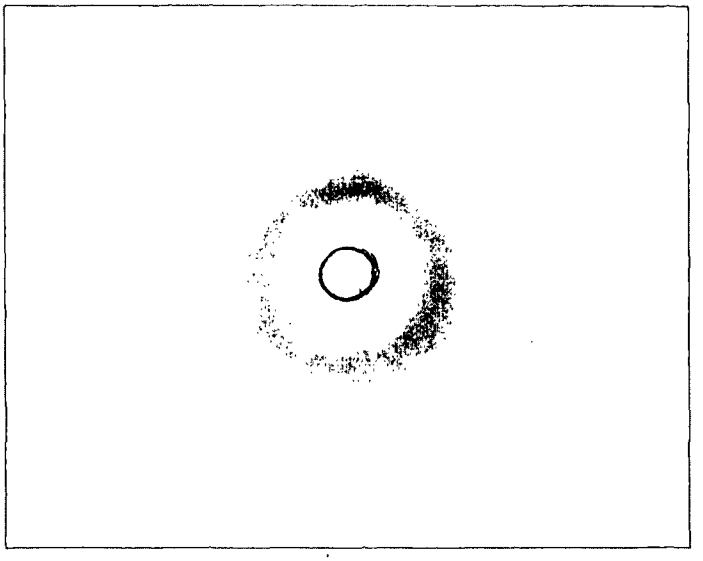

A

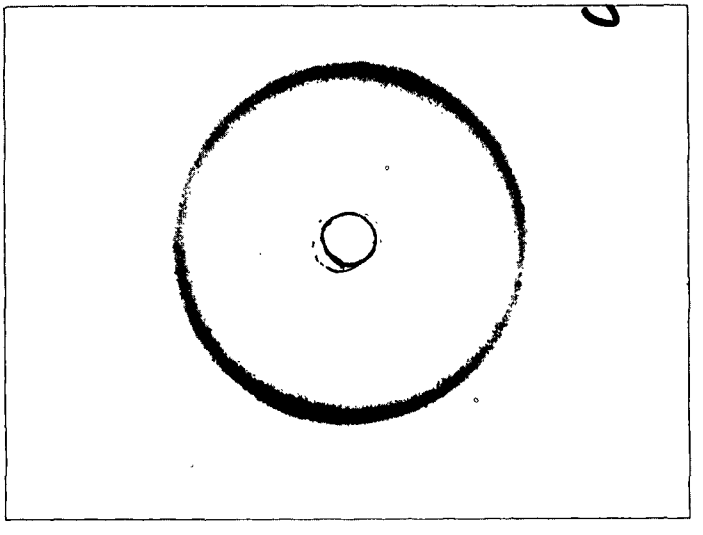

B

Figure 9. The Laue X-ray Diffraction Diagram of Never-Dried Pulp Pad at 460% M.C. (A); the Same Pad After Air Drying to 9.7% M.C. (B). The Fiber Orientation is Random in the Plane of the Pad

rings are readily visible. Apparently, large changes in the cellulose fine structure occur during drying.

The Debye-Scherrer diffraction pattern arises from randomly oriented crystallites. Consequently, the intensity of the scatter from a given set of crystallite planes is distributed in space as a cone. On the x-ray film the cone is exhibited as an equal intensity circle. The scatter is distributed equally around 360°. If, however, the crystallites have a preferred orientation, the resulting scatter is concentrated in narrow arcs with the same radius as in the previous case. This phenomenon is demonstrated in Fig. 10. The x-ray diffraction pattern A is that of a pulp pad at 460% M.C. (o.d. basis). The pattern B is that of a waterlogged holowood section. Several intensity maxima are clearly visible in the latter case. This pattern is a characteristic fiber diagram and is similar to the published patterns of dry wood sections and of dry, well-oriented fiber bundles (72, 117-120). Interpretations of the cellulose fine structure in the wet state can be made from patterns like B in the manner described in (107-111, 119-127).

The resulting crystallinity index values cannot, however, be compared to those obtained by the powder pellet or random sheet techniques. In the present case, the background is not uniform and the scatter from highly ordered regions is concentrated in narrow arcs, while in the latter case scatter is spread over 360°. Furthermore, in the latter case, the scatter originating from the 021 planes overlaps with that from the 002 plane. This results in a distortion of the 002 peak as can be seen in Fig. 11. In addition, the radial tail of the 021 plane diffraction maxima contributes to scatter at 18.5°. Nevertheless, for the powder diagrams, the scatter at this point is attributed solely to the amorphous background. These factors distort the crystallinity index values.

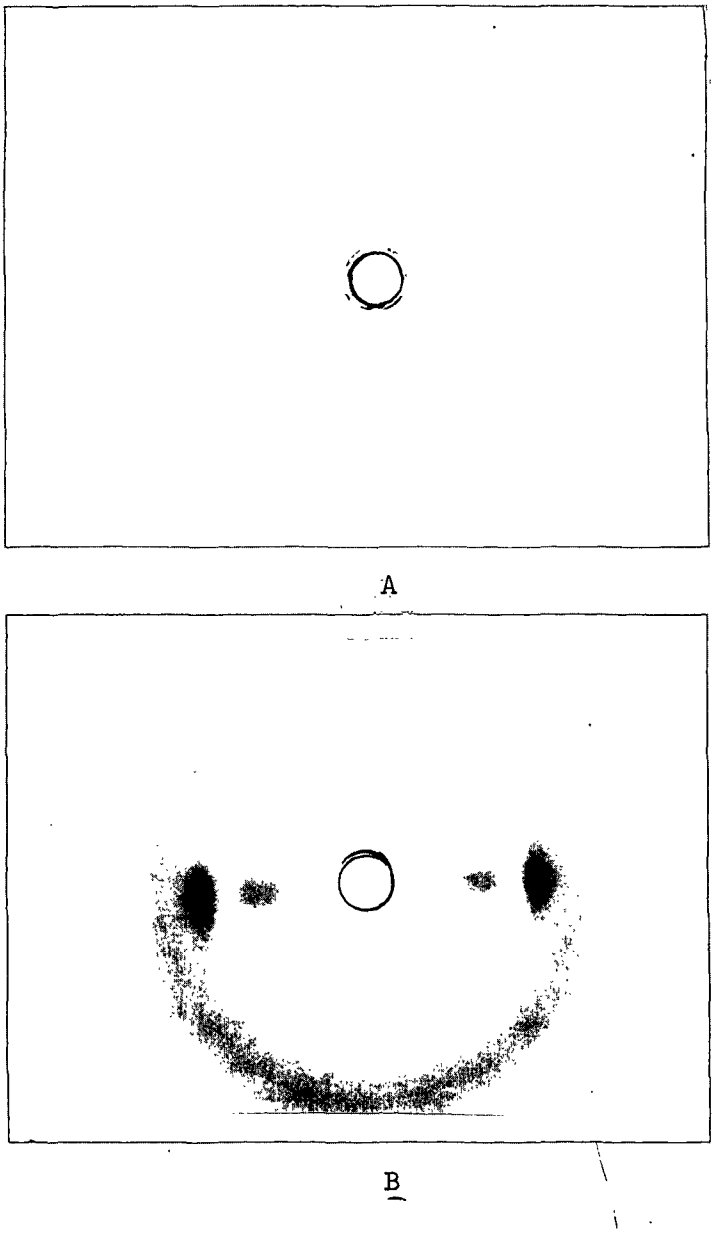

Figure 10. The Laue X-ray Diffraction Diagrams: A, Never-Dried Pulp Pad at 460% M.C.; B, Same Thickness Waterlogged Holowood Section with the Native Tracheid Alignment Preserved

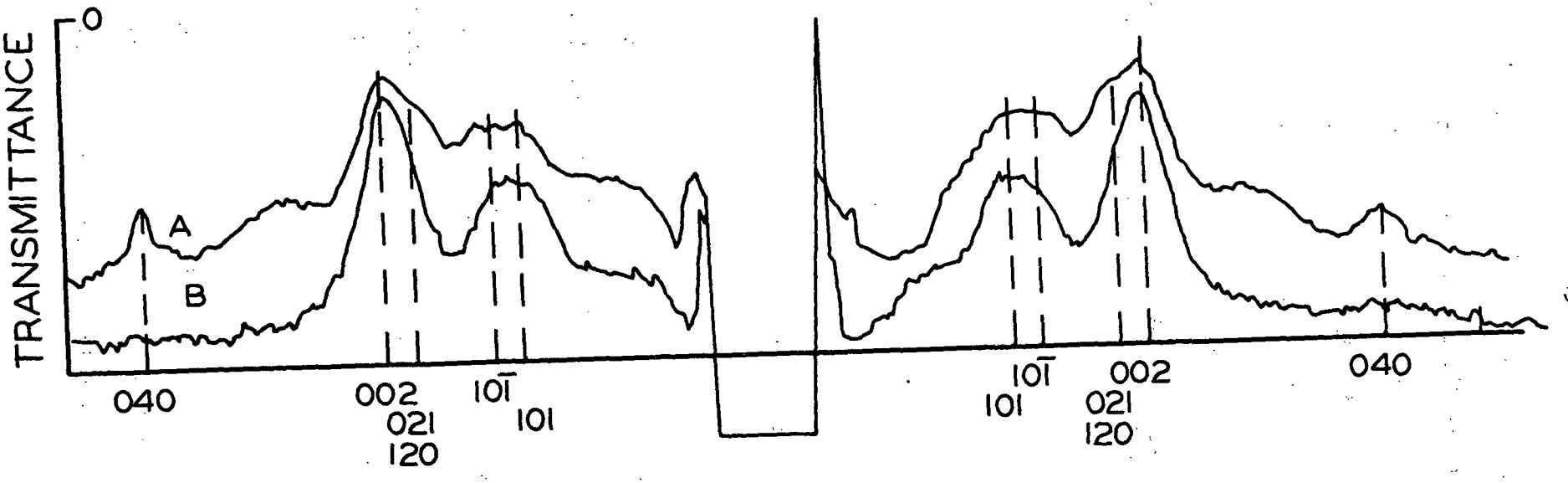

Figure 11. Radial Transmittance Traces with the Major Contributing Crystalline Planes Labeled: A, the Air-Dried Pulp Pad at 9.7% M.C., 30 Minute Exposure; B, the Air-Dried Holowood Section at 9.7% M.C., 15 Minute Exposure

The data in Table I illustrate the difference between the crystallinity index determined from the x-ray diffraction pattern of randomly formed pulp pads and that of corresponding holowood sections with the native tracheid orientation preserved. The crystallinity index in the latter case in considerably higher than that determined from the pad diagram.

TABLE I

X-RAY CRYSTALLINITY OBTAINED FROM RANDOM SHEET DIAGRAM VERSUS THAT FROM HOLOWOOD DIAGRAM

Sample[a]	Crystallinity Index
Pulp Pad I	46.80
Pulp Pad II	49.13
Holowood Section I	74.08
Holowood Section II	76.53

[a]All samples are air dried.

The effect of water on the x-ray diffraction diagram of the holowood section is illustrated in Fig. 12 and 13. In the case of the dry holowood, the background is considerably lighter than in the diffraction diagram obtained from the same section before it is dried. The same number of diffraction maxima, however, are visible in each case. The presence of water does not block out the faint diffraction maxima originating from the 021 and 040 planes. This has significance, since the masking effect of water is not sufficient to dissipate the coherent diffraction originating from these crystallite planes.

Orientation of Crystallites

Since the native tracheid alignment is preserved in the test sections, the crystallite orientation is more reproducible than that from the tracheid bundles generally used to obtain orientation data. Two factors contribute

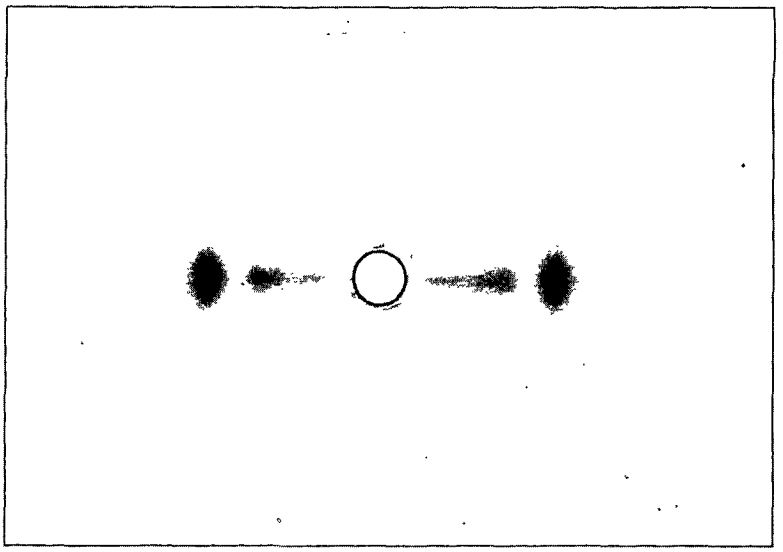

A

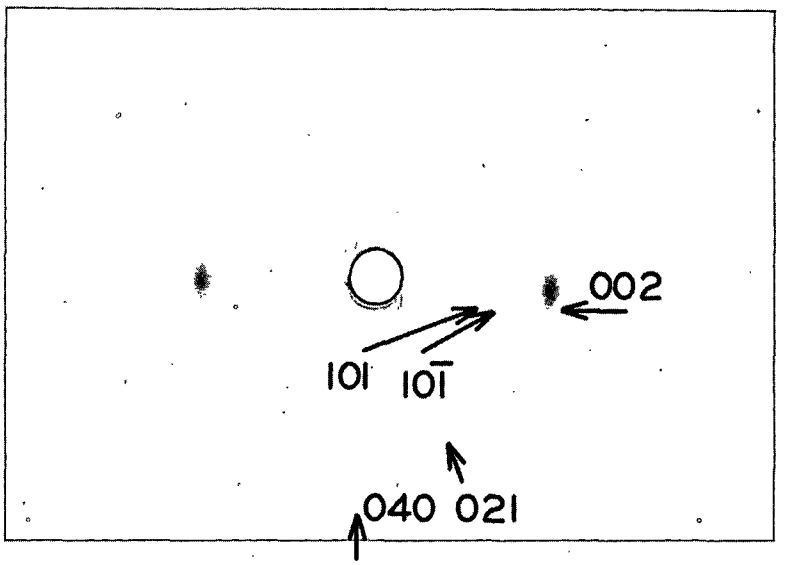

B

Figure 12. The Laue X-ray Diffraction Diagrams: A, Never-Dried Holowood Section in the Waterlogged Condition; B, Same Section After Conditioning to 9.7% M.C. at the Room Temperature, 15-Minute Exposure

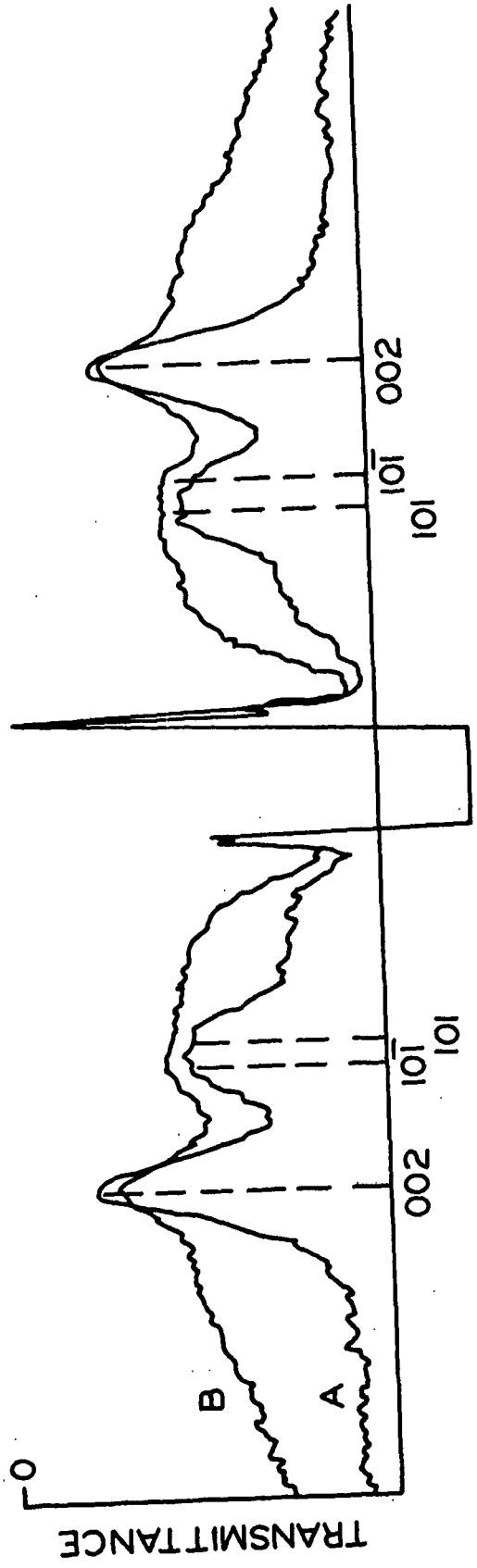

Figure 13. Radial Transmittance Trace with the Major Contributing Crystallite Planes Labeled: A, the Air-Dried Holowood Section 9.7% Moisture Content, 15 Minute Exposure; B, the Waterlogged Holowood Section, 60 Minute Exposure

to this advantage. One, the variation due to the imperfect parallel bundling of tracheids, is minimized. In holowood sections, the imperfections in the tracheid alignment do not change and hence contribute a constant quantity to the tangential spread. Secondly, the uncertainty due to the unknown distribution of radial and tangential walls facing the x-ray beam is also eliminated.

The effect of the crystallite orientation on the x-ray diffraction pattern is illustrated schematically in Fig. 14. The more parallel the crystallites are to the fiber axis, the narrower the diffraction arc due to the 002 planes.

Sisson and Clark (121, 122) were the first to measure this relationship. The width at the half height of the circumferential trace of the 002 maxima distribution curve is a measure of the orientation angle of the crystallite b-axis with the fiber axis. This technique is illustrated in Fig. 15 as CW 1/2H. Later, DeLuca and Orr (125) modified this technique by obtaining the width at the 40% height of the distribution curve claiming better correlation between the experimental values and the actual orientation. The Sisson and Clark technique is applied in this study since it is more widely used and since the purpose in this study is to establish changes in the orientation of highly ordered regions instead of to determine the average microfibril orientation.

Another convenient technique for detecting crystallite orientation changes is that of Meylan (123), also illustrated in Fig. 15. In this technique, tangents are drawn to the circumferential distribution curve. The distance between the intersects of the base line and the two tangents is a measure of the orientation of crystallites. This technique does not give the actual orientation angles, but is a reliable means of establishing the changes in crystallite orientation. This technique is also employed in the present study.

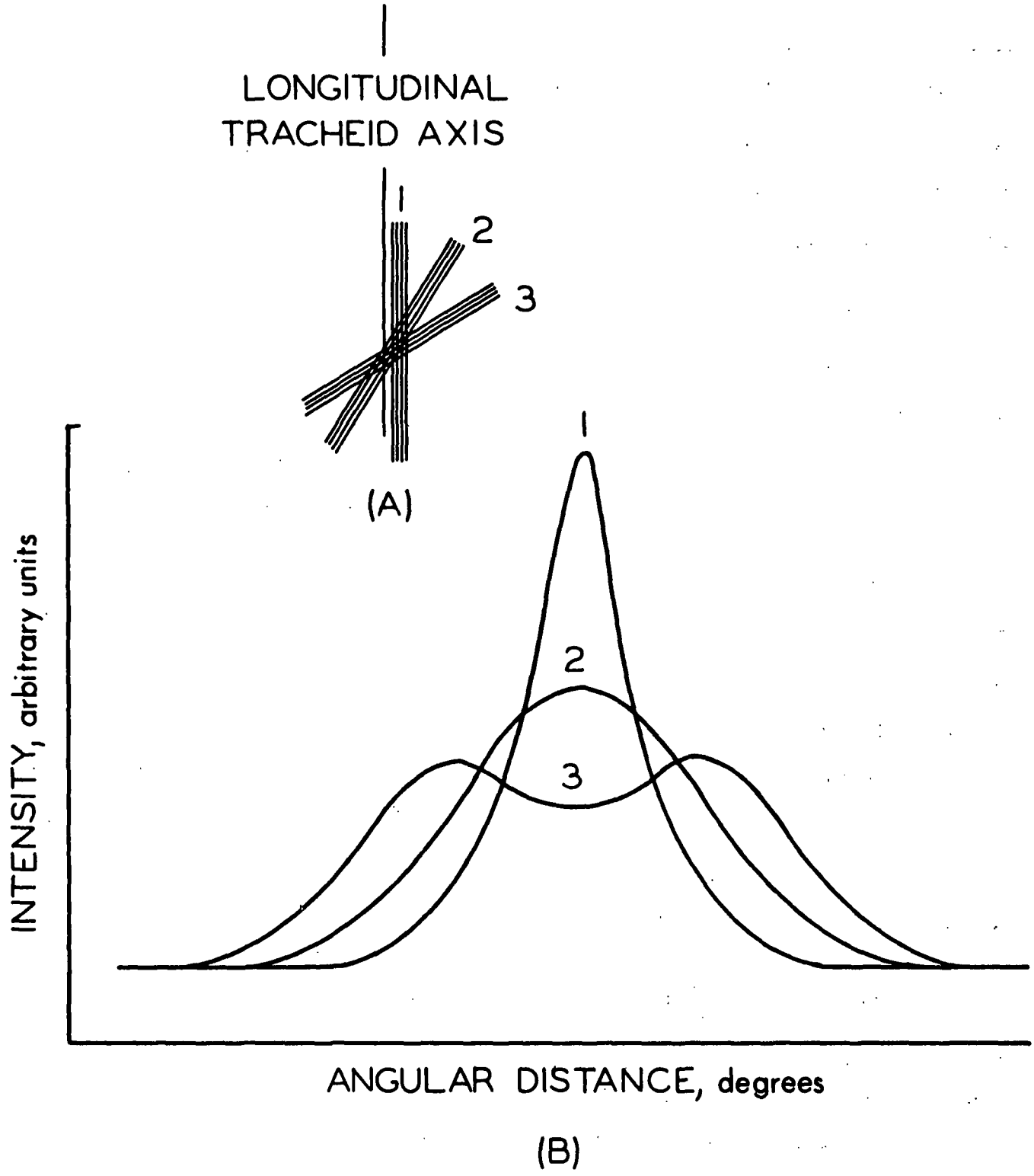

Figure 14. A Schematic Description of the Effect of the Crystallite Orientation (A) on the Resulting Distribution Curve as Seen in the Circumferential Intensity Traces

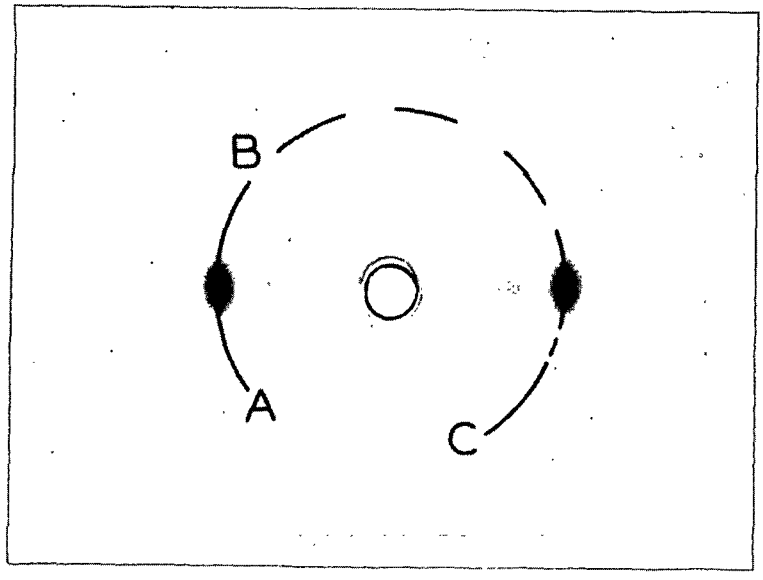

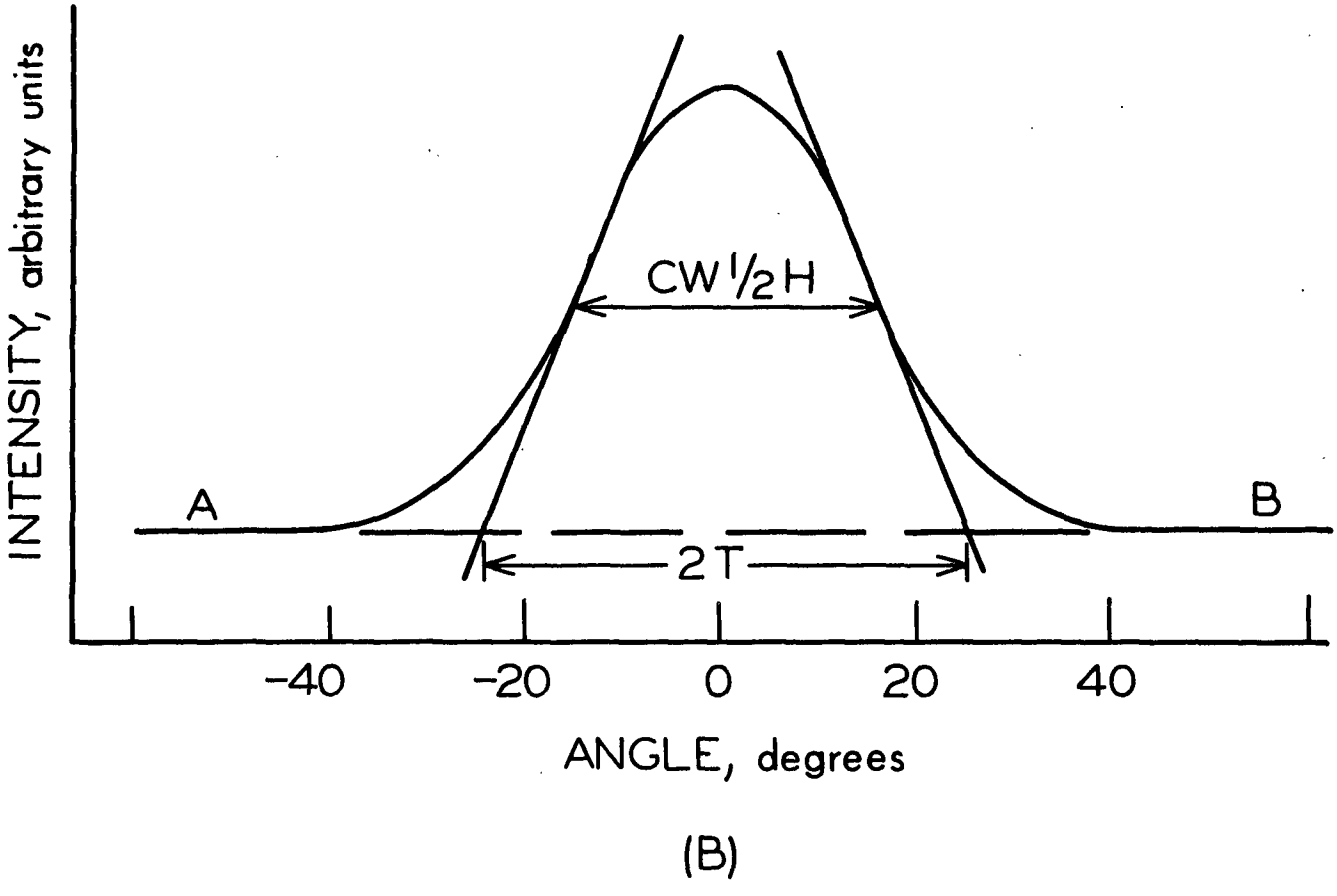

Figure 15. The Laue X-ray Diffraction Diagram of Green Waterlogged Tangential Wood Section (A); Circumferential Intensity Distribution Curve from Which the Crystallite Orientation Parameters are Determined

Degree of Order of Highly Ordered Cellulose

A further advantage of performing the x-ray diffraction analysis on the holowood sections is that the average degree of order of the crystalline region can be determined with less complication than from the conventional powder diagram. The 2θ angle of the 021 plane is 21.0° and that of the 002 plane is 22.6°. In the powder diagram, the scatter is spread about 360°, resulting in a radial overlap of the 021 and 002 plane diffraction distributions. In the fiber diagram the 021 plane diffraction maxima deviates 60° from the equator, while the 002 is on the equator. Hence, the 021 plane does not interfere with the 002 plane diffraction maxima in the cases where the preferred orientation of the crystallites is at a small angle with the fiber axis, which is the case in the present study.

Determining the degree of order of the crystalline region involves the measurement of the radial width of the 002 plane diffraction maxima, as illustrated in Fig. 8 on page 43. According to Scherrer (126), the mean dimension (D) of the crystallites in a powder is related to the pure x-ray diffraction broadening (β) by the equation: $D = K \lambda/\beta \cos \theta$, where K equals 0.9, λ is the wavelength, and β is the radial width as half intensity maxima in radians. For the 002 plane of cellulose I, Bragg angle θ is equal to 11.3°. Others have verified this relationship for various crystalline materials (127). For cellulose, however, this relationship is not rigorously applicable. The lattice distortions, which are not yet well characterized, have a similar broadening effect on the width at half intensity maxima as the small particle size. Furthermore, the width at the half-intensity maxima does not give particle size distribution which may be a variable parameter. For these reasons, the size of the crystallites are not reported in this study although the Scherrer relation is widely applied in cellulose literature.

Since a purpose of the present study is to demonstrate the variable nature of cellulose fine structure in the wet state, changes in the radial width at the half height are interpreted as an increase or a decrease in the degree of order of cellulose in the highly ordered regions. This may involve both changes in the lattice distortion and modification in the crystallite sizes.

Preparation of X-ray Data

The following procedures were used to obtain the x-ray data. The test sections (1.5 mm. by 1.5 mm. by 20 mm.) were cut from the waterlogged wood or pulping liquor-saturated holowood by a hand microtome and a razor blade. The sectioning was performed so that the test section surfaces were parallel to the tracheid tangential and radial walls. This enabled the exposures to be made so that either radial or tangential tracheid walls were perpendicular to the primary beam. The plastic test section holder was designed with a one millimeter diameter hole at the center. The test section was placed in a 1.6-mm. deep, 2-mm. wide, and a 2.5-cm. long slot, also located in the center of the test section holder. Two drops of distilled water or pulping liquor were dropped in the slot to ensure that the sample remains saturated throughout the exposure. The test section holder was covered with aluminum foil with a 1.5-mm. diameter hole cut to coincide with the 1-mm. hole in the test section holder, where the primary x-ray beam entered the test sample.

Care was taken to expose the same area of the test section each time the exposure was made. Approximately 600 tracheids contribute to the resulting diffraction pattern.

The source of x-rays was a Norelco x-ray apparatus with copper Kα radiation generated at 35 kilovolts and 20 milliamperes. A nickel foil filter was used. The exposures were made in the Laue camera designed and built by Jentzen (116) (Appendix IV). The narrow pencil of x-rays was formed in an 8-cm. collimator. The distance from the diffracting test section to the film was about 6 cm. The undiffracted beam was captured by a beam catcher, which was aligned for each exposure.

Kodak Medican No-Screen X-ray film was used throughout the investigation. The exposure time varied from 15 minutes for dry samples to 1.5-2.0 hours for the wet samples. The longer exposure time was necessary for the earlywood sections. Kodak X-ray Developer, Kodak Ektaflo Indicator Stop Bath and Kodak X-ray Fixer were used for the film development.

The film calibration was performed by exposing 2.5 cm. by 5 cm. areas of film for 5 to 90 seconds at a distance of 100 cm. from the x-ray source. The Cu Kα radiation was generated, with the tube operating at 11 kilovolts and 8 milliamperes. The film calibration curve is linear on a semilog scale and is presented in Appendix V. This curve shape agrees with that discussed in Klug and Alexander (127).

The microdensitometer setup used by Jentzen (116) was reassembled for quantitative analyses of the diffraction patterns. The film was centered on a table capable of both linear translation and rotation in the plane of the film at constant speed. An inverted microscope focused the light on the film. The transmitted light was then focused on the photocell by another microscope. A plate with a pinhole was mounted on top of the eyepiece of the second microscope permitting viewing of a 0.5-mm. diameter area of the film at any given

time during scanning. The ratio of radial width at half height of the 002 peak to the diameter of viewing area was about 10.

The radial scan was obtained across the two 002 plane maxima from A to B as shown in Fig. 7 on page 41. The circumferential scan is from A to B to C as shown in Fig. 15 on page 55.

The unexposed but developed area of the film was used as the 100% transmittance reference. The zero transmittance was that of a thin metal plate. Any film exhibiting less than 20% transmittance at the 002 plane diffraction maxima was considered overexposed and discarded. The percent transmittance was converted to intensity by the film calibration curve. The intensity values for radial scans were divided by $\cos^3 2\theta$ to correct for a planar film position (127), and divided by $(1 + \cos^2 2\theta)/2$ to correct for polarization of diffracted x-rays. For circumferential scans corrections are not necessary, since the scans are made at constant Bragg angle. For the calculation of crystallinity index the intensities were expressed on an equal "mass times time" basis.

RESULTS AND DISCUSSION

TRACHEID WALL COMPONENT REMOVAL

The data presented in Table II are the weight losses occurring during standing in reaction liquor, subsequent water washing, and hygrothermal treatment of holowood. The total loss in the ovendry weight of the original wood during this treatment sequence is defined as the apparently solubilized wood components. While the blocks are submerged in reaction liquor for 30 days about one-third of the apparently solubilized components are removed from the block. During 120 days in the reaction liquor only about 50% of the apparently solubilized components are removed. The water washing at room temperature for 50 hours is effective in removing from 31% (for 120 days, 56.8% yield pulp) to 59% (for the 10 day, 80.4% yield sections) of the apparently solubilized wood components. Hygrothermal treatment for 8 hours results in additional removal ranging from 24% for 120-day pulp to 85% for the 2-day, 90.1% yield sections.

The data are too limited to draw any conclusions of whether the hygrothermal treatment of wood has appreciable effects on the pattern of component removal from the tracheid walls during the subsequent delignification.

CHEMICAL COMPOSITION OF HOLOWOOD

The pulps at different degrees of delignification were water washed for 50 hours in distilled water, and hygrothermally treated for eight hours at 95°C. before the determination of the chemical composition. The data in Table III are given as percent on the ovendry basis of wood. The yield drops to about 64% within the 65 days of reaction with only a trace of lignin present in the pulp. Some undefined hemicelluloses, rich in mannan and containing some

TABLE II

WOOD COMPONENT REMOVAL DURING THE SEQUENCE OF REACTION, WATER WASHING, AND HYGROTHERMAL TREATMENT

Elapsed Days of Reaction	Weight (Gain) Loss During the Treatment[a], %: Submersion in Reaction Liquor	50-Hour Water Washing	8-Hour Hygrothermal Treatment	Final Yield, %
From green, waterlogged wood:				
2	(2.7)	1.5	8.4	90.1
5	(2.8)	6.1	11.3	82.6
10	(0.3)	11.6	8.0	80.4
15	3.5	11.9	6.5	78.1
20	0.0	13.3	8.4	78.3
30	7.8	12.5	8.2	71.5
60	10.3	14.0	10.4	65.3
90	19.9	11.7	7.8	60.0
120	19.8	13.3	10.3	56.8
From hygrothermally treated wood:				
2	(1.7)	4.5	6.5	89.0
5	(2.0)	4.9	8.8	86.3
10	(2.1)	7.5	9.8	82.7
15	4.7	9.7	8.2	77.6
20	6.8	7.2	8.9	77.1
30	9.8	9.0	9.2	72.0
40	13.5	8.8	9.3	68.4
50	15.5	8.5	10.0	66.0
60	16.9	11.7	7.4	64.0
90	19.5	12.9	9.1	58.5
106	22.3	12.9	8.0	56.8

[a]Loss in the ovendry weight of blocks into the medium during the indicated lengths of time (into reaction liquor, wash water at 24°C., or hot water at 95°C., respectively). The block surfaces were blotted to remove excess liquor or water before determination of wet weight and oven drying. The ovendry weight includes any solids in the liquor or water in the blocks. For example: % in Column 2 = (ovendry weight of reacted wood and solids in liquor in block)/(ovendry weight of green waterlogged wood).

TABLE III

THE CHEMICAL COMPOSITIONS OF THE HOLOCELLULOSES[a]

Days of Reaction	Anhydrosugars from Holocellulose[b], %					Lignin Content, %[b]		Yield, %[b]
	Glucose	Galactose	Mannose	Xylose	Arabinose	Klason	Acid Soluble	
Delignified from the green wood:								
0	44.2	2.2	13.2	3.3	0.8	28.2	--	100
8	44.7	2.0	12.6	2.9	0.4	7.1	2.71	81.5
14	44.1	1.9	12.2	2.9	0.5	4.5	2.72	78
27	44.0	1.7	11.2	2.7	0.3	2.4	2.13	72
44	41.0	1.5	9.9	2.9	0.5	1.5	2.44	67
65	43.0	0.9	8.7	2.4	0.3	trace	--	64
89	42.2	0.8	8.2	1.9	0.2	--	--	60
110	43.5	1.1	7.8	1.7	0.2	--	--	58.5
120	43.7	0.6	7.4	1.5	0.1	--	--	57
Delignified from the hygrothermally treated wood:								
20	49.1	1.6	11.6	3.1	0.2	1.7	1.99	77
29	49.4	1.4	10.7	2.3	0.2	0.8	--	72
54	46.5	0.9	8.3	1.8	0.2	--	1.27	65
70	41.3	0.5	8.0	2.0	0.2	--	--	60.5
83	41.4	0.5	7.8	1.7	0.2	--	--	58
103	41.3	0.1	7.0	1.7	0.2	--	--	57

[a]The pulps are water washed and posthygrothermally treated before the chemical analysis.

Methods: Anhydrosugars — Tappi 53, no. 2:257-60(1970).
Klason lignin — The Institute of Paper Chemistry Methods 13 and 428.
Acid-soluble lignin — The Institute of Paper Chemistry Method 13.

[b]The values are expressed as percent based on the unextracted wood o.d. weight.

galactan, xylan, and arabinan, are also removed. The third and fourth months in the reaction liquor results in a further extraction of hemicelluloses.

The observed decrease in the hemicelluloses content during oxidative delignification is in agreement with earlier observations made by Thompson and Kaustinen (128), who found the following relative carbohydrate composition in hydrolyzates of chlorite liquor of mature jack pine: galactose (36.0), glucose (6.6), mannose (19.0), arabinose (8.8), xylose (8.5), uronic acid (17.8), and methoxyl (3.6). Other investigators have also observed a drop in the hemicelluloses content of holocelluloses during oxidative delignification (129-131).

CHANGES IN THE STRUCTURE AND DIMENSIONS OF BLOCKS DURING DELIGNIFICATION

DIMENSIONAL BEHAVIOR IN REACTION LIQUOR

During the penetration of the reaction liquor into the waterlogged unextracted sapwood block (5 cm. by 1 cm. by 1 cm.), the block expands about 1.6% in the tangential direction, shrinks about 0.5% in the radial direction, and is essentially unchanged in the longitudinal direction. The tangential expansion is shown versus time in Fig. 16. The expansion is greatest during the first 60 hours and subsequently levels off.

The dimensional responses are in the same direction and have the same magnitudes as the changes observed during the first hygrothermal treatment of green wood (Appendix I). A good explanation for the dimensional changes is lacking, although in the latter case they are generally attributed to the "growth stress" release (94-96).

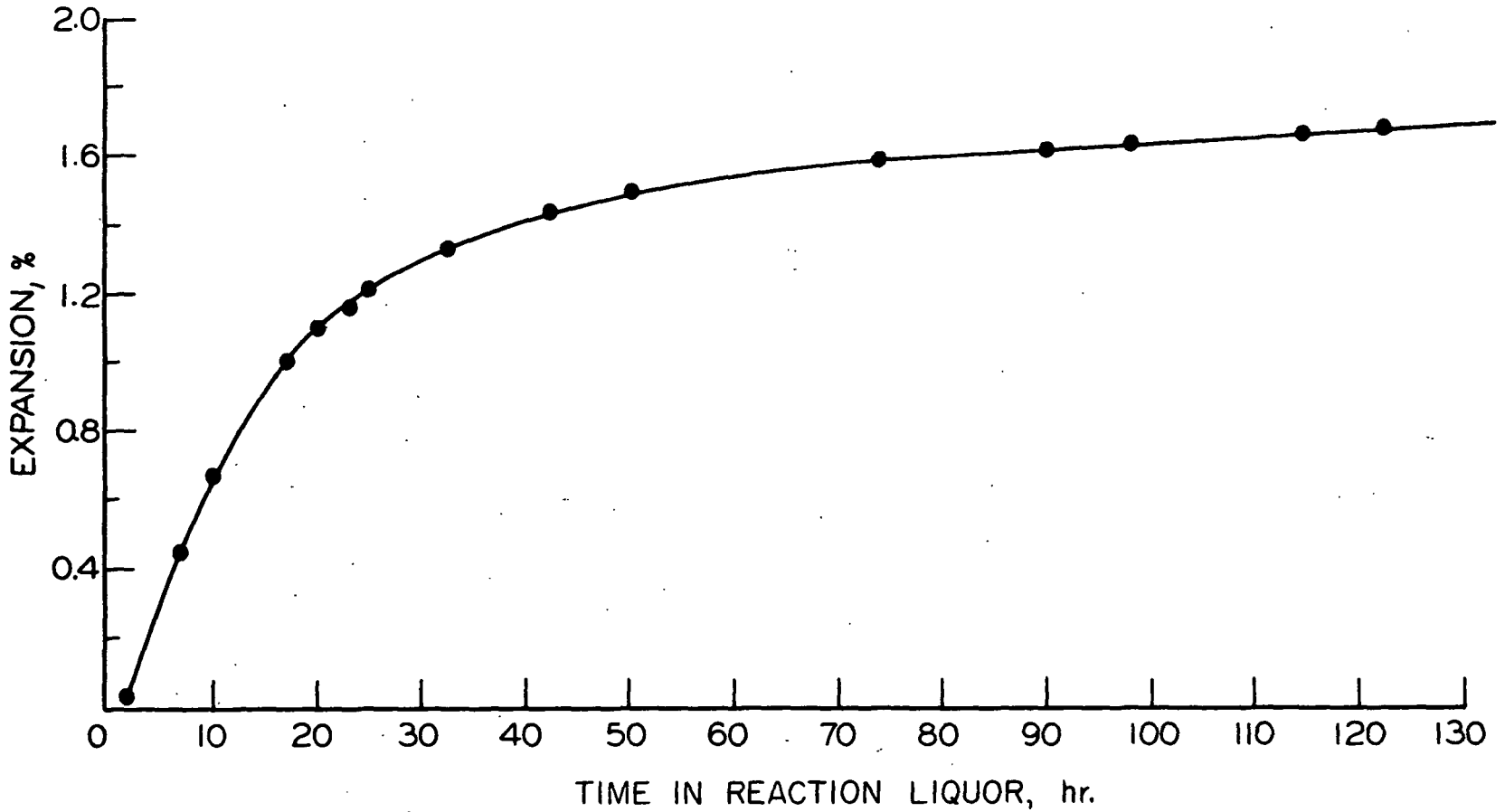

Figure 16. Tangential Expansion of Green Waterlogged Sapwood upon Submersion into the Pulping Liquor at Room Temperature

During the months in the reaction liquor, the block expands slowly in the tangential direction (Table IV). In eight months, the tangential expansion reaches about 5.5%, but the radial dimension is still about 0.6% less than the original water-swollen dimension. The total volumetric expansion of the holowood in reaction liquor is only about 5%.

TABLE IV

CHANGES IN THE DIMENSIONS OF THE SECTIONS[a] IN THE REACTION LIQUOR

Elapsed Days in the Reaction Liquor	Dimension Change[b] of the Sections, %		
	Longitundinal	Radial	Tangential
3	+0.17[c]	-0.47	+1.60
8	-0.08	-0.77	+1.59
11	+0.11	-0.51	+1.54
18	+0.11	-0.83	+1.51
32	+0.28	-0.57	+2.15
48	-0.12	-1.08	+2.03
56	+0.13	-0.81	+2.10
67	+0.24	-0.47	+2.54
108	+0.26	-0.40	+3.82
225	+0.11	-0.57	+5.72
265	+0.33	-0.61	+5.32

[a] Initial thickness is 2 mm., and length and width are 2 cm.

[b] Determined by an x-y digital comparator developed by K.W. Hardacker of The Institute of Paper Chemistry staff in 1967 (unpublished work).

The centrifugally determined swollen specific volumes of unwashed pulps (Table V) further support the concept of tracheid wall dimensional stability in the reaction liquor. The swollen specific volume of unwashed pulp in the liquor appears to increase about 17% during reaction. However, this increase does not directly reflect the volumetric behavior of an individual tracheid. As the delignification proceeds, the swollen specific volume of pulp increases, since the number of tracheids in a gram of pulp increases. In order to follow volume changes of individual tracheids, it is necessary to determine the volume of water in a fixed number of tracheids, for example, that produced from a gram of wood. In the present study this value will be called the tracheid wall water-holding capacity, which is obtained by multiplying the centrifugal water retention value by the yield, and has the units of cubic centimeters of water per gram of wood. As can be seen in the fourth column of Table V, the tracheid wall water-holding capacity does not change appreciably during the range of delignification investigated. Also, the specific volume of the tracheid decreases, since the specific volume of the lignin which is being removed is 0.715 cc./g. and that of the remaining cellulosic substances is 0.628 cc./g. (132, 133). Hence, a correction must be made for the volume of removed materials. As seen in the last column of Table V, the tracheid wall does not swell appreciably in the reaction liquor.

The dimensional stability of the holowood tracheid walls in the reaction liquor has some bearing on the recent studies of the mechanism of delignification by such oxidizing agents as sodium chlorite (70°C.) (134) and peracetic acid (135). According to these workers, the tracheid wall pore sizes have an effective restricting dimension which controls the diameter of the molecules that can diffuse out of the tracheid walls. Hence, the diffusion of large but solubilized lignin molecules out of the tracheid walls is restricted by the small size of the tracheid wall pores. Since the tracheid walls do not swell

TABLE V

TRACHEID WALL LIQUOR-HOLDING CAPACITY
IN THE REACTION LIQUOR

Elapsed Days of Reaction	Swollen Specific Volume of Unwashed Pulp,[a] cc./g.	Centrifugal Liquor Retention Value,[b] cc./g.	Averaged Interpolated Yield of Unwashed Pulp,[c] %	Tracheid Wall Liquor-Holding Capacity,[d] cc./g. wood	Volume of the Removed Components,[e] cc./g. wood	Corrected Volume of Tracheid Wall Pores,[f] cc./g. wood
44	2.25	1.63	85.8	1.40	0.10	1.30
54	2.37	1.75	85.7	1.50	0.10	1.40
80	2.23	1.61	83.8	1.35	0.12	1.23
89	2.50	1.88	79.8	1.50	0.14	1.36
110	2.52	1.90	77.9	1.48	0.16	1.32
120	2.65	2.03	73.9	1.50	0.19	1.31

[a] The swollen specific volume is expressed as the volume occupied by centrifuged unwashed pulp (see page 36) per gram of ovendry unwashed pulp and equals CWR + 0.62 cc./g.

[b] The centrifugal liquor retention value is the volume of liquor held by a centrifuged pad of unwashed pulp per one gram of ovendry unwashed pulp after centrifugation at 1000 g for 30 minutes.

[c] The yield was interpolated from data in Table II, Column 2, page 61.

[d] Liquor-holding capacity is the volume of liquor held by a centrifuged pad of unwashed pulp produced from one gram of wood and was calculated by multiplying the CWR value by the yield of unwashed pulp.

[e] It is assumed that the specific volume of the removed materials is that of the lignin and equals 0.715 cc./g. (132, 133).

[f] The corrected volume of the tracheid wall pores is that volume of pores which was not created by physical removal of wall components, and is obtained by subtracting the volume of the removed components from the tracheid wall liquor-holding capacity. This value is not absolute since some liquor is held in the capillaries between tracheids and since CWR value depends on conditions of centrifugation.

appreciably during reaction, the tracheid wall pores enlarge only slightly more than the volume of previously removed components. As a result, the diffusion of solubilized lignin out of the tracheid walls is restricted.

SWELLING OF HOLOWOOD DURING WATER WASHING

Tarkow and Feist (73) found that the volume of tracheid walls in 20-mil-thick cross sections of sitka spruce holowood, as determined by the solute exclusion technique, more than doubles during the sodium chlorite delignification. The swelling of the holowood in the reaction liquor observed in the present study is only about 5%. However, when a block is removed from the reaction liquor and water washed, it expands in all the directions.

The tangential expansion data are presented in Fig. 17. The extent of tangential expansion is plotted against the time of washing. Each of the curves presented is the dimensional behavior of a given block immediately after removal from the reaction liquor and on submersion in distilled water. The number on the curve indicates the number of days of reaction before testing. The tangential expansion during 50-hour water washing of block delignified from the green condition for 65 days is only about 3%. At this stage of reaction, only a trace of lignin remains. The subsequent reaction results in up to 20% tangential swelling during 50-hour water washing.

The radial expansion of a block with only a trace of lignin present is essentially the same as that of a block with 7% lignin (Fig. 18). These blocks expand initially in the radial direction about 0.2% but begin to shrink at the latter stages of washing. The holowood blocks that have been in reaction liquor twice as long as is necessary to remove all but a trace of lignin, expand slowly in the radial direction during the initial phase of water washing. After

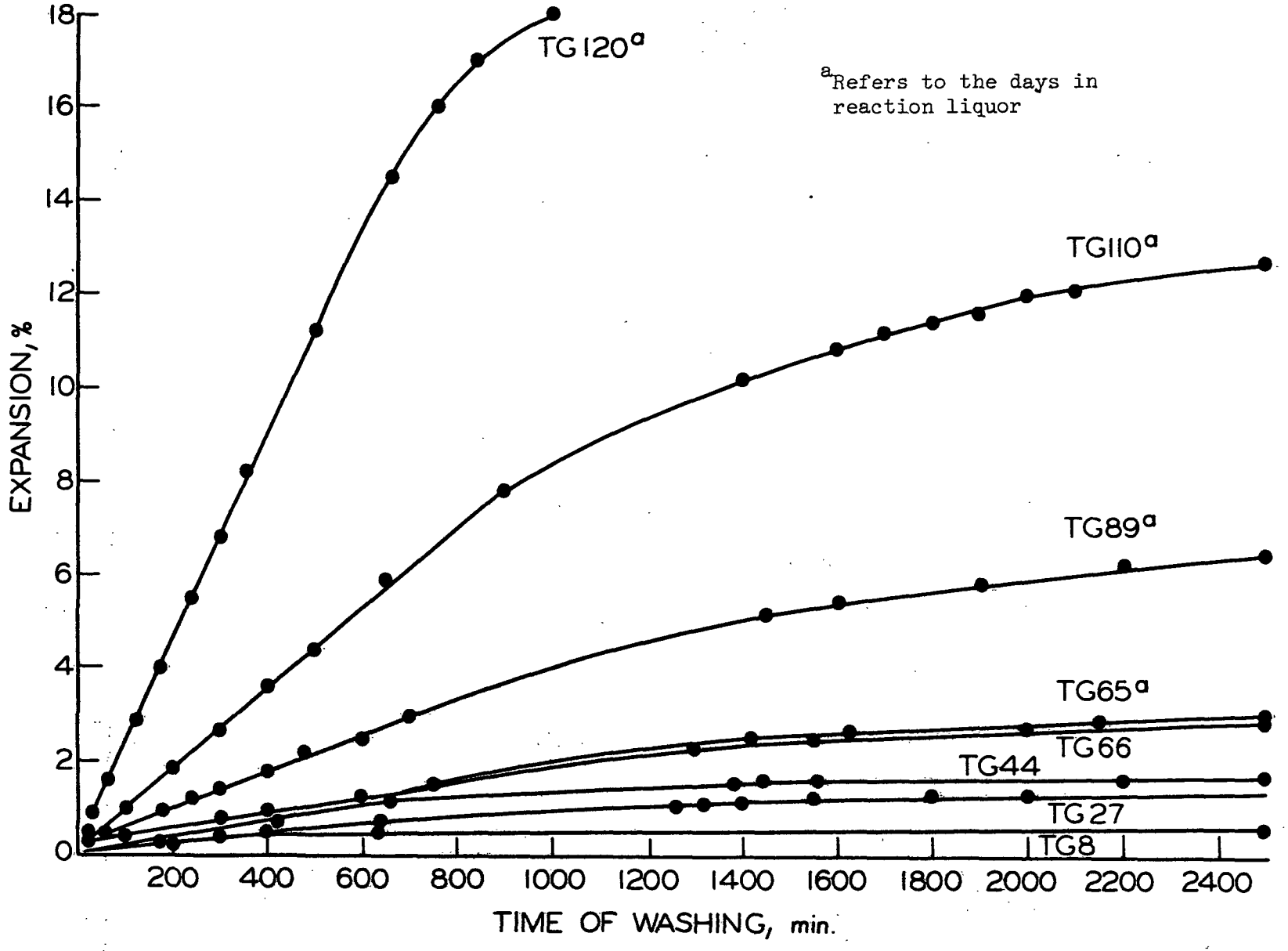

Figure 17. The Tangential Expansion on Washing of Holowood Blocks Delignified from the Green Condition

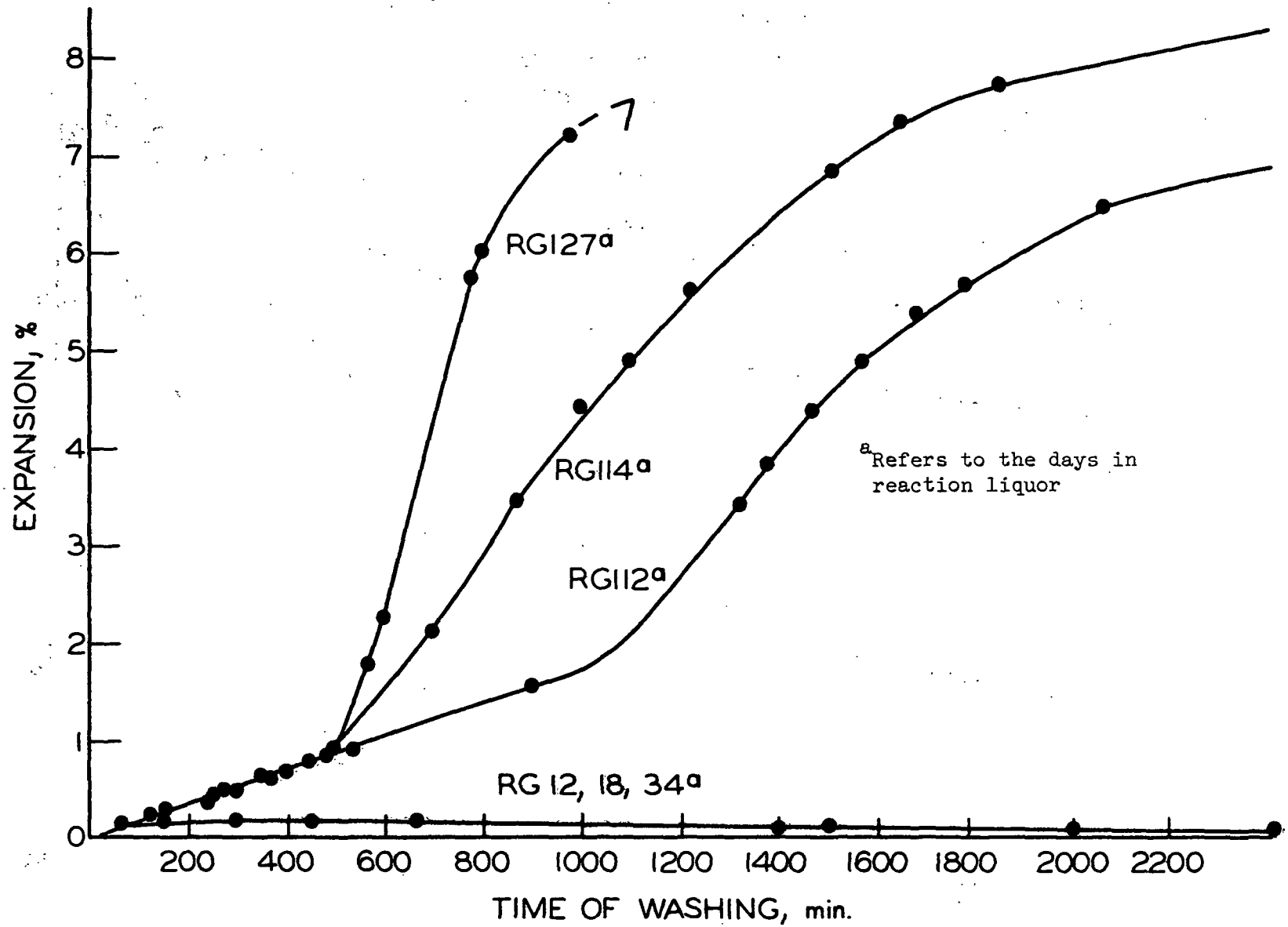

Figure 18. The Radial Expansion on Washing of Holowood Blocks Delignified from the Green Condition

a few hours of washing the rate of expansion accelerates and approaches that of the tangential expansion.

The longitudinal expansion of the holowood blocks on washing is less than 1% beyond the green dimension. The longitudinal expansion curves are presented in Fig. 19.

Considering the tangential expansion simultaneously with the radial expansion, the total volumetric expansion continues at constant rate for a considerable length of time. This is illustrated in Fig. 20. Apparently, the driving force causing swelling increases during water washing while the resistance to swelling increases as the tracheid walls deform. After about 8 hours of water washing the plasticity of both tangential and radial walls is about equal resulting in the same amount of expansion in both walls.

The swelling behavior of the tracheid walls is confirmed by the swollen specific volume determined by the centrifugal water retention technique. These values are converted to tracheid wall water-holding capacity as described earlier (page 66) and are presented in Table VI. The water-holding capacity of the water-washed tracheid walls increases up to 66% with the largest increase for pulp that has been in the liquor twice as long as is necessary to solubilize all but a trace of lignin.

Some of the additional water held in the tracheid walls of the delignified fibers is held in the spaces previously occupied by lignin, and therefore does not contribute to the swelling of the tracheid walls. After correcting for the volume of this water, the remaining increase in the tracheid wall water-holding capacity indicates swelling of the tracheid walls (Table VII).

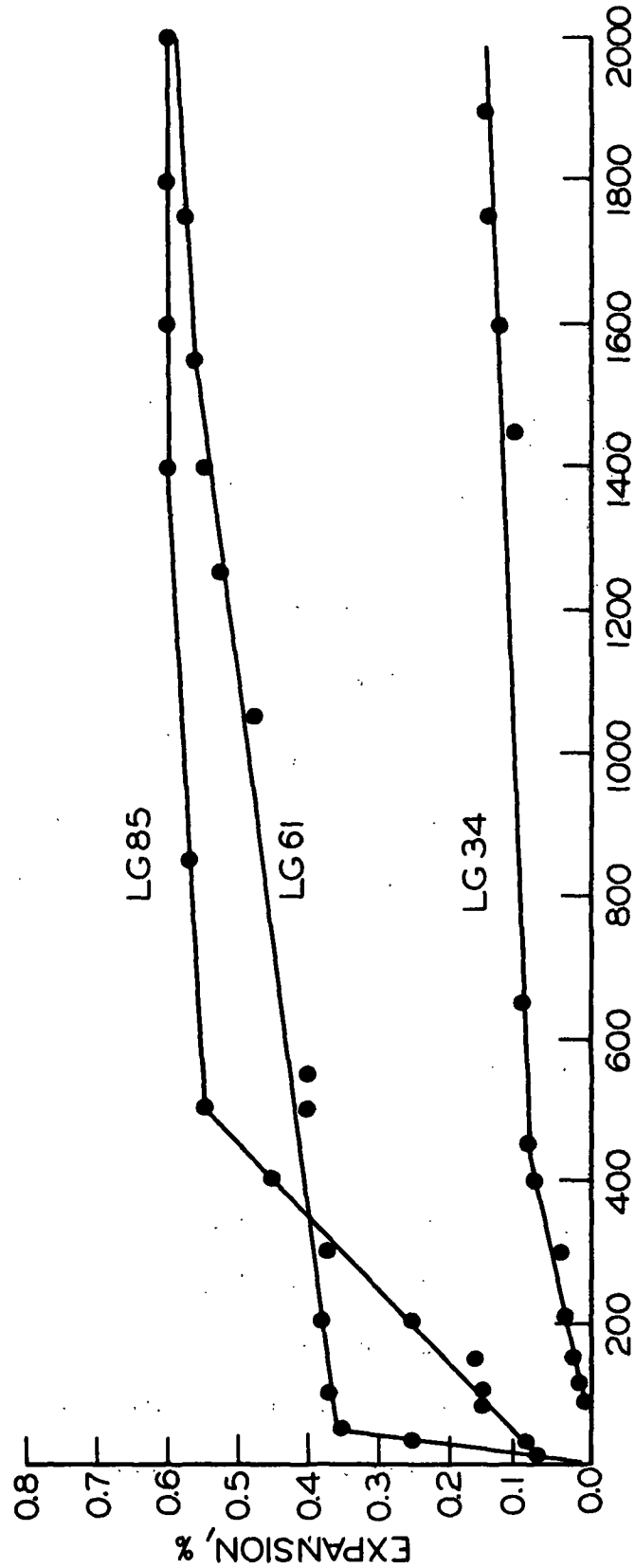

Figure 19. The Longitudinal Expansion of Longitudinal Holowood Blocks on Washing After Delignification in the Green Condition

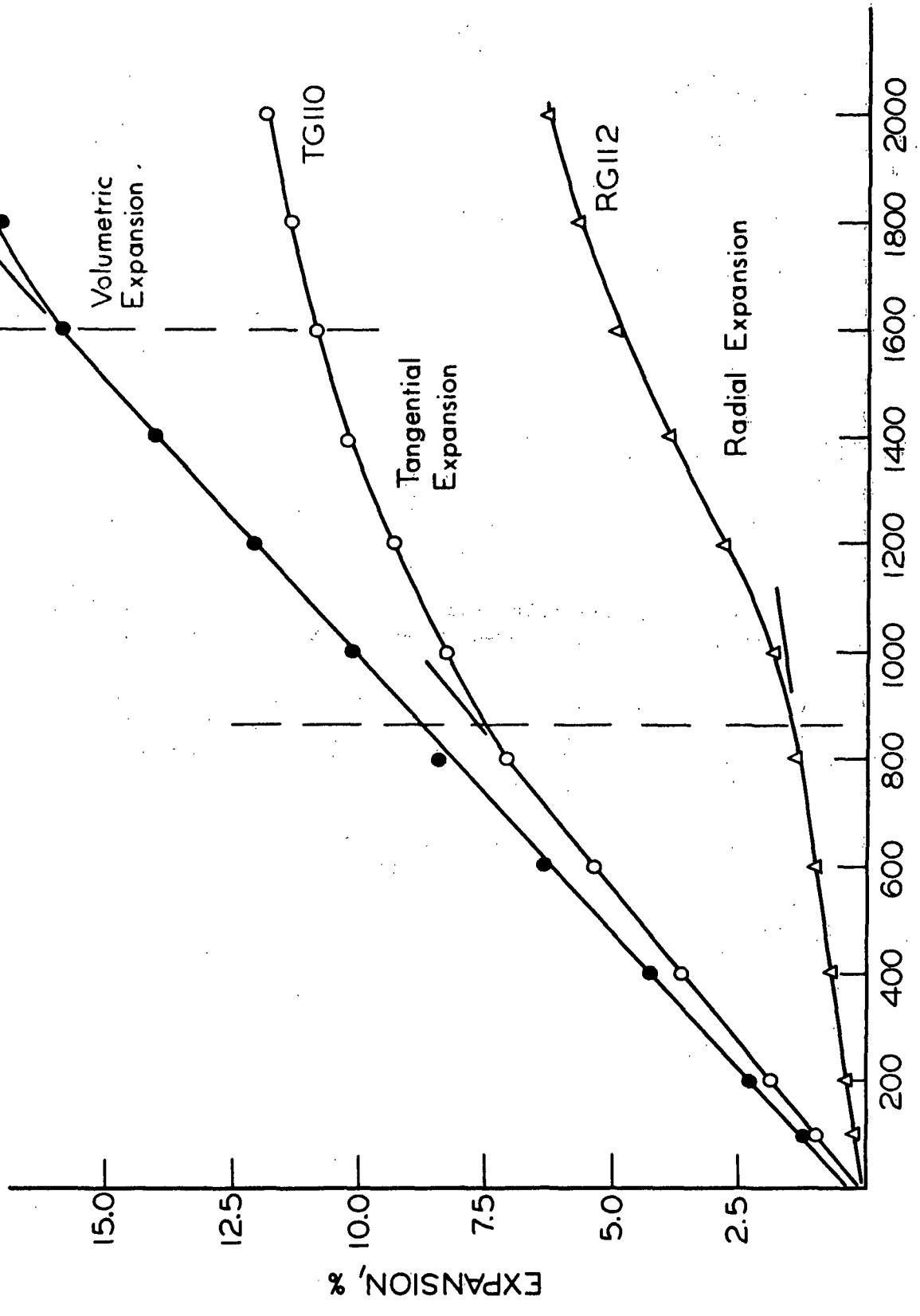

Figure 20. The Percent Volumetric Expansion of the Holowood Block on Washing After Delignification from the Green Condition

TABLE VI

WATER-HOLDING CAPACITY OF PULP
AFTER WATER WASHING

Elapsed Days in Reaction Liquor	Swollen Specific Volume,[a] cc./g.		Tracheid Wall Liquor or Water-Holding Capacity,[b] cc./g. wood		Increase in the Water-Holding Capacity During Washing,[c] %
	In Reaction Liquor	After Water Wash	In Reaction Liquor	After Water Wash	
G 44	2.25	2.65	1.40	1.55	10.7
G 54	2.37	3.19	1.50	1.90	26.7
G 80	2.23	3.33	1.35	1.90	40.7
G 89	2.50	3.74	1.50	2.12	41.3
G 110	2.52	4.36	1.48	2.39	61.5
G 116	2.42	4.24	1.37	2.28	66.4
G 120	2.65	4.61	1.50	2.41	60.7

[a] Swollen specific volume equals CWR value (at 1000 g. for 30 min.) plus 0.62 cc./g., and is expressed as cc./g. of ovendry pulp in unwashed or washed condition.

[b] Tracheid wall water-holding capacity is obtained by multiplying CWR value by yield of unwashed or water washed pulps, respectively. The yields are interpolated from Columns 2 and 2 + 3, respectively from Table II, page 61. For washed pulps: G 44 to G 120, the yields are 76.4, 74.2, 69.6, 68.0, 63.8, 63.0, 60.5.

[c] Since the CWR value depends on conditions of centrifugation, these values are not unique and are used only to indicate a trend.

TABLE VII

NET TRACHEID WALL SWELLING
DURING WATER WASHING

Sample	Corrected Volume of the Tracheid Wall Pores in Liquor,[a] cc./g. wood	Water Washed Pulp		Increase in the Volume of the Tracheid Wall Pores Due to Swelling,[d] %
		Water-Holding Capacity,[b] cc./g. wood	Volume of Removed Components,[c] cc./g. wood	
G 44	1.30	1.55	0.17	7.0
G 54	1.40	1.90	0.19	23.6
G 80	1.23	1.90	0.21	37.4
G 89	1.36	2.12	0.23	39.7
G 110	1.36	2.39	0.26	58.8
G 116	1.21	2.28	0.26	66.3
G 120	1.31	2.41	0.28	62.6

[a] Last column from Table V, page 67.

[b] Water-holding capacity of the washed pulp is the volume of water held by a centrifuged pulp pad expressed as cc./g. wood and was calculated by multiplying CWR value by the yield of washed pulp. Yields were interpolated from data in Table II, page 61.

[c] All the removed components are assumed to have the same specific volume as lignin: 0.715 cc./g.

[d] Column 5 = [(Col. 3 - Col. 4 - Col. 2)/Col. 2] x 100. The water held in the pores previously occupied by removed components is not considered to contribute to the swelling of the tracheid walls.

The amount of tracheid wall swelling during water washing is small in the pulps delignified for less than two months. However, the subsequent standing in liquor results in over 40% increase in the swelling of the tracheid walls as determined in the water-washed condition by the centrifugal water-retention technique. These data are in good agreement with the dimensional behavior of holowood blocks during water washing. In both cases, the large increase in swelling occurs after reaction for more than two months. During this time period the yield drops from about 64% to about 57%, mainly due to decrease in the hemicelluloses content.

Since the tracheid walls swell while the hemicellulose content decreases, the swelling cannot be attributed to the amount of hemicelluloses. However, it is likely that the nature of the remaining hemicelluloses is modified, resulting in an increased tendency of the tracheid walls to swell. Also, the removal of the three-dimensional lignin network is necessary but not sufficient for the swelling to occur. However, the essential solubilization of lignin and the presence of high concentration of hemicelluloses do not cause swelling of the holotracheid walls, since in this case swelling would take place in the reaction liquor. The significant experimental observation made on the holowood blocks and confirmed on pulps is that swelling of the tracheid walls does not commence until water washing.

The solute exclusion technique is carried out on the water-washed samples and not directly in the liquor (52, 86, 134). Since the water-washing step is critical in determining the extent of tracheid wall swelling, the solute exclusion technique, as applied in the literature, does not measure the development of pore sizes during pulping but also includes the response of delignified tracheid walls to water washing.

The effect of preheating wood on the swelling behavior of the holowood blocks during water washing is very dramatic. In Fig. 21, Curve G is for the blocks delignified from the green condition. The blocks delignified after preheating (Curve PH) exhibit a considerably greater swelling tendency. Each data point represents the extent of tangential expansion of the given block during 50 hours of water washing. (For the Curve PH, individual expansion curves are presented in Appendix VI.) The onset of the drastic expansion takes place after about 50 days of reaction for the blocks delignified from hygrothermally treated wood and about 25 days later for the blocks delignified from the green condition.

Comparison of Curves G and PH with the yield Curve Y in Fig. 21 shows that major changes in the chemical composition occur during the first two months of reaction, while major changes in the tracheid wall swelling during water washing occur after reaction has proceeded for more than two months.

Even though the amount of tracheid wall components removed during reaction and water washing (Table II, page 61) is not markedly changed by preheating of wood, the holowood block expansion on water washing is increased drastically. The absence of difference in amount of components removed, even though the tracheid wall pore volume increases more for preheated reacted wood, seems to indicate that some mechanism other than the physical entrapment of solubilized molecules is also involved in the removal of solubilized molecules out of the tracheid walls.

SWELLING OF HOLOWOOD DURING HYGROTHERMAL TREATMENT

During the latter stages of water washing of holowood blocks, the rate of swelling decreases and the block dimensions appear to reach an equilibrium

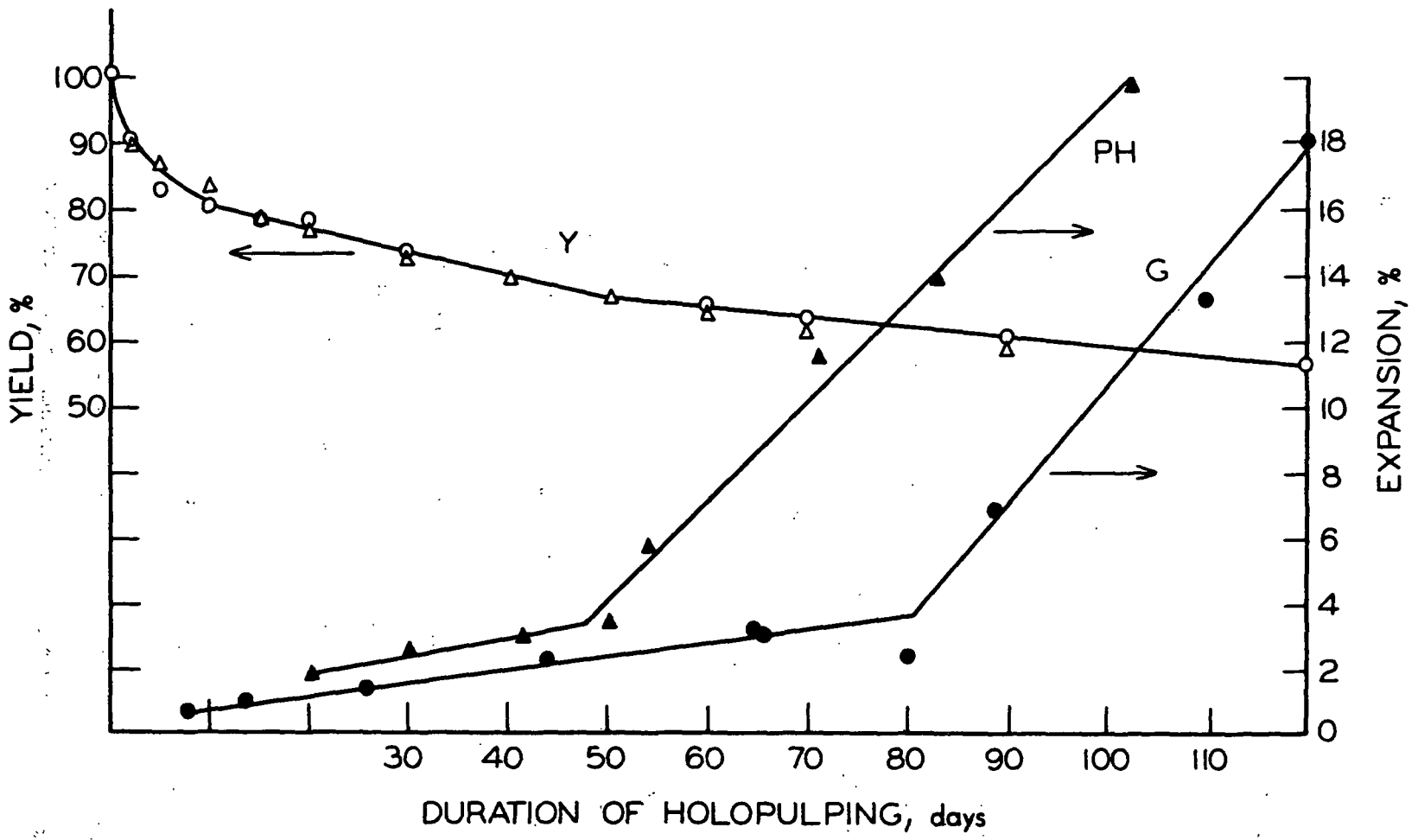

Figure 21. The Tangential Expansion of Holowood Blocks During Water Washing After Reaction for the Indicated Number of Days and Yield, (Y). PH Denotes Blocks Reacted from the Preheated Condition, and G Denotes Blocks Reacted from the Green Condition

(Fig. 17). However, subsequent hygrothermal treatment results in a considerable additional expansion as illustrated in Fig. 22 and 23. The holowood block reacted for 110 days from the green condition expands 15.5% in the tangential direction during the hygrothermal treatment. The total tangential expansion, beyond the water-swollen dimension of the green wood, is 29.4%. This figure takes into account the 0.75% expansion occurring during cooling back to room temperature.

The hygrothermal treatment of the wood blocks before delignification also has an accelerating effect on the rate of swelling during the hygrothermal treatment of the holowood. The rate and the amount of expansion during hygrothermal treatment increases with increasing time of residence in reaction liquor for holowood delignified from green wood (Fig. 22) and for hygrothermally treated wood delignified to about 70% yield. At lower yields the rate of expansion continues to increase, but the final magnitude decreases (Fig. 23). Apparently, the maximum tangential expansion of the holowood blocks during washing and hygrothermal treatment is about 30% before the tracheid-to-tracheid bonding is sufficiently destroyed for the block to lose its coherence.

The tracheid wall water-holding capacity decreases during the hygrothermal treatment of pulps (Table VIII). The decrease is greatest for pulps that have been in the reaction liquor the longest time.

This decrease in the tracheid wall swelling implies a decrease in the tracheid wall average pore size. However, about 8.7% (ovendry weight of wood) of the wood components are removed during the hygrothermal treatment of holowood (Table II, page 61). This is equal to 24% of removed components for holowood reacted for 120 days and 85% for holowood reacted for two days. These data

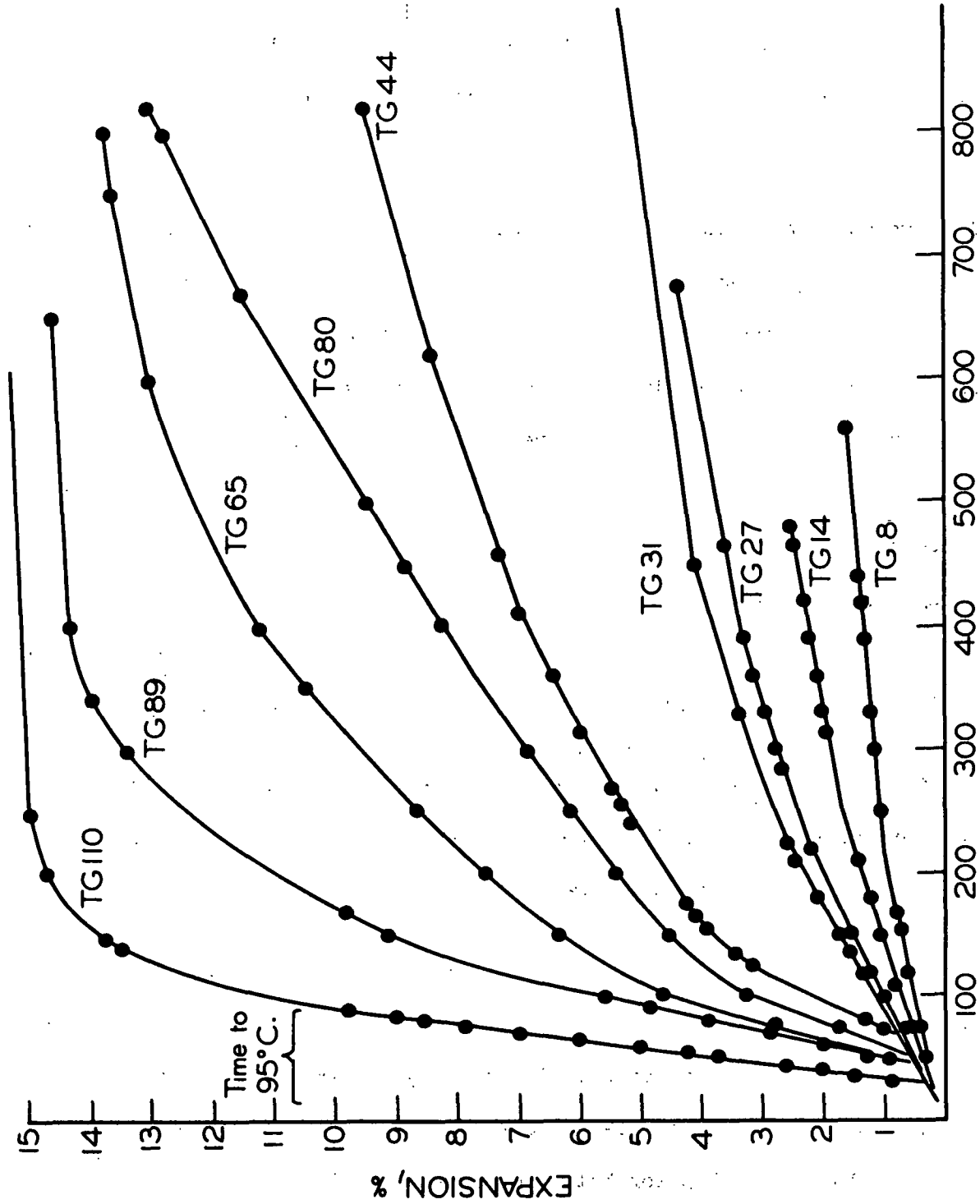

Figure 22. The Percent Tangential Expansion of Holowood Blocks on Heating After Delignification from the Green Condition

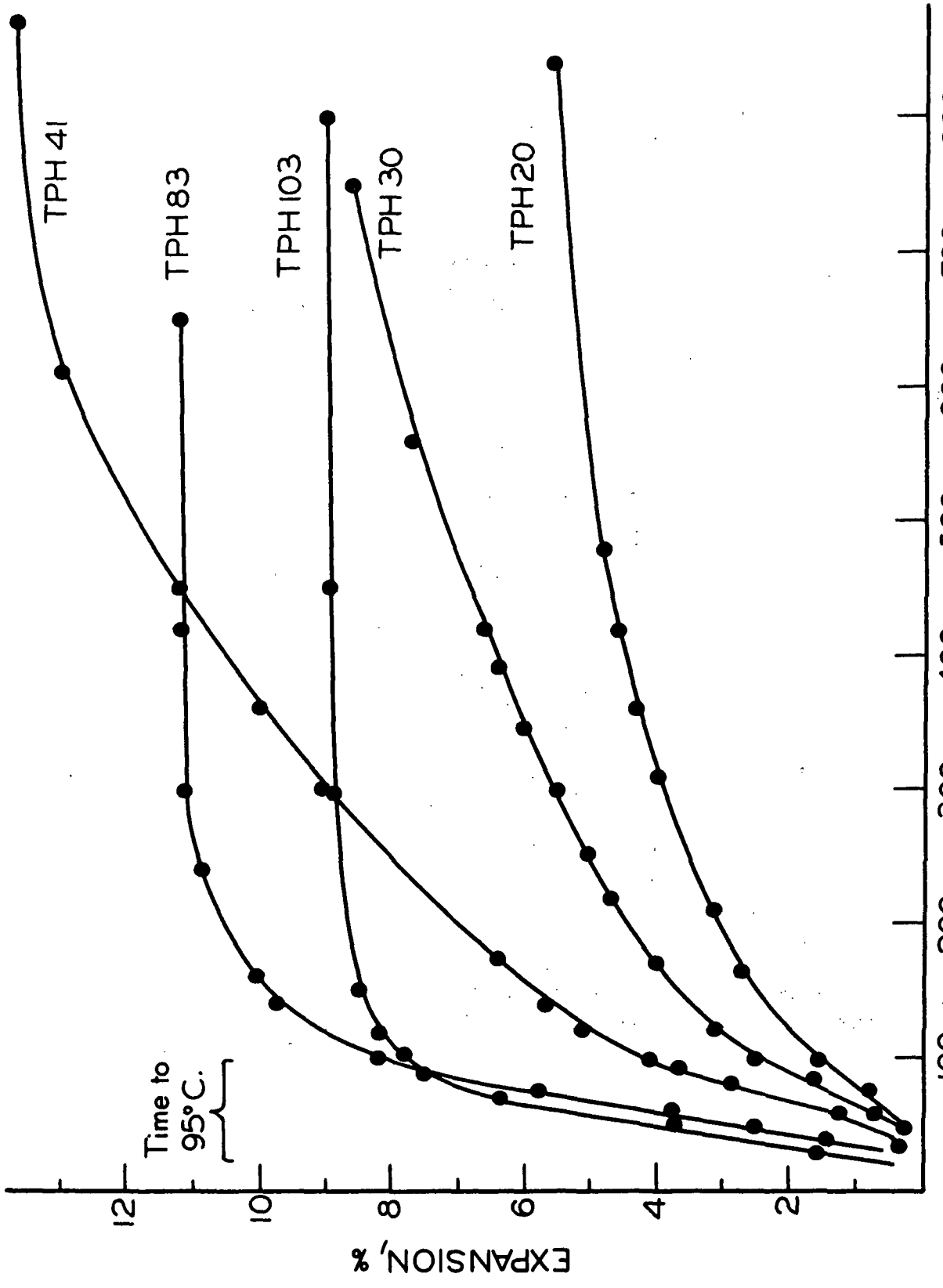

Figure 23. The Percent Tangential Expansion of Holowood Blocks on Hygrothermal Treatment After Delignification from the Preheated Condition and Subsequent Water Washing

suggest that besides the physical entrapment concept (134, 135) some other factors may be involved in resisting the removal of solubilized materials out of the tracheid walls.

TABLE VIII

SWOLLEN SPECIFIC VOLUME AND THE WATER-HOLDING CAPACITY OF HYGROTHERMALLY TREATED PULPS

Sample	Swollen Specific Volume, cc./g. pulp		Tracheid Wall Water-Holding Capacity,[a] cc./g. wood		Decrease in Tracheid Wall Swelling During Hygrothermal Treatment,[b] %
	After Water Washing	After Hygrothermal Treatment	After Water Washing	After Hygrothermal Treatment	
G 29	2.93	2.97	1.87	1.69	12.8
G 44	2.65	3.01	1.55	1.60	1.3
G 54	3.19	3.19	1.90	1.67	10.0
G 66	3.49	3.76	2.15	2.04	8.4
G 80	3.33	3.32	1.90	1.70	13.1
G 89	3.74	3.56	2.12	1.82	16.0
G 110	4.36	3.74	2.39	1.84	24.7
G 116	4.24	4.32	2.28	1.76	24.1
G 127	4.62	4.00	2.48	1.96	22.2

[a] Water-holding capacity of washed, and washed then hygrothermally treated pulps is the volume of water held by a centrifuged pulp pad expressed as cc./g. wood and was calculated by multiplying CWR value by the yield of pulp in washed, and in washed then hygrothermally treated condition, respectively. The yields were interpolated from data in Table II, page 61.

[b] Column 6 = [(Column 4 - Column 5 + 0.715 cc./g. x weight of components removed during hygrothermal treatment)/Column 4] x 100; (weight of removed components is interpolated from the data in Column 4 of Table II, page 61). The water held in the spaces previously occupied by the tracheid wall components is removed during hygrothermal treatment of washed pulp.

CHANGES IN THE CELLULOSE FINE STRUCTURE AS DETERMINED IN THE WET STATE DURING THE CONVERSION OF WOOD TO HOLOWOOD

The holowood block expansion and the decrease in the tracheid wall water-holding capacity result in a dilemma. The expansion of the holowood block could take place by an expansion of the middle lamellae without a change in the tracheid wall volume, or by an increase in the tracheid wall thickness outward. The decrease in the tracheid wall water-holding capacity, however, indicates a decrease in the tracheid wall volume.

According to Stone and Scallan (52), the amount of inaccessible water increases more than the volume of tracheid wall components removed during pulping, and the tracheid walls swell. Their model (page 24) suggests that wall swelling takes place in the amorphous mantle surrounding the highly ordered regions of cellulose, forcing them further apart.

The decrease in the swollen specific volume of pulp during hygrothermal treatment, while the block dimensions continue to expand, however, suggests that the density of tracheid walls increases. This could take place by stretching of the lamellae resulting in a decrease in the void volume within the lamellae.

The concepts of amorphous mantle swelling and the stretching of the lamellae can be differentiated by performing the x-ray diffraction analysis on the wet holowood sections. If the crystallinity index and the degree of order of the highly ordered regions increase, the stretching of the lamella is confirmed. On the other hand, if these parameters are unaffected, or if they decrease during water washing and the hygrothermal treatment of holowood, the swelling of the amorphous mantle takes place.

CELLULOSE FINE STRUCTURE IN THE GREEN WOOD TRACHEIDS

The results of the x-ray diffraction analyses on green wood sections are presented in Table IX. The hygrothermal treatment of green wood, which does not cause a significant removal of tracheid wall components, results in a slight increase in the crystallinity index of specimens still in the wet state. This is interpreted to mean an increase in the amount of highly ordered cellulose, which is arbitrarily defined as that fraction of cellulose which contributes to the scatter of x-rays by 002 planes.

The accompanying decrease in the radial width at half height is an indication of an increase in the degree of order of the highly ordered region of cellulose. Several factors, such as an increase in the crystallite size, relaxation of stresses in the crystalline region, and a decrease in the other crystallite lattice defects, contribute to the radial narrowing of the width at half height of the 002 crystallite plane maxima.

The structure of cellulose in the green wood tracheids can be altered by such a process as hygrothermal treatment. Apparently, the observed increase in the degree of order of cellulose is a continuation of crystallization occurring during maturation of the tracheid as described by Berkley and Kerr (64) and Preston (65, 68).

The locations of the exposed populations of tracheids (about 600 tracheids per exposed volume) are illustrated in Fig. 24. The same locations were viewed before and after hygrothermal treatment.

TABLE IX

THE X-RAY CRYSTALLINITY OF GREEN WOOD AS AFFECTED BY THE HYGROTHERMAL TREATMENT

Sample	Number of Exposures	Average Crystallinity Index		Average Radial Width at the Half Height	
		Green Wood	Heated Wood	Green Wood, degrees	Heated Wood, degrees
Tangential tracheid walls perpendicular to the x-ray beam					
Earlywood I	4	60.91	62.17	12.88	12.70
Mean change[a]		+1.22		-0.18	
Standard error[b]		1.10		0.19	
Latewood I	4	66.66	67.05	13.11	12.81
Mean change		+0.40		-0.30	
Standard error		1.03		0.17	
Whole growth ring	8	56.67	57.16	13.10	12.32
Mean change		+0.49		-0.78	
Standard error		0.52		-0.07	
Radial tracheid walls perpendicular to the x-ray beam					
Latewood I	4	64.44	65.74	13.46	12.90
Mean change		+1.30		-0.55	
Standard error		0.82		0.26	
Latewood II	4	68.42	69.73	12.76	12.35
Mean change		+1.31		-0.40	
Standard error		1.40		0.12	
Average:					
Mean change		+0.87		-0.50	
Standard error		0.40		0.07	
95% Confidence limits		±0.83		±0.15	

[a] Mean change is the average of the differences between measurements made on same populations of tracheids in a wood section at different treatment levels.

[b] Standard error is that of the mean change.

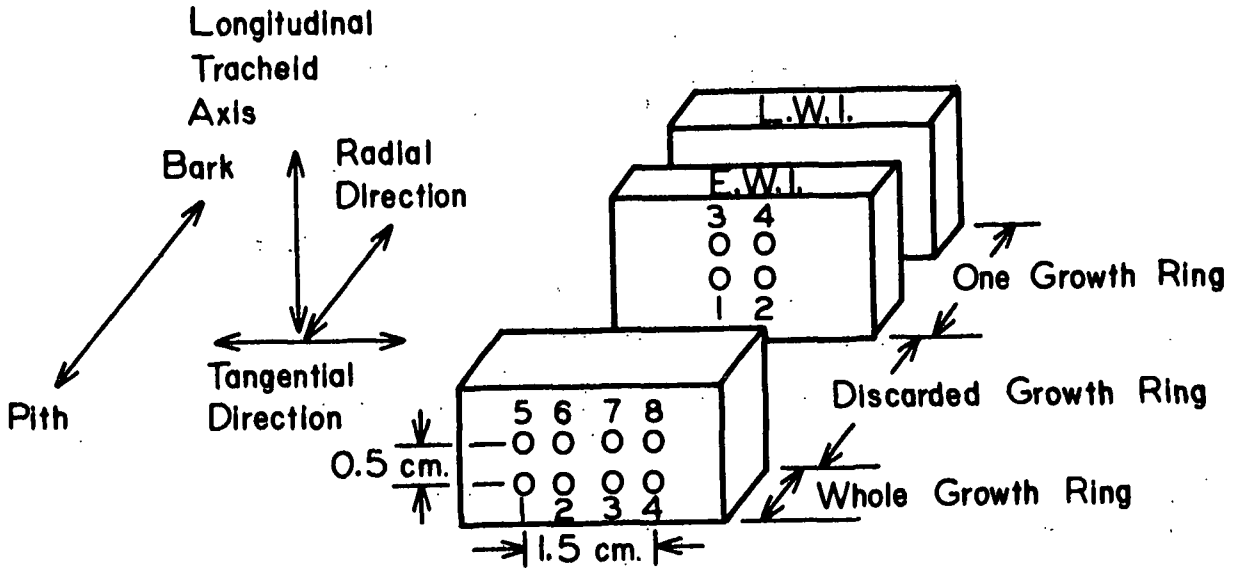

Figure 24. The Location of Tangential Exposure Areas of Wood Sections of Table IX

A large difference in the crystallinity index exists between the earlywood (60.91) and the latewood (66.66) tracheids. In addition, the crystallinity index is variable from one growth ring (60.91-66.66) to another (56.67). Hence, it was necessary to view the same population of tracheids throughout the experimental sequence consisting of exposures on green wood, hygrothermally treated wood, holowood in liquor, water-washed holowood, and hygrothermally treated holowood. However, the exposures on sections at different extents of delignification in the liquor are made on different sections. Since these sections were from three different growth rings, they cannot be directly compared. However, the paired comparisons of same populations of tracheids at different treatment levels can be made, and the statistical analyses are carried out accordingly.

There, also, is a difference in the crystallinity index depending on whether the tracheids are viewed in tangential or radial orientation. Hence, meaningful results were obtained in the present study because precautions were

made to view the same population of tracheids, with known orientation throughout the experimental sequence.

The average orientation of crystallites (Table X) does not appear to change appreciably during hygrothermal treatment of green wood, when the tracheids appear to expand about 1.6% tangentially and shrink about 0.7% radially. Any changes in crystallite orientation caused by these changes in the tracheid dimensions are too small to be detected by the x-ray diffraction analysis.

CELLULOSE FINE STRUCTURE IN THE REACTION LIQUOR

The action of reaction liquor on the tracheid walls causes a decrease in the crystallinity index on the average from 57.75 to 46.11 (Table XI) indicating a decrease in the amount of highly ordered cellulose. These data are collected on the adjacent populations of tracheids within the same growth ring through the whole growth ring with tangential tracheid walls perpendicular to the x-ray beam. Hence, in this case, the obtained values can be compared as a function of time of delignification. The crystallinity index decreases from 57.87 to 48.02 during the first 11 days in the reaction liquor with an additional decrease to 42.58 during the following month. Up to about 15% of the wood components are removed from the sections during this period.

The radial width at the half height appears to increase during the first 20 days from about 12.25 to 12.90 for the two samples analyzed. If real, this increase would indicate a decrease in the order of highly ordered regions. For the samples which have been in the reaction liquor for one to one and one-half months, the radial width at half height appears to have recovered to the same level as that in the hygrothermally treated wood. The decrease in the crystallinity index accompanied by this apparent recovery of order in the highly

TABLE X

ORIENTATION OF CRYSTALLITES OF GREEN WOOD

Sample	Number of Exposures	Average Circumferential Width at the Half Height, degrees		Average Circumferential 2T Width, degrees	
		Green Wood	Heated Wood	Green Wood	Heated Wood
Tangential tracheid walls perpendicular to the x-ray beam					
Earlywood I	4	17.71	17.61	35.65	36.46
Mean change[a]		-0.10		+0.81	
Standard error[b]		0.31		0.75	
Latewood I	4	16.49	16.26	35.33	34.43
Mean change		+0.03		-0.90	
Standard error		0.04		1.19	
Whole growth ring	8	15.32	15.74	30.30	31.12
Mean change		+0.42		+0.82	
Standard error		0.16		0.72	
Average:					
Mean change		+0.19		+0.39	
Standard error		0.11		0.50	
95% Confidence limits		±0.23		±1.07	
Radial tracheid walls perpendicular to the x-ray beam					
Latewood I	4	15.04	14.80	31.84	31.55
Mean change		-0.24		-0.29	
Standard error		0.31		0.53	
Latewood II	4	14.21	13.92	30.16	29.31
Mean change		-0.28		-0.85	
Standard error		0.23		0.33	
Average:					
Mean change		-0.26		-0.57	
Standard error		0.19		0.31	
95% Confidence limits		±0.45		±0.74	

[a] Mean change is the average of the differences between measurements made on same populations of tracheids in a wood section at different treatment levels.

[b] Standard error is that of the mean change.

TABLE XI

EFFECT OF REACTION LIQUOR ON THE
X-RAY CRYSTALLINITY OF SECTIONS

Elapsed Days in Reaction Liquor	Approximate Component Removal into Liquor	Crystallinity Index		Radial Width at Half Height		Circumferential Width at Half Height	
		Original Wood	Holowood	Original Wood, degrees	Holowood, degrees	Original Wood, degrees	Holowood, degrees
11	-2.0	57.87	48.02	12.00	12.86	15.64	15.52
18	5.9	56.38	47.23	12.50	12.95	16.43	16.10
29	9.5	58.86	46.62	12.24	12.23	15.07	16.32
46	14.7	57.88	42.58	12.64	12.54	15.71	15.62
Average		57.75	46.11	12.35	12.65	15.71	15.89
Mean change		-11.64[a]		+0.30[b]		+0.18	
Standard error[c]		1.39		0.24		0.35	
95% Confidence limits[c]		±4.42		±0.76		±1.10	

[a] Decrease indicates a decrease in the amount of highly ordered cellulose.

[b] Increase indicates a decrease in the order of the highly ordered fraction of cellulose.

[c] Calculated from paired comparisons of exposures made on the same populations of tracheids.

ordered regions of cellulose implies that the disordering has taken place in the less ordered regions of the highly ordered region of cellulose. The most highly ordered cellulose appears to be resistant to the disordering effect of the reaction liquor.

The changes in the orientation of highly ordered regions of cellulose are within experimental error. The tracheids expand only about 2% tangentially and shrink about 0.7% radially during the first one and one-half months in the reaction liquor.

CELLULOSE FINE STRUCTURE AS AFFECTED BY THE WATER WASHING OF HOLOWOOD

X-ray Crystallinity

The data in Table XII are collected on sections from three different growth rings and therefore cannot be compared vertically. However, in each case the same population of tracheids is viewed before and after water washing. This design of experiments permits the paired comparisons of washed and unwashed sections at each level of delignification. The statistical analyses are carried out on the difference between measurements made on the same populations of tracheids at different treatment levels.

Throughout the reaction range investigated, the removal of the reaction liquor and of the solubilized tracheid wall components results in a recovery of the crystallinity index. Since this increase resulted from an increase in the height of the 002 diffraction maxima, an increase in the amount of highly ordered cellulose is suggested. During water washing of holowood reacted for 11 days, when 7.5% of the wood components are removed, the crystallinity index increased by 10.42 arbitrary units. For the holowood reacted for 97 days, the wood component removal was 13.0% during water washing, while the crystallinity

TABLE XII

EFFECT OF THE WATER WASHING ON THE HOLOCELLULOSE X-RAY CRYSTALLINITY

Elapsed Days in Reaction Liquor	Crystallinity Index		Radial Width at the Half Height	
	In Reaction Liquor	After Water Washing	In Reaction Liquor, degrees	After Water Washing, degrees
Tangential tracheid walls perpendicular to the x-ray beam				
1	51.47	50.24	12.67	12.80
4	54.32	58.14	13.18	12.68
11	48.02	58.44	12.86	13.04
18	47.23	53.70	12.95	12.61
29	46.62	53.55	12.23	12.65
46	42.58	49.99	12.54	12.16
62	52.30	60.36	12.54	12.29
97	54.77	66.30	12.50	12.14
Mean change[a]	+6.93		-0.14	
Standard error[b]	1.22		0.12	
95% Confidence limits	±2.94		±0.28	
Radial tracheid walls perpendicular to the x-ray beam				
1	49.99	58.13	13.47	13.47
4	56.69	56.87	13.44	13.44
16	38.91	54.34	13.12	12.83
29	48.25	55.36	12.25	13.05
46	46.18	46.08	12.64	12.11
62	38.16	42.54	12.02	12.49
97	46.38	56.95	12.96	12.56
Mean change	+7.95		+0.01	
Standard error	1.77		0.18	
95% Confidence limits	±4.40		±0.46	

[a] Mean change is the difference between measurements made on same populations of tracheids in holowood sections in liquor saturated and water-washed conditions.

[b] Standard error is that of the mean change.

index increased by 11.53 arbitrary units. Hence, the recovery of the crystallinity index is not only related to physical removal of the tracheid wall components.

The amount of highly ordered fraction of cellulose is not accompanied by a detectable change in the radial width at half height; the newly formed highly ordered regions of cellulose appear to have the same degree of order as the previously existing highly ordered regions.

The expansion of the holowood blocks (p. 69) and the increase in the swollen specific volume of pulps (p. 74) during water washing is accompanied by an increase in the amount of highly ordered cellulose. Hence, it is important to distinguish what components actually swell, and what components actually become more highly ordered.

The increase in the amount of highly ordered regions of cellulose are expected to make the microfibrils less extensible. Hence, it is incorrect to consider the tracheid walls as swelling, since the framework substance becomes more highly ordered. The tracheid walls take up water and the outside dimensions expand, but at least the highly ordered regions of cellulose do not swell.

If the microfibrils are considered as inextensible highly ordered structures, the tracheid wall lateral expansion is expected to shorten the tracheid, resulting in a shrinkage of the holowood block. However, the block expands about 0.6% longitudinally as it expands tangentially 20.0% and 7.75% radially. Therefore, the microfibrils are actually extensible and the intermicrofibrillar bonding is infrequent and/or can be easily broken. The lamellae are built up of these rather loosely held, extensible microfibrils.

As the tracheid expands, the lamellae are stretched, causing alignment of cellulose molecule segments in the regions of cellulose which have a degree of order approaching that of highly ordered cellulose. The amount of highly ordered cellulose increases. In addition, the alignment of neighboring highly ordered regions is improved.

If the holowood tracheid behaves dimensionally in the same way as the total holowood block, and if the sliding of microfibrils relative to their surrounding is small, then the maximum extension of the microfibrils in the tangential walls is 9.5% and 4.0% in the radial walls. However, the actual dimensions of the tracheids were not measured. Hence, the above values can be considered only as rough approximations of actual extension of the microfibrils.

The concept of aligning cellulose molecule segments during straining appears to be consistent with Stöckmann's (136) entropy deformation mechanisms. According to him, the elementary fibril must possess less-ordered regions throughout the fibril cross section, allowing for molecular segments to undertake position changes during straining. However, it must be kept in mind that the present data refer to the never-dried sapwood holotracheids, and may not be applicable after the samples are dried.

Orientation of Crystallites

Since the tracheid cross dimensions appear to increase more than the length of the tracheid, the crystallite average orientation angle with respect to the tracheid longitudinal axis is expected to increase. For the holowood sections pulped less than one month, the circumferential width at half height increases from 16.77° to 17.31°, or 0.54° in the case of tangentially exposed sections (Table XIII). For the holowood sections reacted from one and one-half

TABLE XIII

EFFECT OF THE WATER WASHING ON
THE ORIENTATION OF CRYSTALLITES

Elapsed Days in Reaction Liquor	Circumferential Width at Half Height		Circumferential 2T Width	
	In Reaction Liquor, degrees	After Water Washing, degrees	In Reaction Liquor, degrees	After Water Washing, degrees
Tangential tracheid walls perpendicular to x-ray beam				
1	17.42	18.32	38.14	36.85
4	18.47	18.84	37.04	37.73
11	15.52	16.46	29.86	31.92
18	16.10	16.48	32.31	33.16
29	16.32	16.46	31.25	32.62
Average	16.77	17.31	33.32	34.46
46	15.62	17.36	30.01	33.39
62	17.63	18.75	35.46	36.34
97	15.97	18.24	30.55	34.56
Average	16.41	18.12	32.01	34.77
Mean change[a]	+0.98		+1.75	
Standard error[b]	0.26		0.56	
95% Confidence limits	±0.61		±1.08	
Radial tracheid walls perpendicular to x-ray beam				
1	14.81	14.94	30.72	30.65
4	15.77	16.57	31.09	32.51
16	15.64	15.80	30.78	32.20
29	14.29	15.69	28.31	31.03
Average	15.13	15.75	30.23	31.60
46	14.16	15.69	28.96	31.64
62	15.09	16.99	30.53	34.04
97	14.15	17.04	28.93	33.05
Average	14.47	16.57	29.47	32.91
Mean change	+1.26		+2.11	
Standard error	0.51		0.63	
95% Confidence limits	±1.26		±1.54	

[a]Mean change is the difference between measurements made on same populations of tracheids in holowood sections in liquor saturated and water-washed conditions.

[b]Standard error is that of the mean change.

to three months, the corresponding figures are 16.41° and 18.12° or an increase of 1.71°. The increase in the circumferential width at the half height for sections exposed with radial tracheid walls perpendicular to the x-ray beam are 0.62° for the sections reacted less than 30 days, and 2.10° for the sections pulped for one and one-half to three months. Clearly, the tracheid wall expansion is accompanied by a shift in the crystallite orientation angle with respect to fiber axis.

CELLULOSE FINE STRUCTURE OF HOLOWOOD AS AFFECTED BY HYGROTHERMAL TREATMENT

X-ray Crystallinity

The hygrothermal treatment of the holowood sections results in an increase in the crystallinity index throughout the reaction range investigated (Table XIV). The increase is especially apparent in the cases where the radial tracheid walls are perpendicular to the x-ray beam. Apparently, the intermicrofibrillar bonding is predominant on the radial walls due to natural disruptions such as pits and ray parenchyma crossings resulting in changes in the microfibril orientation. These intermicrofibril bonds resist the sliding of microfibrils along their surfaces, resulting in a more severe stretching of the cellulose molecules in the somewhat ordered region of microfibrils in the radial walls.

The decrease in the radial width at half height is on the average from 12.83° to 11.83°, or 1.00° for the tangentially exposed holowood sections. The decrease for the radially exposed sections is 0.90°. These changes suggest a strong increase in the degree of order of the highly ordered fraction of cellulose. Presumably, the stretching of the tracheid wall lamellae and the stretching of the microfibrils are sufficient to cause strong alignment of both

TABLE XIV

EFFECT OF THE HYGROTHERMAL TREATMENT ON
THE HOLOCELLULOSE X-RAY CRYSTALLINITY

Elapsed Days in Reaction Liquor	Crystallinity Index		Radial Width at the Half Height	
	After Water Washing	After Hygrothermal Treatment	After Water Washing, degrees	After Hygrothermal Treatment, degrees
Tangential tracheid walls perpendicular to the x-ray beam				
1	50.24	56.82	12.80	11.98
4	58.14	60.71	12.68	11.94
11	58.44	56.40	13.04	12.30
18	53.70	55.02	12.61	11.80
29	53.55	55.13	12.65	12.73
97	66.30	69.08	12.14	11.48
120-1	59.65	61.00	13.32	11.52
2	57.45	63.36	12.95	11.49
3	54.22	59.49	13.07	11.74
4	55.22	59.98	13.00	11.34
Average	56.69	59.70	12.83	11.83
Mean change[c]	+3.01		-1.00	
Standard error[d]	0.82		0.18	
95% Confidence limits	±1.82		±0.40	
Radial tracheid walls perpendicular to the x-ray beam				
1	58.13	61.79	13.47	12.50
4	56.87	60.69	13.44	12.22
16	54.34	55.70	12.83	12.62
29	55.36	62.31	13.05	12.58
46	46.08	47.38	12.11	11.63
62	42.54	55.93	12.49	10.75
97	56.95	68.48	12.56	11.36[b]
120-A[a]	47.12	65.92	12.22[b]	8.52[b]
120-B[a]	55.35	62.50	11.86	11.11
120-C[a]	57.29	62.87	11.94	10.88
Average	53.00	60.35	12.64	11.74
Mean change	+7.35		-0.90	
Standard error	1.79		0.16	
95% Confidence limits	±3.98		±0.35	

[a] A = Earlywood; B = transitionwood; C = latewood.

[b] Sample 120-A is omitted from the statistical analyses due to the extraordinarily large changes.

[c] Mean change is the difference between measurements made on same populations of tracheids in holowood sections in water washed and hygrothermal conditions.

[d] Standard error is that of the mean change.

the microfibrils and the somewhat aligned cellulose molecules, increasing the amount of highly ordered cellulose at the expense of less ordered cellulose.

Orientation of Crystallites

The average orientation angle of the crystallites with respect to the tracheid longitudinal axis in tangential sections does not change by a detectable amount during hygrothermal treatment of holowood. However, the average orientation angle of crystallites in the radially exposed sections decreases (Table XV).

Since the holowood block continues to expand more in tangential and radial directions than in the longitudinal direction, the average orientation angle of the crystallites is expected to continue to shift away from the tracheid longitudinal axis. However, the shift in the crystallite average orientation is toward the tracheid axis, especially in the radially exposed sections (16.49° to 15.72°). This shift is accompanied by an increase in the crystallinity index (53.00 to 60.35). These data suggest that the additional crystallization takes place in the microfibrils which have the increasingly highly ordered regions more closely parallel to the tracheid longitudinal axis than the previously crystallized regions.

CELLULOSE FINE STRUCTURE IN THE NEVER-DRIED HOLOTRACHEID LAMELLAE

On the basis of the x-ray diffraction analyses, it can be concluded that, as the holowood block expands, and the tracheid wall water holding capacity decreases, the tracheid wall lamellae do not swell. Instead they are stretched to the point where they actually lose water, and the degree of

TABLE XV

EFFECT OF THE HYGROTHERMAL TREATMENT
ON THE ORIENTATION OF CRYSTALLITES

Elapsed Days in Reaction Liquor	Circumferential Width at Half Height		Circumferential 2T Width	
	After Water Washing, degrees	After Hygrothermal Treatment, degrees	After Water Washing, degrees	After Hygrothermal Treatment, degrees
Tangential tracheid walls perpendicular to the x-ray beam				
1	18.32	18.12	36.85	36.99
4	18.84	18.68	37.73	38.30
11	16.46	15.52	31.92	31.80
18	16.48	16.50	33.16	33.84
29	16.46	16.51	32.62	32.58
97	18.24	17.81	34.56	35.21
120-1	17.42	17.47	35.80	33.80
2	17.88	18.83	35.60	35.89
3	18.93	17.53	35.86	35.91
4	17.93	18.32	35.26	34.47
Mean change[b]	-0.16		-0.06	
Standard error[c]	0.21		0.26	
95% Confidence limits	±0.46		±0.57	
Radial tracheid walls perpendicular to the x-ray beam				
1	14.94	15.10	30.65	29.23
4	16.57	15.54	32.51	31.72
16	15.80	15.55	32.20	30.98
29	15.69	13.98	31.03	29.63
46	15.69	15.50	31.64	29.63
62	16.99	15.35	34.04	31.14
97	17.04	15.80	33.05	31.36
120-A[a]	17.23	15.64	34.11	33.48
120-B[a]	17.53	17.64	33.17	33.18
120-C[a]	17.38	17.11	32.24	32.89
Mean change	-0.77		-1.14	
Standard error	0.24		0.32	
95% Confidence limits	±0.53		±0.71	

[a] A = Earlywood; B = transitionwood; C = latewood.
[b] Mean change is the difference between measurements made on same populations of tracheids in holowood sections in water washed and hygrothermal conditions.
[c] Standard error is that of the mean change.

order of cellulose increases. Based on this evidence, the model of tracheid wall lamellae advanced by Stone and Scallan (52) does not fully describe the fine structure of never-dried lamellae, since it does not provide a mechanism for the increase in the degree of order of cellulose as the tracheid dimensions increase. The concept of cellulose possessing different degrees of order as described by Howsmon and Sisson (37) and the fringed fibril model of cellulose (42) do provide mechanism for this increase. The present data suggest that the never-dried microfibrils are extensible, and that the straining causes an increase in the degree of order of cellulose molecules within the microfibril as well as in the better alignment of microfibrils in the lamellae.

FACTORS CAUSING THE CHANGES IN THE CELLULOSE FINE STRUCTURE IN THE WET STATE

INTRODUCTION

The experimental evidence presented in the previous section establishes the concept that the cellulose fine structure is modified already in the wet state during the tracheid wall component removal. However, up to this point, the factors causing the stretching of the framework constituents, which in turn cause the increase in the degree of order of cellulose, have not been discussed.

During water washing for 48 hours the swollen specific volume of the 57% yield pulp increases by 82%. On resubmersion in reaction liquor, the swollen specific volume decreases and approaches that in the unwashed condition (Table XVI). The subsequent water washing results in the recovery of the swollen specific volume to the same level as with the first water washing. The chemical composition of the pulp does not appreciably change during this reversible swelling process. Hence, the swelling and shrinking of the tracheid

wall cannot be attributed to the hydrophobic or hydrophilic character of the tracheid wall components. The concentration of ions in the environment, however, does change. Therefore, it is reasonable to expect that the expansion and shrinking of the tracheid wall may be caused by ionized group effects. In the following section these factors are elucidated by considering the mechanisms which are involved in swelling of holocellulose in the ionic medium.

TABLE XVI

SWOLLEN SPECIFIC VOLUME OF 57% YIELD PULP IN WATER AND IN REACTION LIQUOR

Treatment	Swollen Specific Volume, cc./g.	
	Sample I	Sample II
In reaction liquor	2.65	2.65
After the first water washing	4.75	4.90
After resubmersion in the reaction liquor	3.30	3.42
After the second water washing	5.00	4.88

SWELLING MECHANISMS IN THE ELECTROLYTE SOLUTIONS

According to Stamm (132) the swelling of cellulosic substances in the electrolyte solutions can be explained by the following mechanisms:

1. The water, bound to the ions immobilized in close proximity to the surface ions, causes the swelling (137).
2. Electrical charge develops on the swelling material as a result of selective adsorption of ions causing repulsion of like charges on the neighboring surfaces opening up the structure and permitting water to enter mechanically (137-140).

3. Donnan membrane equilibrium is set up within the swelling material, with higher concentration of ions within the swelling material than in the bulk solution. The developed osmotic pressure causes water to diffuse into the material (141, 142).

Yorston (143) has proposed a fourth mechanism of swelling which is a modification of the second mechanism. In this case the cellulose is considered to have a negative surface charge. An electrostatic repulsion develops due to the formation of electrical double layers on the neighboring cellulose surfaces. As a result, the wall pores are enlarged and the amount of capillary water increases. This mechanism is supported by Thomas (129) and by Jacquelin (144).

The fifth mechanism of swelling involves Donnan potential swelling forces. Unlike mechanism three, the uneven ionic distribution does not arise from the electrolyte, but from the immobility of the anions of the polymer ionizing groups. These ionogenic groups are internal to the amorphous components of the tracheid walls and hence cause osmosis of water into these regions (145-147).

The first of the above cited mechanisms, the swelling by water of hydration, is related to the now popular concept of "water structure making ions" and "water structure breaking ions" (148). However, this mechanism is discarded as not being the controlling mechanism on the following grounds. In order for the cellulosic materials to swell by the mechanism of the water of hydration of the absorbed cations, the cation concentration should be above 2N (132, 149-150). In the present study the bulk solution concentration is 0.1N and below. Furthermore, the swelling by this mechanism increases as the ion concentration increases. In the present case, the swelling occurred during water washing as cation concentration decreases. Finally, the Na^+ is a "structure making" ion, while K^+ is a "structure breaking" ion. However, no differences were observed between the effects of Na^+ and of K^+ ions.

Cellulosic Substances in Water

In order for either the electrostatic repulsion effect or the Donnan potential effect to be operating, the holocellulose surfaces have to possess a negative surface charge in water. The negative surface charge is well documented. According to Heymann and Rabinov (151), the "cation-free" cellulose has distinct acid properties in water. He considers the cellulose fiber as a multivalent giant anion, which is surrounded by an atmosphere of hydrogen ions due to the dissociation of acidic groups. Stamm (132) observed that even the finely ground wood flour dispersed in water assumes a negative surface charge. According to Goring and Mason (152), the whole pulp fiber carries a negative charge when suspended in water. Furthermore, Asunmaa and Schwab (49) suggest that the 100 A. diameter microfibrils of holocellulose in fibrillated condition carry a surface charge.

Several authors have determined the zeta-potential (ζ) of cellulosic substances and found it to vary between -11 mv. for viscose rayon and -45 mv. for beaten cotton (152, 153). Kanamaru and Takada (153) found that the ζ decreases as a result of standing in distilled water. Furthermore, the higher the crystallinity of the cellulose is, the smaller is the drop in ζ. Goring and Mason (152) found for the bleached sulfite pulp that ζ is -29.2 mv. in 2.5×10^{-5}N KCl, and -8.8 mv. in 2×10^{-2}N KCl.

Bjorkqvist and Jorgensen (154) found the holocellulose to contain considerably more acidic groups than pure cellulose. They suggest that the majority of carboxyl groups in spruce and birch holocellulose belong to the hemicellulose fraction. This view is supported by Asunmaa and Lange (155), who determined the carboxyl group distribution through the tracheid walls of spruce holocellulose and found it to be similar to hemicellulose distribution. The carboxyl

groups are almost linearly distributed throughout the tracheid walls with the maximum in the outer layers and the minimum around the lumen. Kantouch, et al. (156) observed an increase in the carboxyl content of the cotton cellulose on reaction with sodium chlorite. The effect is more pronounced after prolonged reaction. Hence, not only is the carboxyl content of holocellulose high due to the high hemicellulose content, but also the reaction of cellulose with sodium chlorite promotes the formation of carboxyl groups.

Donnan Potential in the Cellulose-Electrolyte System

The Donnan potential develops if the ion distribution is uneven, resulting in an osmosis of water, which swells the cellulose (157). The swelling continues until the osmotic pressure is balanced by the forces arising from the cohesion of limited swelling cellulose gel (158). If the electrolyte concentration of the bulk solution is increased, the Donnan potential is suppressed. For the cellulose-potassium chloride system, the Donnan potential is completely suppressed at a concentration above approximately 0.4 molar (159). At lower concentration the Donnan potential develops and swelling occurs. Neale and Standing (146) have found the Donnan potential of cellophane to vary from 0.23 mv. at 1.03M KCl to 57.11 mv. at 0.001M KCl. Recently, Sivaraja Iyer and Jayaram (159) confirmed the above results. Osmotic pressure due to Donnan potential could result in the expansion of the tracheid walls by swelling of the amorphous regions within as well as between the lamellae.

Electrostatic Repulsion Effect of Electrical Double Layer

A simplified model of the electrical double layer and its potential distribution is shown in Fig. 25. The liquid phase consists of the Stern immobile layer and of the Gouy-Chapman diffuse layer. The Stern immobile layer contains

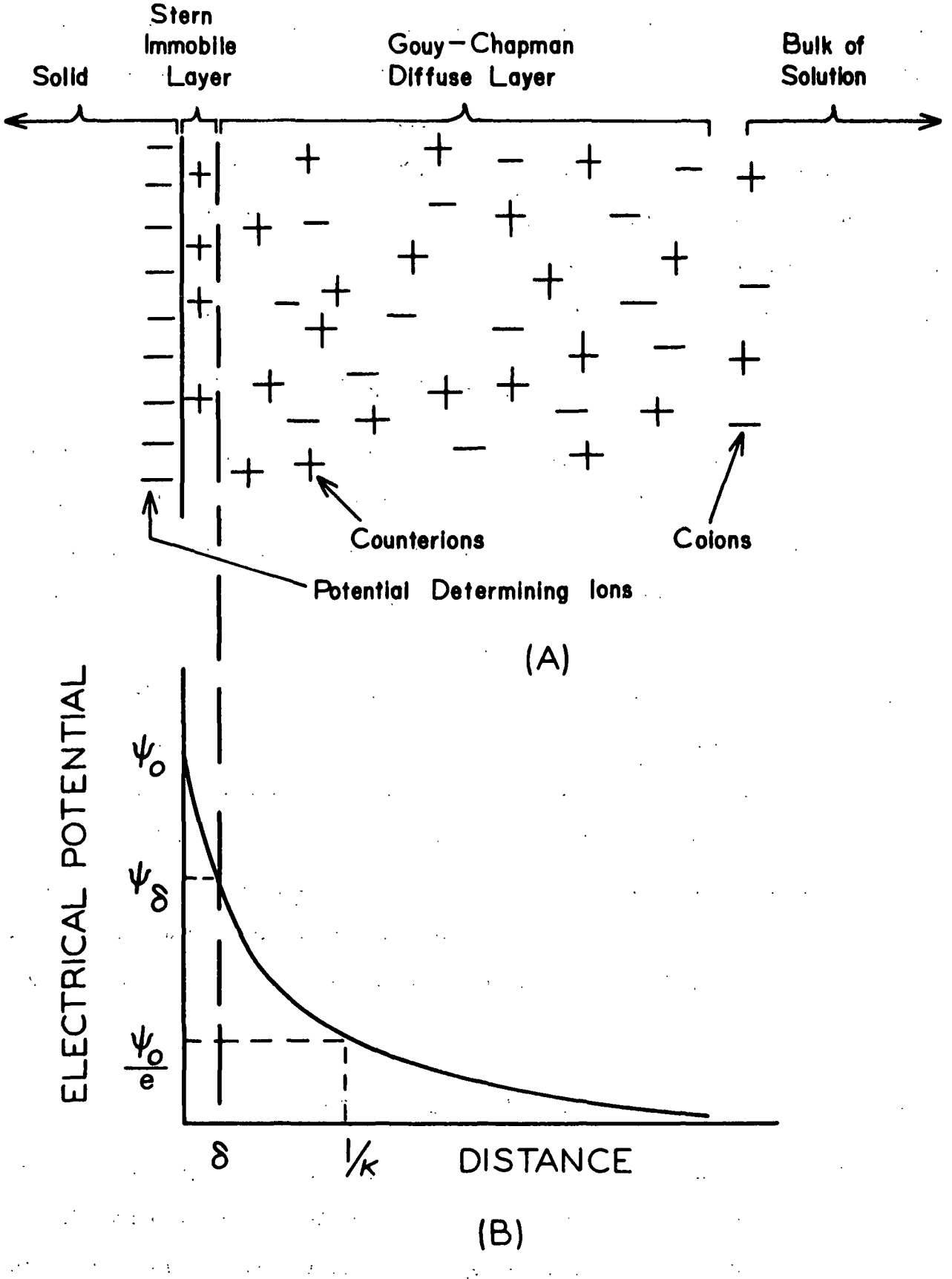

Figure 25. A Simplified Model of the Electrical Double Layer, (A); and its Potential Distribution, (B). Adopted from Verwey and Overbeek (162)

the thin layer of chemisorbed but hydrated counterions. The Gouy-Chapman diffuse layer has the rest of the counterions and extends to the bulk solution. The following other terms are used to describe the electrical double layer:

ψ_o = the surface potential

ψ = the electrical potential at some distance x from the surface

δ = the thickness of the immobile Stern layer

ψ_δ = the potential at the outer Helmholtz plane, the potential drop across the diffuse layer

ζ = the experimentally determined potential at the hydrodynamic plane of shear

κ = Debye-Huckel parameter; $1/\kappa$, an approximation of the double layer thickness (160-162)

Electrostatic Repulsion Effect of Electrical Double Layer

As the electrolyte concentration in the bulk solution decreases, an increasing number of sodium ions are removed from the Stern layer by thermal motion into the Gouy-Chapman diffuse layer increasing the domain of the double layer. The expansion of the electrical double layer is illustrated in Fig. 26 as the expansion of the electrical potential distribution curve. Thus, the lower the electrolyte concentration, the more gradually the potential falls off with distance from the charged surface. With the surface charge of 25 mv. the effective double layer domain extends over 100 A. in 0.001N electrolyte (161). These values can be considered as reasonable estimates for the holotracheid lamellae during water washing.

The interaction of the two neighboring lamellae is illustrated in Fig. 27. According to Verwey and Overbeek (162), the repulsive effect is operative between two lamellae separated by less than a hundred Angstrom units to several

hundred Angstrom units apart, depending on the surface charge and the electrolyte concentration. Hence, the electrostatic repulsive effect tends to widen the spacing between charged surfaces.

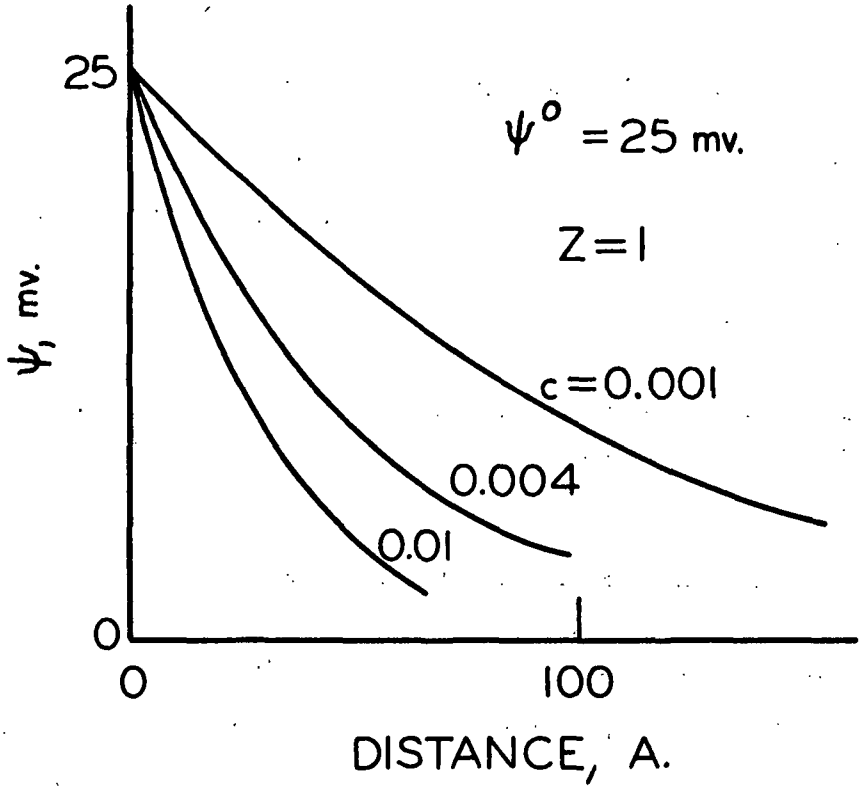

Figure 26. The Expansion of the Electrical Double Layer is Illustrated as the Development of the Electrical Potential Distribution Curve when the Electrolyte Concentration Changes from 0.01N to 0.004N to 0.001N for One to One Electrolyte. From Adamson (161)

The electrostatic repulsion effect can be considered to act on all the surfaces possessing a surface charge. The distance between the neighboring lamellae of the tracheid walls can be controlled by this mechanism. Furthermore, the electrical double layers can be present on the surfaces of paracrystalline bundles of molecules and crystalline regions.

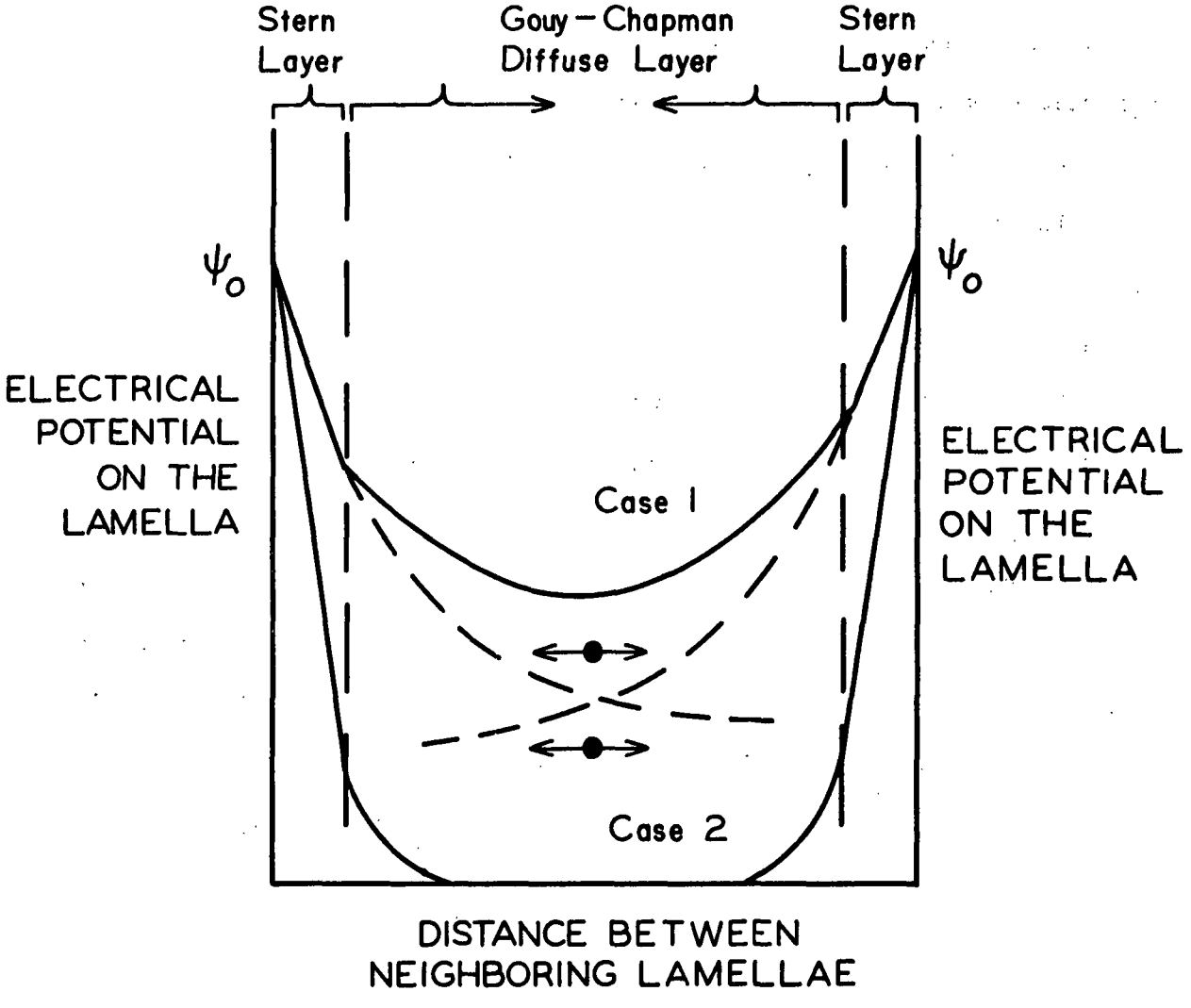

Figure 27. The Electrical Potential Distribution Curves of Two Interacting Double Layers. In Case 1, the Electrolyte Concentration is Low and the Gouy-Chapman Diffuse Layer is Expanded Resulting in a Repulsive Interaction Tending to Move the Surfaces Further Apart. In Case 2, the Electrolyte Concentration is High and the Gouy-Chapman Diffuse Layer is Collapsed Resulting in Negligible Interaction Between the Charged Surfaces

According to Campbell's (163) original model of swelling of cellulose in water, the surface molecules of the amorphous regions are anchored to the body of the structure with a portion of the molecules or a group of molecules dissolved. Goring and Mason (152) modified this concept to include the electrostatic repulsion effects as depicted in a simplified manner in Fig. 28. They proposed that there is a diffuse boundary of considerable thickness called the β-layer in which the partially dissolved molecules and groups of molecules, bearing an electrical charge, extend into the liquid phase. Each such unit is surrounded by its own Gouy-Chapman diffuse double layer. They calculated the approximate double layer thickness to be 20 A. in 0.02N solution and to expand to about 300 A. in the 1.0×10^{-4}N KCl. This, of course, results in an electrostatic repulsion between the neighboring charged cellulose molecular segments and groups of molecular segments. According to this idealized model, the electrostatically swollen β-layer would be several thousand Angstrom units thick if the macromolecule segments can unravel and become fully extended. For holotracheid walls with a high hemicellulose content, this swelling mechanism could play a considerable role during water washing.

EFFECT OF UNIVALENT CATIONS ON THE SWOLLEN SPECIFIC VOLUME OF WATER-WASHED PULP

Since the cellulosic substances possess a negative surface charge in water and the swelling forces attributable to these charges are strongly influenced by the electrolyte concentration, the effect of ionic medium on the swollen specific volume of the 57% yield pulp (p. 36) was studied. The results of treatment with univalent cationic electrolyte solutions are given in Table XVII.

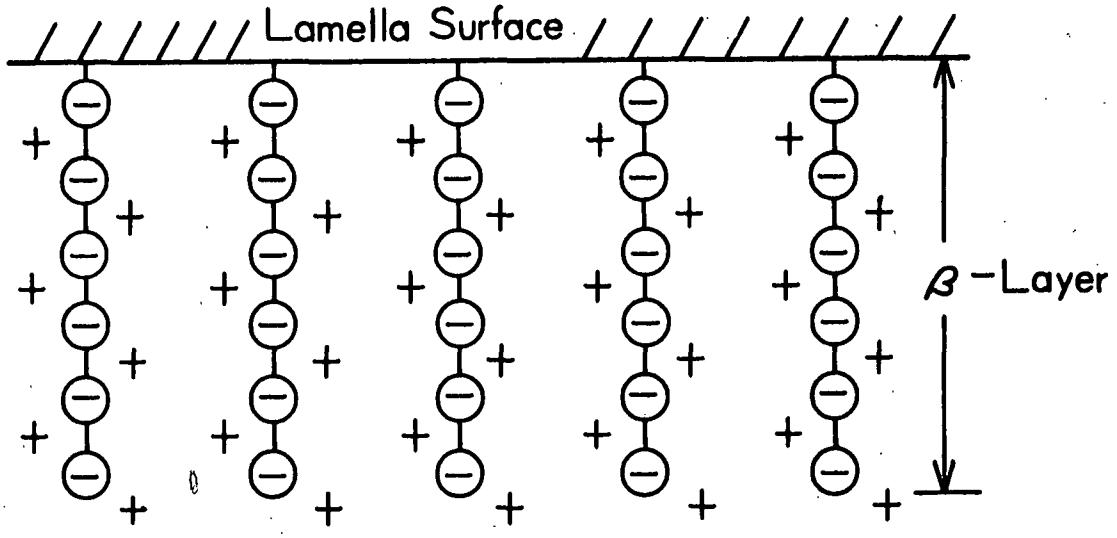

Figure 28. Schematic Representation of Distribution of Ions at the Lamella-Liquid Interphase. Adopted from Goring (152)

TABLE XVII

EFFECT OF UNIVALENT CATIONS ON THE SWOLLEN SPECIFIC VOLUME OF 57% YIELD PULP

Sample	Swollen Specific Volume After Water Washing from Reaction Liquor, cc./g.	Time of Treatment, hr.	Swollen Specific Volume in 0.1N Ionic Medium, cc./g.	Swollen Specific Volume After Second Water Washing, cc./g.
NaCl	5.01	20	3.28	4.58
	5.10	20	3.30	4.56
KCl	5.02	1/6	3.33	4.53
	5.16	2/3	3.43	4.69
	4.73	1 2/3	3.35	4.32
	5.00	20	3.68	4.18
	4.98	20	3.48	4.62
	4.73	20	3.16	4.11
	4.76	20	3.15	4.17
	4.90	48	3.30	3.73
NaOH	4.63	20	3.22	4.08
	4.75	20	3.14	4.05
KOH	4.55	20	3.08	3.99
	4.61	20	3.10	3.99

The tracheid walls respond to the univalent ionic solution in a manner similar to that observed with the reaction liquor. The swollen specific volume of washed pulp decreases about 32% in the 0.1N univalent ionic medium. The rewashing in distilled water for 48 hours results in a 70% recovery of the swollen specific volume loss. The 0.1N KCl solution has the same effect as the 0.1N NaCl regardless of the duration of treatment in the salt solution.

These results are in qualitative agreement with the results of Andersson and Samuelson (164), who observed that the rayon fiber swells as the concentration of K^+, Na^+, or Li^+ decreases from 0.1N to 0.01N. Grundelius and Samuelson (165) observed a similar effect for beaten bleached birch kraft pulp in sodium polymetaphosphate $(NaPO_3)_n$ in the concentration range of 0.1N to 0.05N. Aggebrant and Samuelson (104) made the same observation for purified beaten and unbeaten cotton.

The tracheid walls do not swell in the 0.1N alkaline medium, but in fact shrink in a manner similar to that observed with the other univalent ionic solutions. Also, the shrinking is partially reversible in the sense that rewashing in distilled water results in an increase in the swollen specific volume.

EFFECT OF MULTIVALENT CATIONS ON THE SWOLLEN SPECIFIC VOLUME OF WATER-WASHED PULP

Others have noted that the effects of electrolyte on pulp fiber properties (166-169), pulp slurry properties (170-175), and paper properties (173-175) are dependent on the valence of the cations. To obtain a qualitative verification that the observed swelling and shrinking behavior of the pulp tracheid walls is indeed attributable to cationic effects, the swollen specific volume of pulps was also determined in the multivalent cationic mediums. The results are given in Table XVIII.

TABLE XVIII

EFFECT OF MULTIVALENT CATIONS ON THE SWOLLEN SPECIFIC VOLUME OF 57% YIELD PULP

Sample	Swollen Specific Volume After Water Washing from Reaction Liquor	Time of Treatment, hr.	Swollen Specific Volume in 0.1N Ionic Medium, cc./g.	Swollen Specific Volume After Second Water Washing, cc./g.
$BaCl_2$	4.67	20	3.04	3.18
	4.64	20	2.90	3.28
$Ba(C_2H_3O_2)_2$	4.91	20	2.95	3.12
	4.43	20	2.93	3.20
$FeCl_3$	4.89	1/6	3.09	2.83
	4.72	2/3	3.10	2.88
	4.79	1 2/3	2.99	2.85
	4.76	20	3.08	2.87
	4.79	20	2.93	2.89
	4.43	20	3.04	2.92
	4.65	20	3.09	2.89
	4.76	48	3.15	2.94

The univalent and multivalent cations have a similar effect in decreasing the swollen specific volume of the washed pulps. The valence effect, however, is apparent on the swollen specific volume of the pulp after rewashing in distilled water. For the univalent cation treated pulps, the swollen specific volume loss recovery is 70%, while for the divalent cation-treated pulps the recovery is only 12%. In the case of the pulp treated with 0.1N trivalent cations, the tracheid walls remain in the shrunken condition.

These results agree in principle with the observations that the beating time needed to reach a given freeness increases with the valence of the cation in the dispersing medium (172-174). In the shrunken condition the tracheid walls do not beat as well as in the swollen condition. The results are also in agreement with the fact that multivalent cations are better drainage aids (172-174) and better flocculating agents (167, 168, 171) than the univalent cations.

SORPTION OF CATIONS WITHIN THE HOLOCELLULOSE TRACHEID WALLS

The chief reason for the differences between the effects of univalent and multivalent cations on the tracheid wall dimensional changes is that cations are more difficult to remove from the vicinity of negatively charged surfaces the larger the cation valence. Masters (176) observed that sodium ion can be easily removed from cotton with water washing, and according to Sarkar, et al. (177), the Na^{+} bound to jute holocellulose is completely removed by distilled water washing. On the other hand, Preston (160) observed that cellulose microfibrils adsorb Cu^{++} ions from water solution forming a two-dimensional crystalline array of copper atoms on the surfaces. Cohen, et al. (178) found that water washing is not effective in removing divalent ions such as Mg^{++} and Cu^{++}. Ogiwara and Kubota (179) observed that Ca^{++}, and Fe^{++} in dissolving pulp could not be removed by water washing, but that 0.1N HCl is effective in removing these divalent cations. The Fe^{+3} and Ce^{+4}, however, resist even the acid washing so that only about 20% of these multivalent cations are removed.

It is generally believed that the sorbed cations are associated with the carboxyl groups (177-180). Sjöström, et al. (181) indicate that the divalent cations are associated with carboxyl groups through both valence electrons. Ogiwara, et al. (179, 180) found that the amount of sorbed Ca^{+2} and Fe^{+2} in dissolving pulp is approximately equal to the molar number of total carboxyl groups, while the amount of sorbed Fe^{+3} and Ce^{+4} is equal to the total carbonyl content. Ogiwara and Kubota believe that divalent cations are ionically bonded to carboxyl groups, while the trivalent ions may be bonded by coordinate chelation with carbonyl oxygen (179).

EFFECT OF CATION SCAVENGER ON THE SWOLLEN SPECIFIC VOLUME OF ELECTROLYTE TREATED PULP

If the permanent decrease in the swollen specific volume observed for the di- and trivalent cationic electrolyte treated pulps is indeed due to the presence of the cations within the tracheid walls, then the removal of these cations should result in the recovery of the swollen specific volume. In order to test this hypothesis the cation containing pulps were treated with a cation scavenger, ethylenediamine-tetraacetic acid (EDTA). The results are given in Table XIX.

The runs made on the pulping liquor or monovalent cationic electrolyte treated pulps serve as the controls. Treatment with the 0.1N EDTA results in the reduction of the swollen specific volume of pulps to the same level as the treatment with univalent cations. The effect, however, is reversible, so that 75% of the swollen specific volume loss is recovered on rewashing in distilled water.

The tracheid previously treated with di- and trivalent cationic electrolyte solutions swell during water washing following EDTA treatment. For the divalent cation treated pulps the swollen specific volume loss recovery is about 58%, while for the trivalent cation treated pulps the corresponding recovery is 44%. The lower recovery is again an indication of the increased difficulty of removing cations from the holocellulose as the valence of the cation increases. These results are consistent with those of Cohen, et al. (178), who found that sodium hexametaphosphate exchanges Mg^{++} and Ca^{++} on the carboxyl groups to Na^{+} in bleached spruce sulfite and unbleached eucalypt kraft pulps resulting in a better response to beating.

TABLE XIX

THE EFFECT OF CATION SCAVENGER (EDTA) ON THE SWOLLEN SPECIFIC VOLUME OF ELECTROLYTE TREATED 57% YIELD PULP[a]

Sample	Swollen Specific Volume of Pulps, cc./g. After Rewashing[b]	After Treatment with 0.1N EDTA[c]	After Subsequent Water Washing
Treated with pulping liquor			
	5.00	3.05	4.19
	4.88	3.07	4.23
Treated with univalent cations			
KCl	4.11	2.99	4.18
	4.17	3.03	4.16
NaCl	4.58	3.04	4.13
	4.56	3.08	4.11
Treated with multivalent cations			
$BaCl_2$	3.18	2.99	4.21
	3.23	2.99	4.32
$Ba(C_2H_3O_2)_2$	3.12	2.94	4.25
	3.20	3.17	4.06
$FeCl_3$	2.92	2.85	3.62
	2.89	2.86	3.65

[a]The pulps were first water washed to remove reaction liquor and solubilized components, then treated with the 0.1N solution of indicated electrolytes.

[b]The values in the first column of numbers are the swollen specific volumes after subsequent water washing.

[c]The pulps were centrifuged directly from 0.1N EDTA.

EFFECT OF ACID TREATMENT ON THE SWOLLEN SPECIFIC VOLUME OF PULP

According to the literature (168, 173, 175), the 0.1N acid treatment of kraft and sulfite pulps has effects on flocculation, response to beating, and final paper properties closer to the effects of multivalent cations than univalent cations. In agreement, acid treatment results in shrinking of the tracheid walls, which is permanent in the sense that the subsequent water washing does not result in a recovery of the swollen specific volume (Table XX).

TABLE XX

THE EFFECT OF ACID MEDIUM ON THE SWOLLEN SPECIFIC VOLUME OF 57% YIELD PULP

	Swollen Specific Volume of the Pulps, cc./g.		
Sample	After First Washing	In 0.1N Acid Medium	After Rewashing
HCl	4.57	2.71	3.00
	4.62	2.71	2.89
CH_3COOH	4.63	2.88	3.05
	4.59	2.95	2.93

MODEL OF THE EXPANDED HOLOCELLULOSE TRACHEID WALLS

The holocellulose tracheid walls can expand beyond the water-swollen condition of wood by two main mechanisms: (1) the Donnan potential effect causing swelling within amorphous cellulose and hemicelluloses by virtue of internal ionized groups, and, (2) by the electrostatic repulsion-induced separation of surfaces. The latter effect can be considered to act on all structural elements of the tracheid walls that possess surface charge. These concepts are illustrated in Fig. 29. They qualitatively account for the observed increases in the swollen specific volume of pulps and in the dimensions of the holowood blocks during water washing. They are also in harmony with the

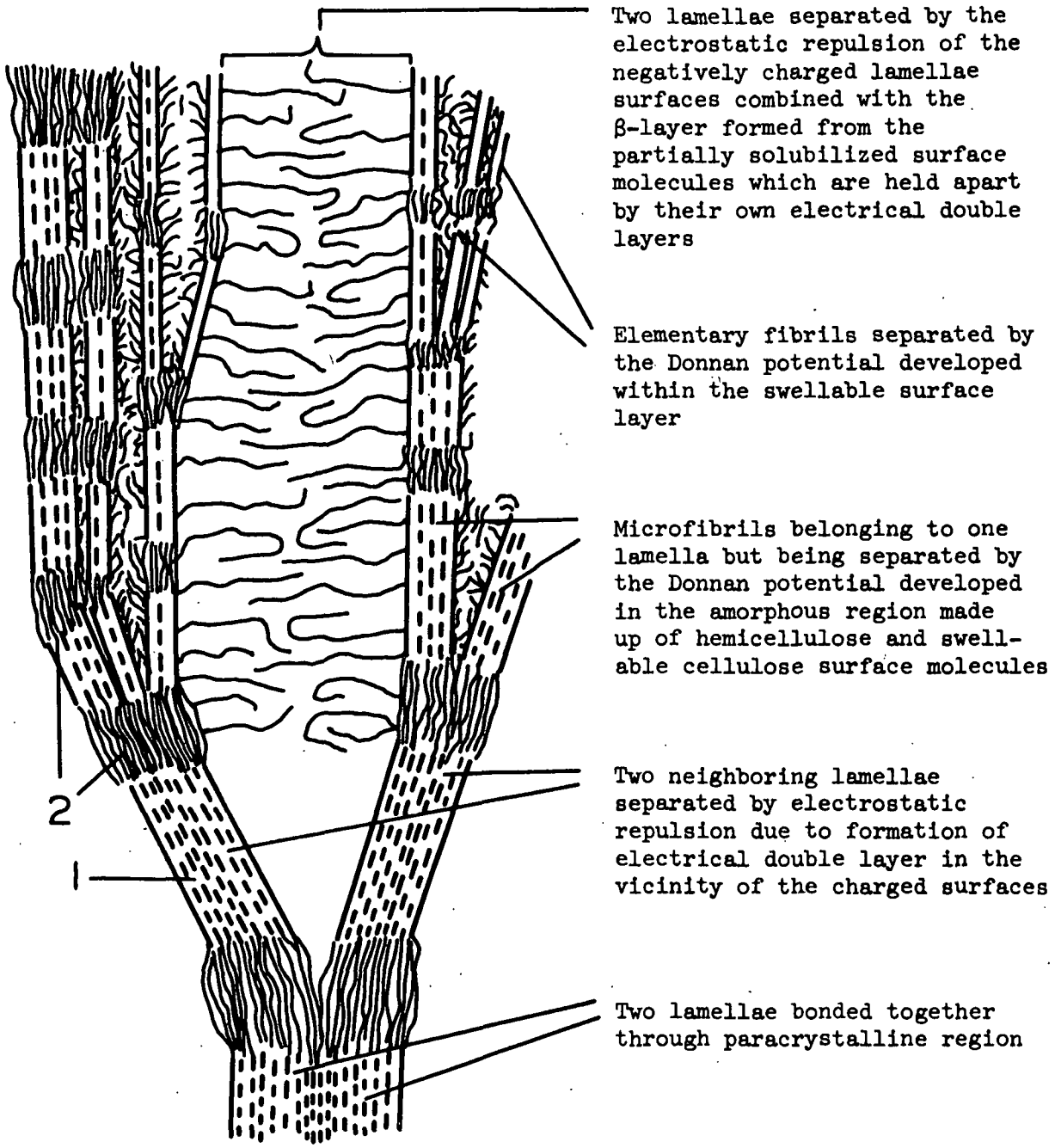

Figure 29. A Schematic Representation of a Cross Section of Two Neighboring Lamellae of Holocellulose Tracheid Wall in the Swelling Condition.

1. The Highly Ordered Region of Lamella Possessing Crystalline Regions Connecting the Adjacent Highly Ordered Fibrils but Interrupted with Amorphous Regions Between Fibrils.

2. The Paracrystalline and Amorphous Regions of Lamellae Made up of Disordered Fibrils

reversibility of dimensional changes of the holocellulose tracheid walls in univalent electrolyte solutions and distilled water.

In the univalent cationic electrolyte solution, the electrostatic interaction of the neighboring carboxyl groups are suppressed by shielding of the negative charge by excess Na^+ ions (182). As the electrolyte concentration in bulk solution decreases during water washing, the Na^+ counterion concentration in the vicinity of the charged surfaces decreases. As a result, the electrostatic double layer of ionized surface groups expands and the Donnan potential of ionized internal groups increases. The increasing electrostatic repulsion effect due to the neighboring electrical double layers tends to separate the adjacent structural elements and the increasing Donnan potential increases the osmotic movement of water into the amorphous regions. Thus, the tracheid walls expand. As the expanded tracheids are submerged in the 0.1N electrolyte solution, the Gouy-Chapman diffuse layer collapses and the Donnan potential decreases; thus, the tracheid walls shrink. On rewashing, the process is repeated.

Based on information in the literature, the divalent cations are bound to carboxyl groups either by salt formation (ion pairing) (179, 181) or by complex formation (183, 184). Tondre and Zana (183) indicate that binding of counterions involves two charged sites when the minimum distance between two charged sites is small (chelation). Ogiwara and Kubota (179) believe that trivalent cations form a chelate bond with the carbonyl oxygen. Consequently, the bound multivalent cations are more difficult to remove from the Stern layer than the univalent cations: the domain of the double layer is small and the Donnan potential is low even in the washed condition. Thus, the tracheid walls expand very little on water washing. The reoccurrence of the tracheid wall expansion on water washing after removal of divalent cations by EDTA confirms the concept

that the ionized groups in the holowood are responsible for the expansion of the holocellulose tracheid walls on water washing.

In the acid medium, the low pH favors formation of nonionized groups (145). The electrostatic interactions between these nonionized groups suppress their dissociation (182) on water washing. Hence, only a low surface charge develops, and tracheid wall swelling by electrostatic repulsion is small. Similarly, the dissociation of internal groups is suppressed, and the Donnan potential swelling forces are low. In addition, hydrogen bonding between carboxyl groups also contributes to the dimensional stability of the tracheid walls.

EFFECT OF THE TRACHEID WALL EXPANSION ON THE CELLULOSE FINE STRUCTURE

The cellulose microfibrils are the framework constituents of the tracheid walls and are arranged more or less parallel in concentric layers forming more or less independent structural units called lamellae. As the amorphous fractions located within as well as between the lamellae swell by the Donnan effect, and as the lamellar separation is further aided by the electrostatic repulsion operating between the neighboring lamellae, the tracheid circumference increases. A possible consequence is that, since the tracheid does not shrink longitudinally, the microfibrils are stretched. Furthermore, they slide along each other's surfaces resulting not only in a higher degree of order within the microfibrils but also the microfibrils themselves are more perfectly aligned.

SUMMARY OF RESULTS

In order to make a judgment whether the cellulose fine structure is modified in the wet state during the tracheid wall component removal, the following observations were made:

1. The component removal (solubilized lignin and hemicelluloses) from the tracheid walls continues through the oxidative delignification, the water washing, and the hygrothermal treatment. The amount of tracheid wall components extracted into reaction liquor and into wash water increases with the time of oxidative delignification while the amount of tracheid wall components removed during the hygrothermal treatment is independent of the length of reaction time and is about 9% of the ovendry weight of unextracted wood.

2. The holowood block retains the tracheid-to-tracheid bonding throughout the reaction range (to 57% yield) as long as it remains in the reaction liquor, but undergoes dimensional changes when soaked in distilled water. The holowood block expands up to 20% tangentially, up to 8% radially, and 0.6% longitudinally during water washing (at 57% yield).

3. The hygrothermal treatment of washed holowood (8 hours at 95°C.) results in an additional expansion of about 15.5% tangentially, 4% radially, and 0.4% longitudinally (at 57% yield). At this point the tracheid-to-tracheid bonding diminishes, particularly along the radial walls.

4. The volumetric expansion of the holowood block in the reaction liquor beyond the water-logged condition of wood is only about 3.5% for 57% yield holowood (120 days). This comprises about 4% tangential expansion and 0.5% radial shrinkage. In 250 days, the tangential expansion is about 5.5%, while the radial shrinkage is still about 0.5%. The swollen specific volume of pulps in reaction liquor increases about 17% during reaction from 71.5% yield (30 days) to 57% yield. However, after correcting for the volume of the removed components, the water-holding capacity of the holocellulose tracheid walls increases only 5%. Hence, the tracheid walls do not swell appreciably in the reaction liquor during the entire delignification period.

5. Water washing of the holowood results in volumetric expansion at any degree of delignification (down to 57% yield). The tangential expansion is only about 3% for holowood delignified to 61% yield but increases to 20% as the yield decreases to 57%. The 70% yield holowood expands 0.2% radially during the first few hours of water washing but subsequently shrinks slightly, while the 57% yield holowood expands throughout water washing and reaches 8% expansion in 50 hours. Water washing results in an increase in the swollen specific volume of pulp and this increase becomes larger as the yield decreases. For the 57% yield pulp, the swollen specific volume increases by 74%, which corresponds to a 66% increase in the tracheid wall water-holding capacity.

6. The hygrothermal treatment results in up to a 24% decrease in the holocellulose tracheid wall water-holding capacity (as determined by

the centrifugal water retention technique) even though the holowood block expands 20% in volume (57% yield pulp).

7. The crystallinity index and the degree of order of the highly ordered regions decrease during the room temperature sodium chlorite delignification as determined on holowood sections still in the reaction liquor.

8. Water washing of holowood sections results in a considerable recovery of the crystallinity index, while the degree of order of the highly crystalline region remains relatively unchanged. The orientation angle of the highly ordered regions relative to the tracheid longitudinal axis widens during water washing. The longer the reaction is carried out, the larger are the changes in the cellulose fine structure during washing.

9. The hygrothermal treatment of the washed holowoods results in a further increase in the crystallinity index and in a considerable increase in the degree of order of the highly ordered regions. The average crystallite orientation angle is relatively unaffected.

10. Hygrothermal treatment of green sapwood results in increases in the crystallinity index and the degree of order of the highly ordered regions.

11. Heating of the air-dried holowood sections at 105°C. and 9.7% moisture content for two hours results in an increase in the crystallinity index and in a strong increase in the degree of order of the highly ordered region.

12. Washed holocellulose tracheids (57% yield) behave dimensionally in a similar manner in the electrolyte solutions as in the reaction medium. When the pulp is submerged in the liquor (1.1N $NaClO_2$ + removed wood constituents) or in a 0.1N electrolyte solution, the swollen specific volume decreases about 32%, indicating shrinking of the tracheid walls.

13. Water washing of reaction liquor submerged, previously washed pulp, results in a 47% increase in the swollen specific volume. The corresponding figures are 33, 9, and -5.5% for pulps submerged in monovalent, divalent, and trivalent cationic electrolyte solutions, respectively.

14. Water washing after treatment with the cation scavenger (EDTA) results in a recovery of the swollen specific volume loss of 75% for univalent, 58% for divalent, and 44% for trivalent cationic electrolyte solution soaked pulps.

15. Treatment with the 0.1N acids and 0.1N alkalies results in a 32% and in a 39% reduction, respectively, in the swollen specific volume of washed pulps. The subsequent water washing results in a 59% recovery of the swollen specific volume loss for alkali-treated pulps. In the case of the acid treatment the tracheid wall shrinkage is irreversible.

CONCLUSIONS

On the basis of the x-ray diffraction analysis on wet holowood sections, it is concluded that the highly ordered regions of cellulose become less ordered during the oxidative solubilization of lignin, and that during the removal of the solubilized components by water washing, the amount of highly ordered cellulose increases.

Since the crystallinity index increases and average orientation of crystallites relative to tracheid longitudinal axis increases during water washing of holowood, and since the crystallinity index and degree of order of highly ordered regions of cellulose increase during hygrothermal treatment of both green wood and washed holowood, it must be concluded that the fine structure of cellulose can be readily modified in the never-dried condition. Changes in the concentration of ionic medium as well as the temperature increase can result in changes in the amount of and in the degree of order of the highly ordered cellulose. Hence, the fine structure of cellulose in any given sample is dependent on the previous treatment sequence. This also suggests that the cellulose fine structure can be manipulated in the never-dried state to optimize desired fiber properties.

Both the hygrothermal treatment of wood and the soaking of the water-logged wood in the oxidizing liquor result in small tangential expansion and radial shrinkage of the wood blocks, suggesting that either softening or partial solubilization of the encrusting lignin is needed if the tracheid walls are to undergo dimensional changes. However, these dimensional changes cannot be attributed solely to lignin removal, since tangential expansion and radial shrinkage are also observed for holowood (about 70% yield) with only about 4% lignin remaining.

Apparently, the cellulose microfibrils, rather than the encrusting and matrix constituents, control the direction and the magnitude of the dimensional changes of tracheid walls. When only a trace of lignin and decreasing amounts of hemicelluloses are present, holowood blocks expand both tangentially and radially with the tangential change being larger, which is similar to that occurring during swelling or drying of wood.

Holowood block expansion simultaneously in tangential, radial, and longitudinal directions, is consistent with the extensibility of the microfibrils in the never-dried tracheid walls.

During water washing, as holowood block dimensions increase in all three morphological directions, the lamellae within the tracheid walls are stretched. The straining of lamellae results in a better alignment of cellulose molecules in the paracrystalline regions as well as alignment of highly ordered cellulose regions, and the increase in the degree of order of cellulose is a consequence of the tracheid walls expansion.

The water washing of holowood results in an increase in the amount of highly ordered cellulose, while the hygrothermal treatment results in both an increase in the amount of highly ordered cellulose and an increase in the degree of order of the highly ordered regions. In both cases, the holowood expands in all morphological directions. The lamellae are stretched and the microfibrils are strained resulting in an increase in the amount of highly aligned (ordered) cellulose. However, the increase in degree of order of these highly ordered regions suggests that additional mechanisms may be involved during hygrothermal treatment.

The increase in the crystallinity index along with the decrease in the radial width at half height of the 002 crystallite plane diffraction maxima during the expansion of the tracheid walls indicates that a model of the tracheid wall lamellae in the never-dried condition must include a mechanism for an increase in the degree of order of cellulose and perhaps even for an increase in the cellulose-to-cellulose bonding.

The holowood and the resulting pulp do not swell more than about 5% beyond the water-logged condition of original wood in the reaction liquor indicating that the removal of lignin does not result in marked swelling. On water washing, however, the holowood expands and the swollen specific volume of pulp increases, with the largest changes observed at the lowest yield (down to 57%) even though the hemicellulose content has decreased. Hence, the dimensional stability of the holowood in the reaction liquor or its expansion on water washing cannot be directly attributed to the amounts of encrusting and matrix constituents of the tracheid walls.

Since the block expansion and the swollen specific volume increase of pulps do not commence until water washing, when not only the solubilized tracheid wall components but also the sodium cations are removed from the tracheid walls, it is hypothesized that these changes are related to the ionogenic groups within the tracheid walls. Apparently, as the sodium cation concentration decreases in the bulk solution during water washing, the Na^+ counterions are removed from the vicinity of the charged surfaces by thermal motion. Consequently, the electrical double layer expands, resulting in an electrostatic repulsion of the charged surfaces. This is accompanied by the development of Donnan potential of ionized internal groups, which causes diffusion of water into

amorphous hemicellulose and cellulose regions within and between lamellae. Thus, the apparent expansion of the tracheid walls could be attributed to the electrical double layer electrostatic repulsion and Donnan potential swelling forces.

ACKNOWLEDGMENTS

I wish to express my deep gratitude and sincere thanks to The Institute of Paper Chemistry for providing the opportunity and the atmosphere inducive to carry out this work. Special thanks for encouragement, continued interest, and guidance willingly provided go to the Thesis Advisory Committee: Drs. N. S. Thompson (Chairman), J. P. Brezinski, and I. H. Isenberg. The critical discussions with Dr. D. G. Williams are greatly appreciated.

The author is indebted to Messrs. P. F. Van Rossum, M. C. Filz, Jr., L. E. Dambruch, K. W. Hardacker, and B. D. Andrews for their help in the construction and assembling of experimental apparatus. Thanks go to Mrs. H. Kaustinen and Mr. J. P. Rademacher for lignin analysis and to L. G. Borchardt for the sugar analyses. The work of C. H. Schabo and F. R. Sweeney for the reproductions is appreciated.

Sincerest thanks go to my wife, Judy, and little daughter, Michele, who have made this effort personally meaningful to me. Not only have they provided daily inspiration but Judy has also shared in the frustrations and rewards involved in thesis research by doing the typing throughout the course of this work.

We are all products of a civilization which emphasizes always black or white, hot or cold, day or night. Always it is either-or, where more-or-less is a better explanation of the facts.

Alfred Korzybski

LITERATURE CITED

1. Rånby, B. C. The fine structure of cellulose fibrils. In Bolam's Fundamentals of papermaking fibers. p. 72. Kenley, Surrey, England, Tech. Soc. of the Brit. Paper & Board Makers' Assocn., Inc., 1958.

2. Thomas, E. N., and Heroitt, J., Nature 136:69-70(1935).

3. Astbury, W. T., Preston, R. D., and Norman, A. G., Nature 136:391(1935).

4. Preston, R. D., and Allsopp, A., Biodynamica 53:1(1939).

5. Preston, R. D. The molecular architecture of plant cell walls. New York, John Wiley & Sons Inc., 1952. 221 p.

6. Nelson, R., J. Polymer Sci. 51, no. 155:27-58(1961).

7. Marton, R., and McGovern, S. D. Relation of crystallite dimensions and fibrillar orientation to fiber properties. In Page and Weiner's TAPPI STAP No. 8, The physics and chemistry of wood pulp fibers. p. 153. New York, TAPPI, 1970.

8. Heyn, A. N. J., J. Polymer Sci., 3A:1251-65(1965).

9. Stone, J. E., and Scallan, A. M., Tappi 50, no. 10:496-501(1967).

10. Stone, J. E., and Scallan, A. M., Cellulose Chem. Technol., no. 2:343-58 (1968).

11. Ahlgren, P. A., Yean, W. Q., and Goring, D. A. I., Tappi 54, no. 5:737-40 (1971).

12. Esau, K. Plant anatomy. 2nd ed. New York, John Wiley & Sons Inc., 1965.

13. Panshin, A. J., and de Zeeuw, C. Textbook of wood technology. Vol. 1. 3rd ed. New York, McGraw-Hill, 1970. 704 p.

14. Isenberg, I. H. The structure of wood. In Browning's The chemistry of wood. p. 7. New York, Interscience, 1963.

15. Kerr, T., and Bailey, I. W. In Panshin and de Zeeuw's Textbook of wood technology. Vol. 1. 3rd ed. p. 35. New York, McGraw-Hill, 1970.

16. Dunning, C. E. An examination of longleaf pine cell wall morphology by electron microscopy of single fibers. Doctor's Dissertation. Appleton, Wis., The Institute of Paper Chemistry, 1968. 409 p.; Tappi 52, no. 7:1326-41(1969).

17. Browning, B. L. The composition and chemical reactions of wood. In Browning's The chemistry of wood. p. 57. New York, Interscience, 1963.

18. Browning, B. L., and Isenberg, I. H. Analytical data and their significance. In Wise and Jahn's Wood chemistry. 2nd ed. Vol. 2. p. 1259. ACS Monograph Series No. 97. New York, Reinhold, 1952.

19. Meier, H. General chemistry of cell walls and distribution of the chemical constituents across the walls. In Zimmermann's The formation of wood in forest trees. p. 137. New York, Academic Press, 1964.

20. Harlow, W. M. The chemistry of the cell walls of wood. In Wise and Jahn's Wood chemistry. 2nd ed. Vol. 1. p. 99. ACS Monograph Series No. 97. New York, Reinhold, 1952.

21. Timell, T. E. Wood and bark polysaccharides. In Côté's Cellular ultrastructure of woody plants. p. 127. Syracuse, New York, Syracuse University Press, 1965.

22. Fergus, B. J., and Goring, D. A. I., Holzforschung 24, no. 4:118(1970); Wood Sci. Technol. 3:117-38(1969).

23. Klauditz, W., Holzforschung 6, no. 3:70-82(1952); 11, no. 4:110-16(1957).

24. Stone, J. E., and Clayton, D. W., Pulp Paper Mag. Can. 60, no. 10:T476-84 (1960).

25. Leopold, B., Tappi 44, no. 3:232-5(1961).

26. Leopold, B., and McIntosh, D. C., Tappi 44, no. 3:235-40(1961).

27. Mark, R. E. Cell wall mechanics of tracheids. New Haven, Yale University Press, 1967. 310 p.

28. Harada, H. Ultrastructure and organization of gymnosperm cell wall. In Côté's Cellular ultrastructure of woody plants. p. 215-33. Syracuse, New York, Syracuse University Press, 1965.

29. Schuerch, C. The hemicelluloses. In Browning's The chemistry of wood. p. 191. New York, Interscience, 1963.

30. Meyer, K. H. High polymers. Vol. IV. Natural and synthetic high polymers. New York, Interscience, 1942. 891 p.

31. Cowdrey, D. R., and Preston, R. D. The mechanical properties of cell wall. In Côté's Cellular ultrastructure of woody plants. p. 473. Syracuse, New York, Syracuse University Press, 1965.

32. Marx-Figini, M., and Schulz, B. V., Naturwissenshaften 53, no. 18:466-74 (1966); Chem. Titles 21:134(1966).

33. Hermans, P. H. Physics and chemistry of cellulose fibres. New York-Amsterdam, Elsevier Publ. Co., 1949. 534 p.

34. Meyer, K. H., and Misch, L., Helv. Chim. Acta., 20:232(1937).

35. Ellefsen, O., and Tonnesen, B. A. Some aspects of the polymorphic forms and structure of cellulose. In Page and Weiner's TAPPI STAP No. 8. The physics and chemistry of wood pulp fibers. p. 50. New York, TAPPI, 1970.

36. Liang, C. Y., and Marchessault, R. H., J. Polymer Sci. 37, no. 132:385-95 (1959); 39, no. 135:269-78(1959).

37. Howsmon, J. A., and Sisson, W. A. Submicroscopic structure. In Ott's Cellulose and cellulose derivatives. 2nd ed. Part I. p. 231. New York, Interscience, 1954.

38. Frey-Wyssling, A., Fortschr. Chem. Org. Naturstoffe 27:1-30(1969).

39. Fahmy, Y., and Mobarak, F., Svensk Papperstid. 74, no. 15:1-9(1971).

40. Heyn, A. H. J., J. Ultrastruct. Res. 26, no. 1/2:52-68(1969).

41. Mühlethaler, K., and Frey-Wyssling, A., Macromol. Chem. 62:23-30(1963).

42. Hearle, J. W. S. The development of ideas of fine structure. In Hearle and Peter's Fibres structure. p. 209. Manchester, Butterworth's, 1963.

43. Frey-Wyssling, A., Science 119:80-2(1954).

44. Hearle, J. W. S., J. Polymer Sci. 20C:215-51(1967).

45. Fengel, D., Tappi 53, no. 3:497-503(1970).

46. Jeffries, R., Jones, D. M., Roberts, J. G., Selby, K., Sismmens, S. C., and Warwicher, J. O., Cellulose Chem. Technol. 3:255-74(1969).

47. Mühlethaler, K. The fine structure of the cellulose microfibril. In Côté's Cellular ultrastructure of woody plants. p. 191. Syracuse, New York, Syracuse University Press, 1965.

48. Sullivan, J. D., and Sachs, I. B., Forest Prod. J. 16, no. 9:83-6(1966).

49. Asunmaa, S. K., and Schwab, D. W. Aspen holocellulose and interfiber bonding. In Côté's Cellular ultrastructure of woody plants. p. 573. Syracuse, New York, Syracuse University Press, 1965.

50. Ritter, G. J., Ind. Eng. Chem. 20:241(1928); Paper Ind. 16:178(1944).

51. Bailey, I. W., and Kerr, T., J. Arnold Arbor. 16:273-300(1935).

52. Stone, J. E., and Scallan, A. M., Pulp Paper Mag. Can. 69:T288-93(1968).

53. Wardrop, A. B., Appita 16, no. 3:XV-XXX(1963).

54. McIntosh, D. C., Tappi 50, no. 10:482-8(1967).

55. Page, D. H., and DeGrace, J. H., Tappi 50, no. 10:489-95(1967).

56. Morehead, F. F., Tappi 46, no. 9:524-30(1963).

57. Kaustinen, H. M. Unpublished work. Appleton, Wis., The Institute of Paper Chemistry, 1971.

58. Jayme, G., and Fengel, D., Holz Roh-Werkstoff 19:50-4(1961).

59. Norberg, P. H., Svensk Papperstid. 73, no. 7:208(1970); 71, no. 23:869-71 (1968).

60. Stone, J. E., Scallan, A. M., and Aberson, G. M. A., Pulp Paper Mag. Can. 67, no. 5:264(1966).

61. Preston, R. D. Observed fine structure in plant fibres. In Hearle and Peter's Fibre structure. p. 235. London, Butterworth, 1963.

62. Wardrop, A. B., Tappi 40, no. 4:225-43(1957).

63. Peterlin, A., and Ingram, P., Textile Res. J. 40, no. 4:345-54(1970).

64. Berkley, E. E., and Kerr, T., Ind. Eng. Chem. 38:304(1946).

65. Preston, R. D. Molecular architecture of plant cell walls. New York, John Wiley & Sons Inc., 1952. 176 p.

66. Rånby, B. G., and Katzmire, J. L. The formation of the cellulose lattice. In Cellulose Research Institute's Proc. First Cellulose Conference. p. 41. Syracuse, New York, Cellulose Research Inst., 1958.

67. Preston, R. D., Wardrop, A. V., and Nicolai, E., Nature 162:957(1958); Biochim. Biophys. Acta 3:549-59(1949).

68. Preston, R. D., Proc. Roy. Soc., B 134:202-18(1947).

69. Clark, G. L., Pickett, L. W., and Farr, W. K., Science 71:293(1930).

70. Berkley, E. E., Textile Research 9:355(1939).

71. Ritter, J. G., and Stillwell, C. W., Paper Trade J. 98:37(May 31, 1934).

72. Murphey, W. K., Forest Prod. J. 13, no. 4:151-5(1963).

73. Tarkow, H., and Feist, W. C., Tappi 51, no. 2:80-3(1968).

74. Stone, J. E., and Scallan, A. M., J. Polymer Sci., C11:13-25(1965).

75. Stone, J. E., Pulp Paper Mag. Can. 65:T3-12(1964).

76. Alexander, S. D., Marton, R., and McGovern, S. D., Tappi 51, no. 6: 277-83(1968).

77. Wardrop, A. B., Nature 164:366(1949); Austral. J. Botany 2:154(1954); 3:3177(1955).

78. Vogel, A., Makromol. Chem. 11:111(1953).

79. Jayme, G., and Roeffael, E., Papier 23, no. 1:1-7(1969).

80. Clark, G. L., Tappi 33, no. 8:108-10, 384-6(1950).

81. Spiegelberg, H. L. The effect of hemicellulose on the mechanical properties of individual pulp fibers. Doctor's Dissertation. Appleton, Wis., The Institute of Paper Chemistry, 1966. 115 p.; Tappi 49, no. 9:388-96 (1966).

82. Emerton, H. W. Fundamentals of the beating process. Kenley, B.P. & B.I.R.A., 1958. 198 p.

83. Dolmetsch, H., Cellulose Chem. Technol. 3, no. 3:253-7(1969).

84. Hermans, P. H., and Weidinger, A., J. Am. Chem. Soc. 68:2547, 2730(1946); J. Polymer Sci. 4:135(1949).

85. Hermans, P. H. Contribution to physics of cellulose fibers. Amsterdam, Elsevier, 1946. 221 p.

86. Hermans, P. H. Physics and chemistry of cellulose fibres. New York-Amsterdam, Elsevier, 1949. 534 p.

87. Vigo, T. L., Mitcham, D., and Welch, C. M., J. Polymer Sci. (B. Polymer Letters) 8, no. 6:385-94(1970).

88. Risch, K. Thesis, Zurich (1930). In Herman's Physics and chemistry of cellulose fibres. p. 192. New York-Amsterdam, Elsevier, 1949.

89. Thompson, N. S., and Kaustinen, O. A., Can. pat. 806,573(Feb. 18, 1969).

90. Thompson, N. S., and Kaustinen, O. A., Tappi 53, no. 8:1502-6(1970).

91. Thompson, N. S., and Kaustinen, O. A., Tappi 47, no. 3:157-62(1964).

92. Hatt, W. K., Forest Service Circular, no. 39, 1906.

93. Koehler, A., Proc. Wood Preservers' Assocn. 29:376-88(1933).

94. MacLean, J. D., Proc. Wood Preservers' Assocn. 48:136-57(1952).

95. Kubler, H., Holz Roh-Werkstoff 17:77-86(1959).

96. Yokota, T., and Tarkow, H., Forest Prod. J. 12, no. 1:43(1962); J. Japan Wood Res. Soc. 7, no. 5:217-21(1961).

97. Stevens, W. C., Timber Technol. 61, no. 2171:427-8(1958).

98. Coward, H. G., and Spencer, L., J. Textile Inst. 14:T28(1923).

99. Jayme, G., and Rothamel, L., Papier 2, no. 1/2:7-18(1948); 9, no. 19/20: 476-82(1955).

100. Thode, E. F., Bergomi, J. G., and Unson, R. E., Tappi 43, no. 5:505-12 (1960).

101. Preston, J. M., Nimkar, M. V., and Gundavde, S. P., J. Textile Inst. 42:T79-90(1951).

102. Silvy, J., Sarret, G., and Jestin, F. Venice, EUCEPA, 1964. 169 p.

103. German Standard Method: Merkblatt IV/33/57 Zellcheming.

104. Aggebrant, L. G., and Samuelson, O., J. Appl. Polymer Sci. 8:2801-12 (1964).

105. Segal, L., Textile Res. J. 32:702(1962).

106. Nelson, M. L., and Schultz, E. F., Jr., Textile Res. J. 33:515(1963).

107. Ellefsen, O., Lund, W. E., Tonnesen, B. A., and Oien, K. Norsk Skogind. 11, no. 9:284-93, 349-55(1957).

108. Hermans, P. H., and Weidinger, A., J. Appl. Phys. 19, no. 5:491-506(1948).

109. Hermans, P. H., and Weidinger, A., Textile Res. J. 31, no. 6:558-71(1961).

110. Segal, L., Creely, J. J., Martin, A. E., Jr., and Conrad, C. M., Textile Res. J. 29, no. 10:786-94(1959).

111. Ant-Wuorinen, O., and Visapää, A., Paperi Puu 47, no. 5:311-22(1965).

112. Ray, P. K., Textile Res. J. 37:434(1967).

113. Ray, P. K., J. Appl. Polymer Sci. 13:2593-600(1969).

114. Caulfield, D. F., and Steffes, R. A., Tappi 52, no. 7:1361-6(1969).

115. Narten, A. H. X-ray diffraction data on liquid water in the temperature range 4°C.-200°C. Oak Ridge, Tennessee, Oak Ridge National Laboratory, ORNL-4578, UC-4-Chemistry Union Carbide Corporation, U.S. Atomic Energy Commission, July, 1970. 70 p.

116. Jentzen, C. A. The effect of stress applied during drying on some of the properties of individual pulp fibers. Doctor's Dissertation. Appleton, Wis., The Institute of Paper Chemistry, 1964. 130 p.

117. Wardrop, A. B., Textile Res. J. 22:288(1952).

118. Clark, G. L., Tappi 33, no. 2:108-10(1950).

119. Kantola, M., and Seitsonen, S. X-ray orientation investigations on Finnish conifers. Suomalaisen Tiedeakatemian Toimituksia, Series A, VI Physica, 80:15 p.(1961).

120. Seitsonen, S. On the analysis of x-ray diffraction patterns of conifer wood. Turun Yliopiston Julkaisuja, Series A, 11:46 p.(1967).

121. Sisson, W. A., and Clark, G. L., Ind. Eng. Chem. Anal. Ed. 5, no. 5:296-300(1933).

122. Sisson, W. A., Ind. Eng. Chem. 27, no. 1:51-6(1935).

123. Meylan, B. A., Forest Prod. J. 17, no. 5:51-8(1967).

124. Sisson, W. A., J. Phy. Chem. 40:343(1936).

125. DeLuca, L. B., and Orr, R. S., J. Polymer Sci. 54:457-70, 471-89(1961).

126. Scherrer, P., Gottinger Machrichten 2:98(1918); In Klug and Alexander's X-ray diffraction procedures. Chap. 9. New York, John Wiley & Sons Inc., 1954.

127. Klug, H. P., and Alexander, L. E. X-ray diffraction procedures. New York, John Wiley & Sons Inc., 1954. 716 p.

128. Thompson, N. S., Kremers, R. E., and Kaustinen, O. A., Tappi 51:123-6, 127-31(1968).

129. Thomas, B. B., Paper Ind. 26:1281(1945); 27:374, 382(1945).

130. Bublitz, W. J., Tappi 34, no. 9:427(1951).

131. Meier, H., Acta Chem. Scand. 14:749(1960).

132. Stamm, A. J. Wood and cellulose science. New York, Roland, 1964. 549 p.

133. Stamm, A. J., and Loughborough, W. K., J. Phys. Chem. 39:121-32(1935).

134. Ahlgren, P. A., and Goring, D. A. I., Can. J. Chem. 49, no. 8:1272-5(1971).

135. Albrecht, J. S. An investigation of the physical-chemical mechanism of selective delignification of wood with peracetic acid. Doctor's Dissertation. Appleton, Wis., The Institute of Paper Chemistry, 1971. 190 p.

136. Stöckmann, V. E. Cellulose elementary fibrils possess entropic deformation mechanism. Paper read at Seventh Cellulose Conference at State University College of Forestry, Syracuse, New York, Syracuse University, June 9-11, 1971.

137. Pauli, W., and Handovsky, H., Biochem. Z. 18:340(1909); 24:239(1910).

138. Bovard, W. M., Paper 22, no. 3:11(1918).

139. Gasell, W. H., and Minor, J. E., Paper 24, no. 12:15(1919).

140. Tolman, R. C., and Stearn, A. E., J. Am. Chem. Soc., 40:264(1918).

141. Proctor, H. R., and Wilson, J. A., J. Chem. Soc. 109:307(1916).

142. Freundlich, H. Colloid and capillary chemistry. p. 553-6. New York, E. P. Dutton and Co., Inc., 1922.

143. Yorston, R. H., Forest Prod. Lab. of Canada, Pulp and Paper Lab Quar. Rev., no. 20:11(Oct.-Dec., 1934); no. 22:1-2(April-June, 1935); BIPC 5:218; 6:216(1935-1936).

144. Jacquelin, G., Svensk Papperstid. 66:801-11(1963).

145. Kibblewhite, R. P., Thompson, N. S., and Williams, D. G., Wood Sci. Technol. 5, no. 2:101-20(1971).

146. Neale, S. M., and Standing, P. T., Proc. Roy. Soc. A 213:530(1952).

147. Farrar, J., and Neale, S. M., J. Colloid Sci. 7:186-95(1952).

148. Dobbins, R. J., Tappi 53, no. 12:2284(1970).

149. Sisson, W. A., and Saner, W. R., J. Phys. Chem. 43:687(1939).

150. Stamm, A. J., J. Am. Chem. Soc. 56:1195(1934).

151. Heymann, E., and Rabinov, G., J. Phys. Chem. 45:1152-66(1941).

152. Goring, D. A. I., and Mason, S. G., Can. J. Res. B. 28:307-38(1950).

153. Kanamaru, K., J. Soc. Chem. Ind., Japan 39:240(1936); Kolloid Z., 84:222 (1938); Kanamaru, K., and Takada, T., Z. Phys. Chem. A 184:179(1939); A 186:1(1940).

154. Bjorkqvist, C., and Jorgensen, L., Acta Chem. Scand. 5:978(1951).

155. Asunmaa, S., and Lange, P. W., Svensk Papperstid. 55:217(1952).

156. Kantouch, A., Hebeish, A., and El-Rafie, M. N., Textile Res. J. 40, no. 2:178(1970).

157. Donnan, F. G., and Herris, A. B., Trans. Chem. Soc. 99:1551(1911).

158. Neale, S. M., J. Textile Inst. 20:T373(1929).

159. Sivaraja Iyer, S. R., and Jayaram, R., J. Soc. Dyers Colorists 86, no. 9:398-402(Sept., 1970).

160. Mitchie, R. I. C., and Preston, R. D., Nature 190, no. 4778:803(May 27, 1961).

161. Adamson, A. W. Physical chemistry of surfaces. 2nd ed. New York, Interscience, 1967. 747 p.

162. Verwey, E. J. W., and Overbeek, J. Th. G. Theory of the stability of lyophobic celloids. Amsterdam, Elsevier Publ. Co., 1948. 205 p.

163. Campbell, W. B. The cellulose-water relationship in paper-making. Forest Service, Bull 84. Ottawa, Dept. Interior, 1933. 52 p.

164. Andersson, B., and Samuelson, O., Svensk Papperstid. 61:1001-9(1958).

165. Grundelius, R., and Samuelson, O., Svensk Papperstid. 65:273-81(1962).

166. Lottormoser, A., Trans. Faraday Soc. 31:411-14(1935).

167. Mason, S. G., Pulp Paper Mag. Can. 48, no. 8:76-80(1947).

168. Andersson, O., Svensk Papperstid. 64:417-93(1961).

169. Kibblewhite, R. P. Intercellular adhesion in resin canal tissue isolated from slash pine chlorite holocellulose. Doctor's Dissertation. Appleton, Wis., The Institute of Paper Chemistry, 1969. 172 p.

170. Bjellfors, C., Eriksson, K.-E., and Johanson, F., Svensk Papperstid. 68, no. 24:865(1965).

171. Walkush, J. C. The coagulation of cellulose pulp fibers and fines as a mechanism of retention. Doctor's Dissertation. Appleton, Wis., The Institute of Paper Chemistry, 1969.

172. MacGugan, I. C., Paper Trade J. 146, no. 2:22(1962).

173. Cohen, W. E., Farrand, G., and Watson, A. J., Appita Proc. 3:72(1949).

174. Thomas, B. B., Tappi 43:447(1960).

175. Nelson, P. F., and Kalkipsakis, C. G., Tappi 47:170(1964).

176. Masters, R., J. Chem. Soc. 121:2026(1922).

177. Sarkar, P. B., Chatterjee, H., and Mazumda, A. K., J. Textile Inst. Trans. 38:T318(1947).

178. Cohen, W. E., Farrand, G., and Watson, A. J., Appita Proc. 4:176(1965).

179. Ogiwara, Y., and Kubota, H., J. Polymer Sci., A-1, 7:2087-95(1965).

180. Ogiwara, Y., Ogiwara, Y., and Kubota, H., J. Appl. Polymer Sci. 12:2575 (1968); A-1, 6:1489(1968).

181. Sjöström, E., Enström, B., and Haglund, P., Svensk Papperstid. 68, no. 6:186-7(1965).

182. Chowdhury, F. H., and Neale, S. M., J. Polymer Sci. 1A:2881-91(1963).

183. Tondre, C., and Zana, R., J. Phys. Chem. 75, no. 21:3367-72(1971).

184. Gaillard, B. D. E., Thompson, N. S., and Morak, A. J., Carbohyd. Res. 11:509(1969).

185. Jayme, G., and Roffael, E., Papier 24, no. 6:335-40(1970).

186. Thompson, N. S., and Hankey, J. D., Tappi 51, no. 2:88-93(1968).

187. Merchant, M. V. A study of certain phenomena of the liquid exchange of water-swollen cellulose fibers and their subsequent drying from hydrocarbons. Doctor's Dissertation. Appleton, Wis., The Institute of Paper Chemistry, 1957; Tappi 40, no. 9:771-80(1957).

APPENDIX I

HYGROTHERMAL TREATMENT OF GREEN WOOD

For the green wood blocks, the first hygrothermal treatment results in a tangential expansion, in a radial shrinkage, and in a negligible change in the longitudinal dimension. The tangential expansion is about 0.45% for the heartwood and 0.95% for the sapwood during heating at 95°C. for ten hours. The effect of temperature on the green wood dimensions is the same whether the heating is done in distilled water or in the saturated air.

Initially, when bringing the test block up to temperature, the block shrinks tangentially about 0.05% during the 20°C. to 40°C. temperature interval. From 40°C. to 60°C. the block is dimensionally rather stable. At 60°C. the block begins to expand tangentially and shrink radially. The rate of dimensional change is accelerated considerably as the temperature is raised above 60°C. The blocks appear to approach an equilibrium value at any given temperature in about three hours. If the temperature is raised, the wood undergoes further tangential expansion and radial shrinkage. Some typical tangential expansion data are presented in Table XXI.

TABLE XXI

PERCENT DIMENSIONAL CHANGE OF TANGENTIAL WATERLOGGED SAPWOOD

Block	Intermediate Temperature, °C.	% Dimensional Change at the Intermediate Temperature		% Dimensional Change at 95°C.	
		2 Hours	4 Hours	2 Hours	4 Hours
T-1	40	0.015	0.020	0.950	1.00
T-2	50	0.060	0.085	0.950	--
T-3	60	0.170	0.220	0.960	1.15
T-4	70	0.400	0.450	0.960	--
T-5	80	0.650	0.675	0.970	--
T-6	95	0.860	0.940	0.975	1.015

During the first and the subsequent coolings both the tangential and the radial dimensions of the wood block increase. However, the block is dimensionally stable down to about 62°C. and only then begins to expand. This expansion is only about one-tenth of the original irreversible dimensional change.

The second and the subsequent heatings result in a decrease both in the tangential and in the radial dimensions.

EFFECT OF IONIC TREATMENT OF WOOD

The results of the hygrothermal treatment on the green wood blocks which are previously treated in 0.1M cationic solution are given in the Fig. 30. The treatment in nearly neutral electrolyte solution containing multivalent cation does not have a detectable effect on the tangential expansion of wood on the first hygrothermal treatment. In the case of 0.1M $Ba(OH)_2$ the dimensional behavior is similar to that in the 0.1M NaOH. The acetic medium seems to depress the tangential expansion. The removal of the native multivalent cations from the wood block by EDTA leaves the block more extensible.

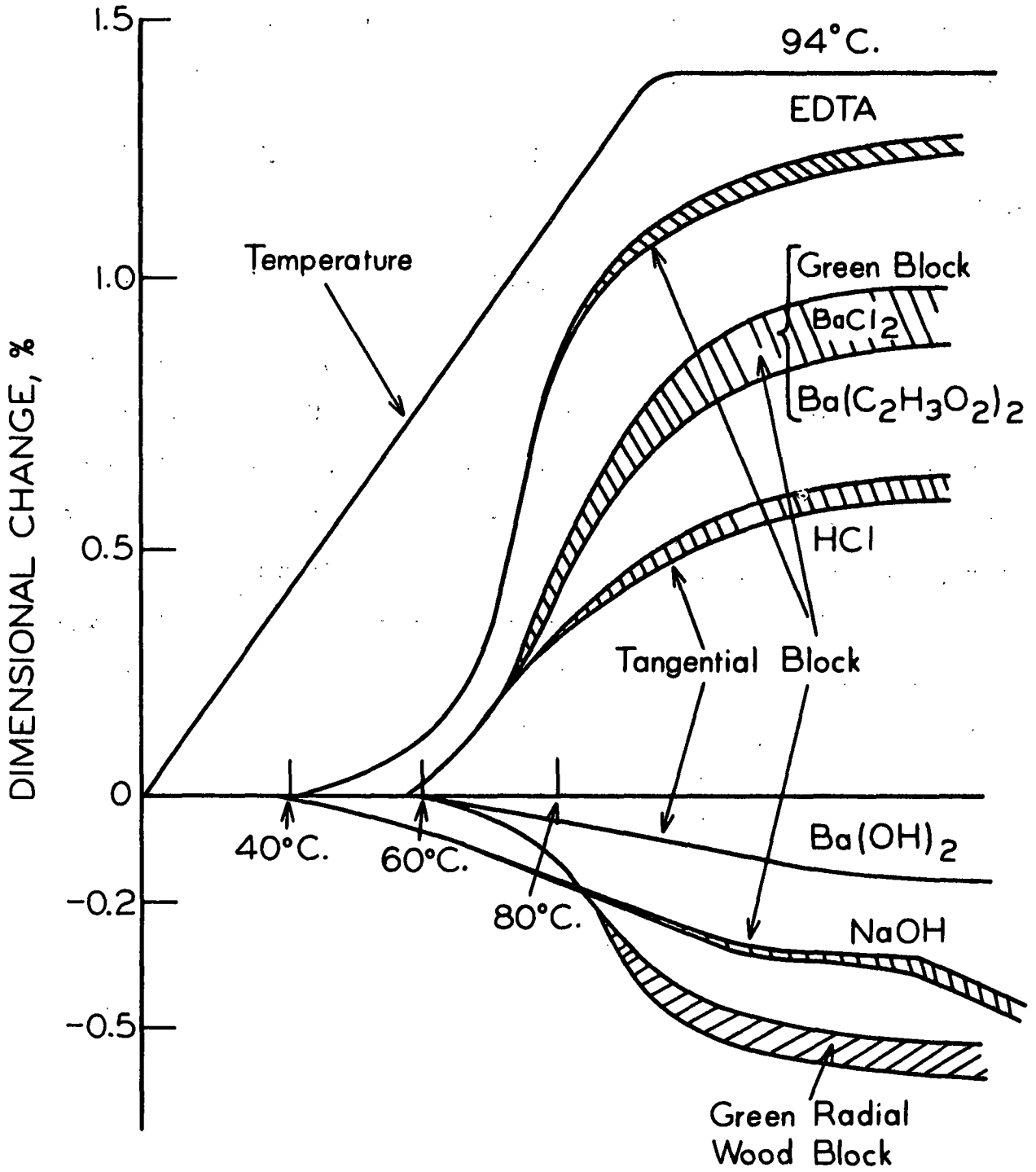

Figure 30. The Dimensional Changes of Green Wood and Impregnated Tangential Wood Blocks on the First Hygrothermal Treatment

APPENDIX II

THE DIMENSIONAL CHANGE MEASURING APPARATUS

The power source for the linear variable differential transformer (LVDT) is the Power/Mate Corporation Powertwin-99. It can take 105-125 v.a.c. input voltage and deliver an output voltage ranging from 12 to 18 v.d.c. In the present case, 15 v.d.c. is employed. The line voltage was found to fluctuate between 112 to 119 volts. The Powertwin-99 is rated to cut down this fluctuation to ± 0.004 volt.

The linear variable differential transformers employed are the Schaevitz Engineering DC-LVDT, DC-A Series, Model 050 DC-A. The full stroke displacement is ± 0.050 inch with corresponding output voltage of ± 10 v.d.c. The readout device is a Sensitive Research Instrument Corporation voltmeter.

To isolate the inherent work bench vibration from the Dimensional Change Measuring Apparatus, pads of Unisorp were placed underneath the aluminum base plate at the corners.

The linearity of the core displacement in relation to the output was tested and found to be linear for the entire displacement stroke. The procedure was as follows: A milled aluminum block is placed on the sample stage in the test chamber. The base-line voltage is adjusted by moving the LVDT body. A series of Starret Thickness Gage plates are carefully placed between the aluminum block and the detection probe. The output voltage is noted.

To determine the dimensional change of the block the following procedure is used: The test block is placed on the stage, a thin cover glass plate is

placed over the top edge of the test block to distribute the detection probe load evenly over the block, and the detection probe is lowered on the block. The detection probe supporting springs are adjusted so that the test block experiences only a few grams load. The base-line voltage is adjusted by moving the LVDT body. The chamber is filled with continually running distilled water. The reading of the output voltage is started.

APPENDIX III

A PRELIMINARY STUDY OF THE CENTRIFUGAL WATER RETENTION TECHNIQUE

The centrifugal water retention value depends on the speed of centrifugation (the centrifugal field strength) as demonstrated in the Table XXII. The field strength of 1000 g is selected for the present study.

TABLE XXII

EFFECT OF CENTRIFUGAL FIELD STRENGTH ON THE CENTRIFUGAL WATER RETENTION VALUE

Centrifugal Field Strength, g	Water Retention Value, cc./g. o.d. pulp[a]
100	8.70
500	5.15
1000	4.28
1500	4.07
2000	3.90
2500	3.63

[a] Water-washed 120-day pulp centrifuged for 30 minutes.

The effect of duration of centrifugation is demonstrated in Table XXIII. The thirty-minute centrifugation time is selected for the present study.

TABLE XXIII

SUMMARY OF THE CENTRIFUGAL WATER RETENTION VALUES AS A FUNCTION OF TIME OF CENTRIFUGATION

Sample	Centrifugal Water Retention Values, cc./g. Time of Centrifugation at 1000 g			
	15 Min.	30 Min.	45 Min.	60 Min.
Holocellulose fiber pads with salts	2.20	2.02	1.93	1.84
Washed holocellulose fiber pads	4.35	4.18	4.01	3.82
Washed and heated holocellulose fiber pads	3.92	3.70	3.51	3.43

APPENDIX IV

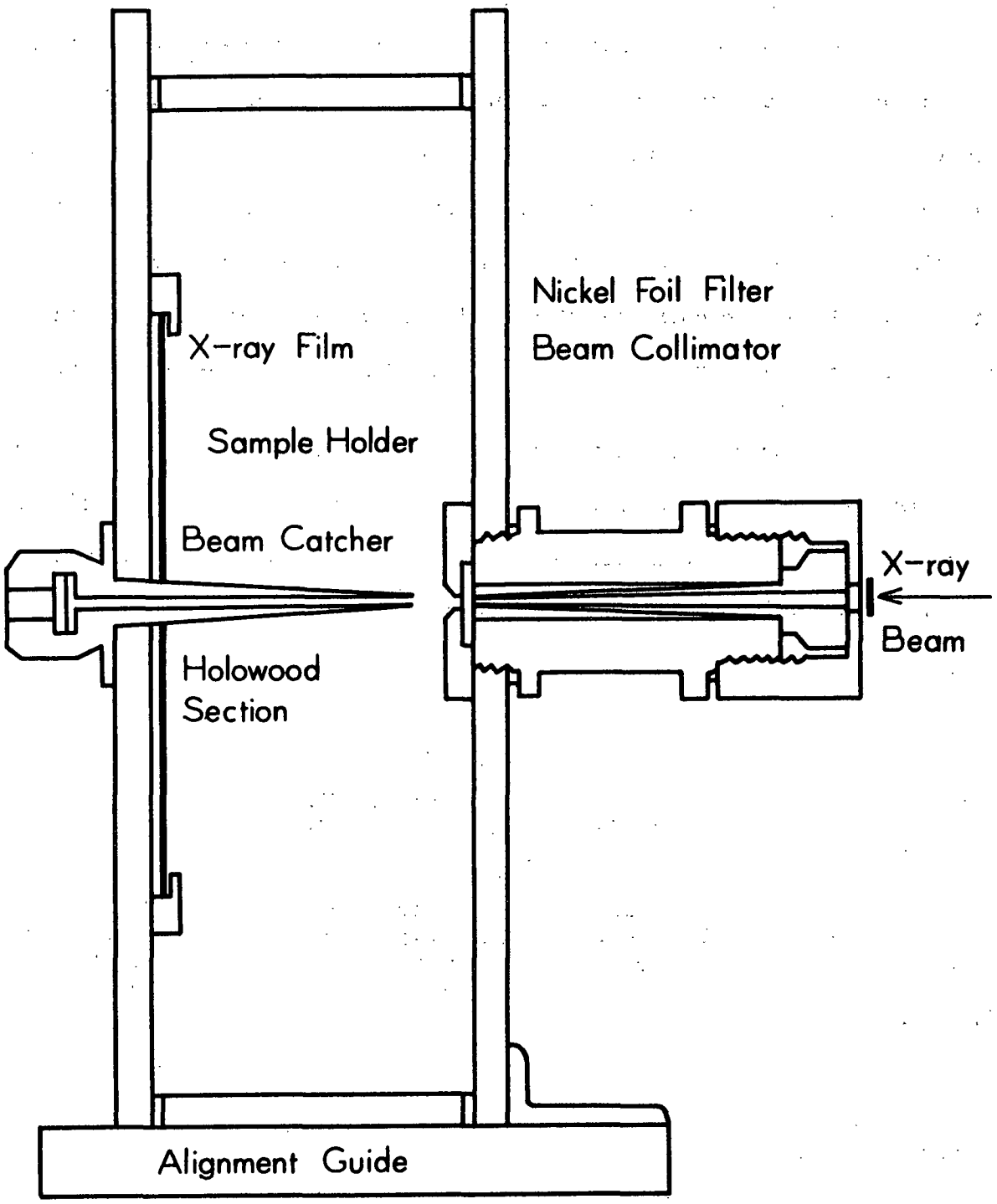

Figure 31. Schematic of Jentzen's Laue X-ray Camera

APPENDIX V

CORRECTION FOR SCATTER BY WATER, AND REACTION LIQUOR

The correction for the scattering due to water and reaction liquor is made by subtracting the intensity of scatter due to these mediums from the total intensity observed on the x-ray film. The intensities of scatter due to these mediums are determined by exposing a one millimeter thick layer of water or reaction liquor between thin cover glass plates to the x-ray primary beam. These intensities are corrected for scatter by glass by exposing the empty glass plate container to the same x-ray beam for the same length of time.

The thickness of the water layer in the wood and holowood sample is calculated from the material balance of the sample. The intensity correction is then performed on the equal time-equal mass basis (Fig. 32). Summary of the data for the water and the reaction liquor scatter of x-rays is given in Table XXIV.

TABLE XXIV

SUMMARY OF THE DATA FOR THE WATER AND REACTION LIQUOR SCATTER OF X-RAYS

Sample	Time of Exposure, hr.	Scatter Intensity at 18.5 Degrees, arbitrary units	Scatter Intensity at 22.8 Degrees, arbitrary units
Glass and air	1	34	30
	2	67	57
	3	96	86
Glass + air + water (1 mm.)	2	98	82
	3	146	123
Glass + air + reaction liquor	1 1/2	64	52

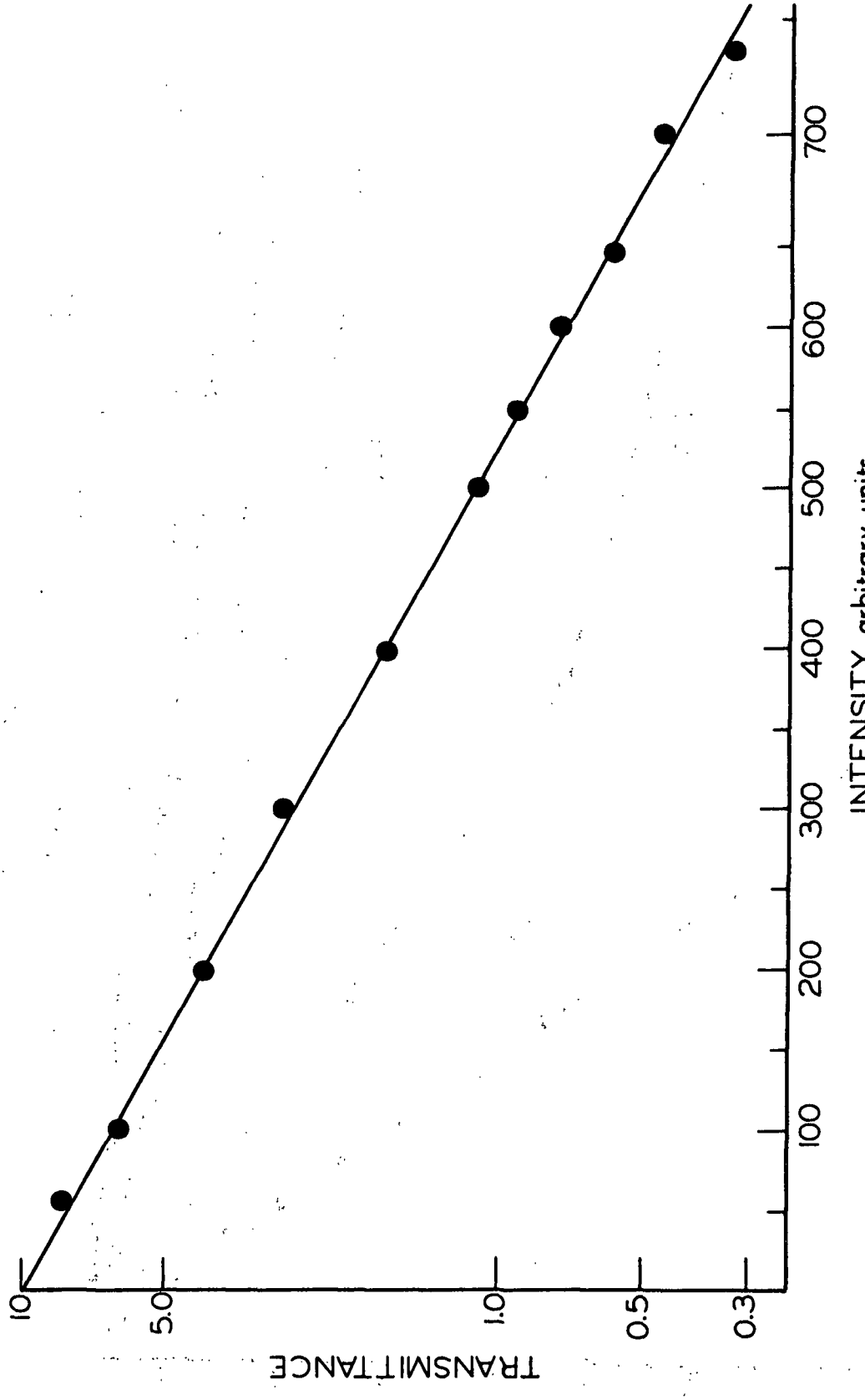

Figure 32. X-ray Film Calibration Curve

APPENDIX VI

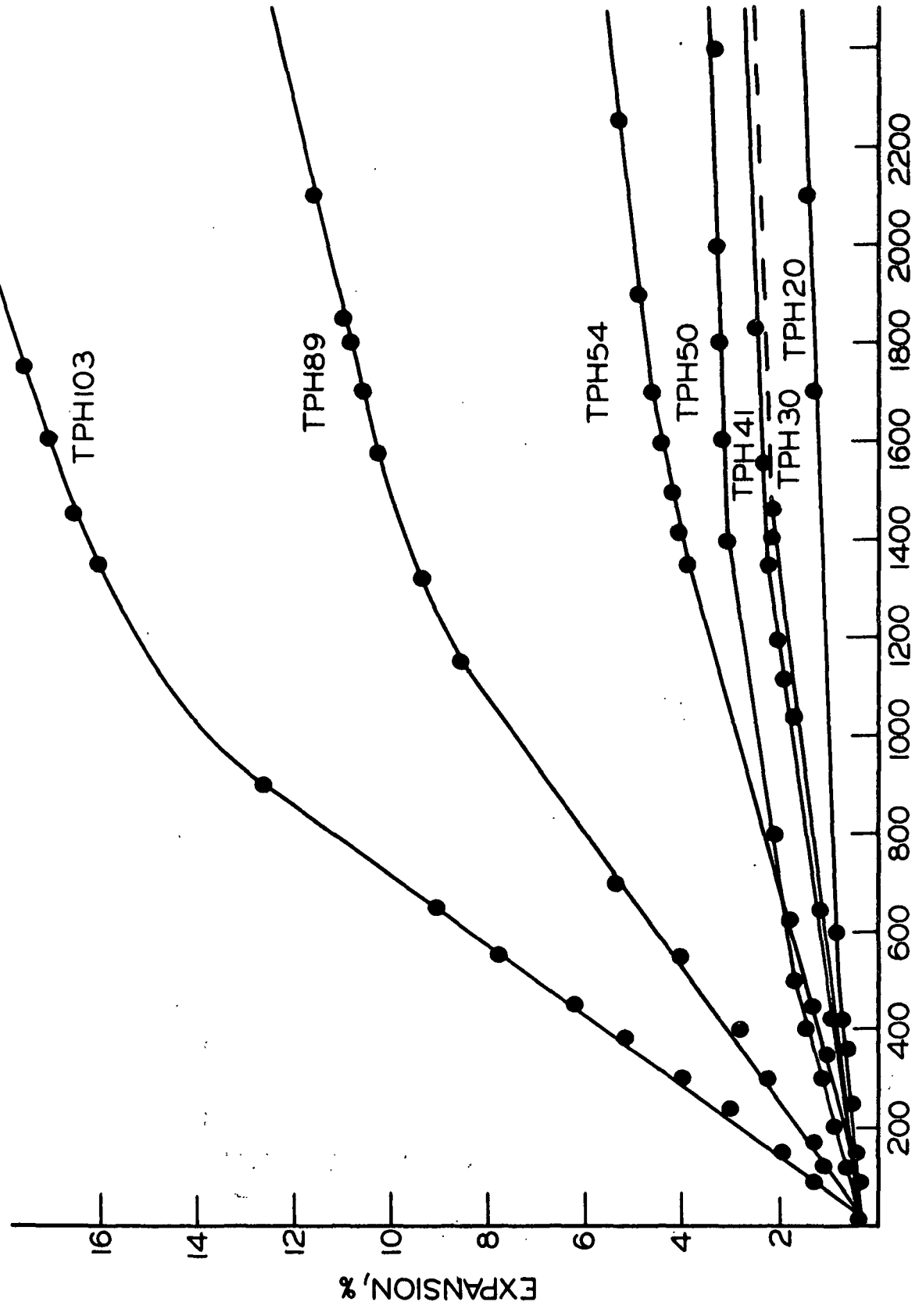

Figure 33. The Tangential Expansion on Washing of Holowood Block Delignified from Preheated Condition

APPENDIX VII

RADIAL EXPANSION OF HOLOWOOD

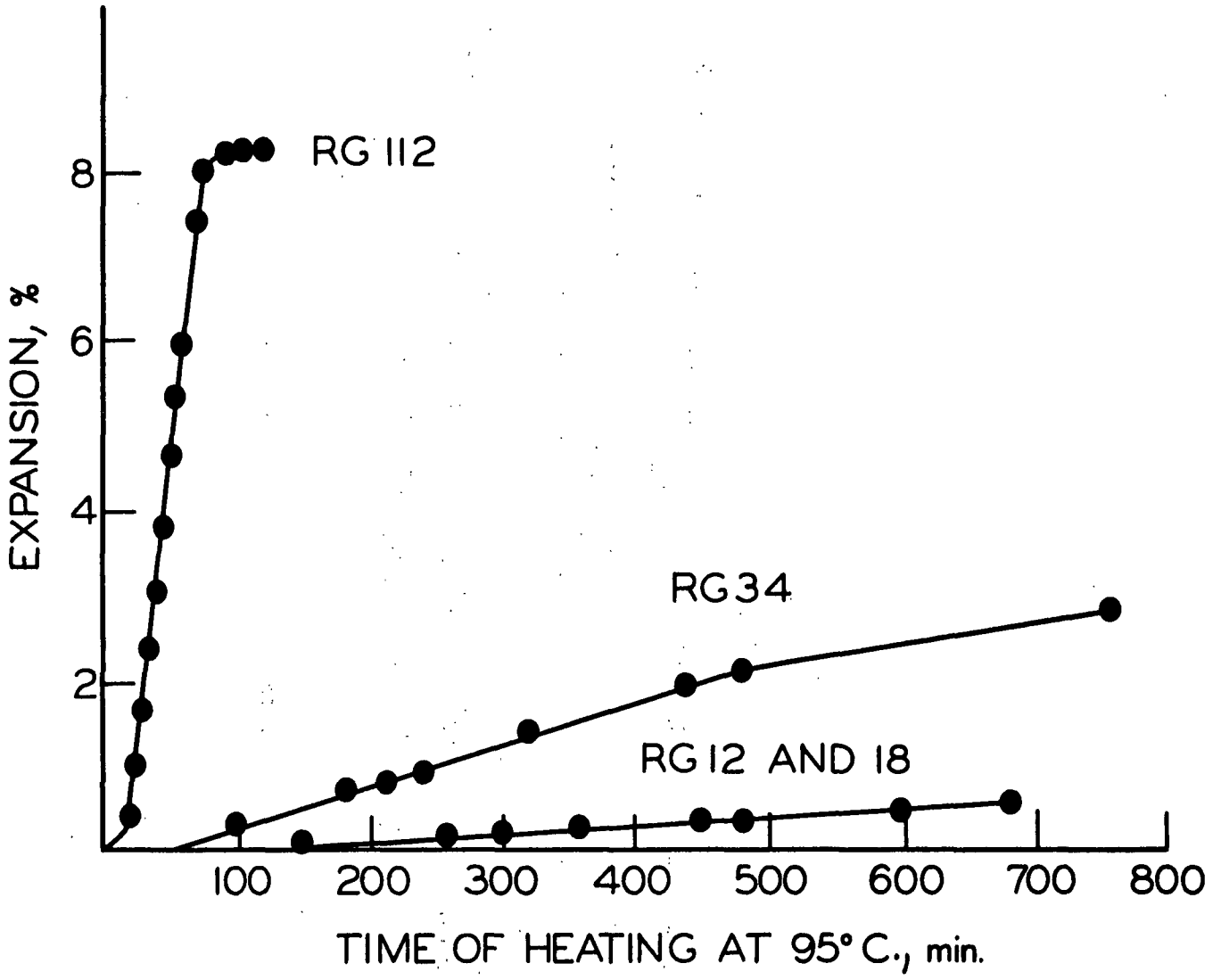

Figure 34. The Percent Expansion of Radial Holowood Blocks on Heating at 95°C. After Delignification from the Green Condition and Subsequent Water Washing

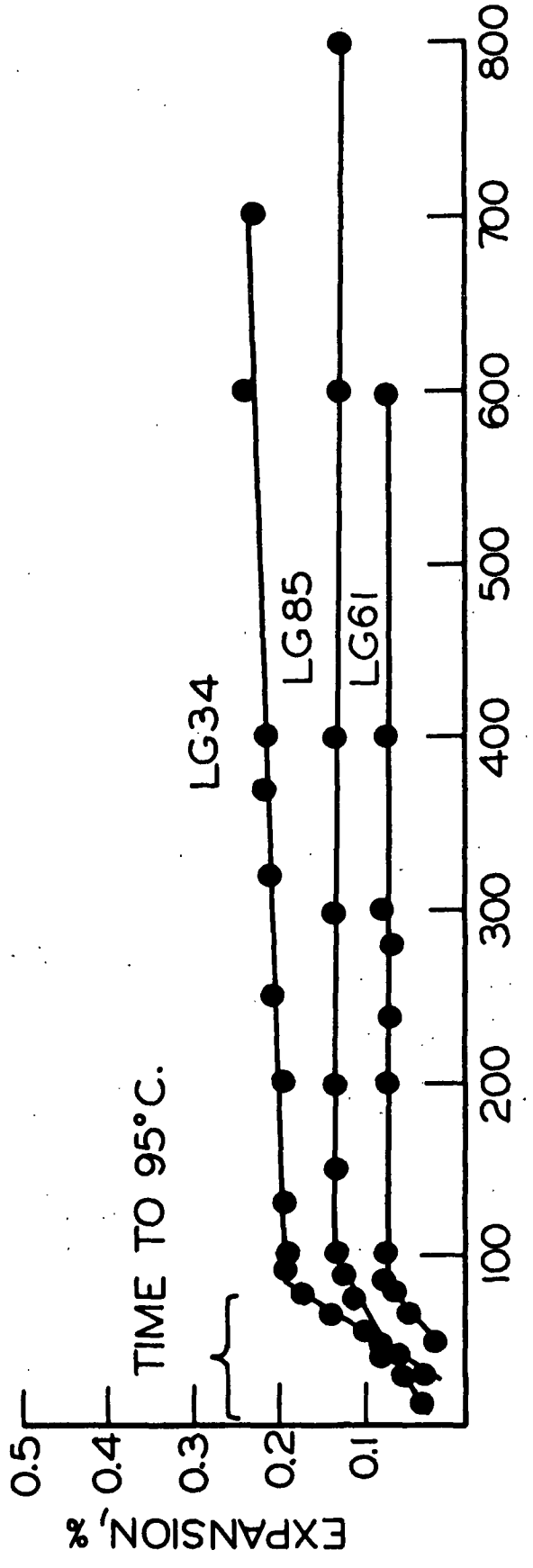

Figure 35. The Percent Expansion of Longitudinal Holowood Blocks on Heating at 95°C. After Delignification from the Green Condition and Subsequent Water Washing

APPENDIX VIII

POWDER DIAGRAM AND THE INHERENT PROCEDURES

In the powder diagram, the 021 peak interferes with the 002 peak since the diffraction is spread over 360°. In the oriented fiber diagram, the diffraction concentrates at two spots for each crystallite plane and the diffraction from the 021 plane is isolated from that of the 002 plane. For these reasons the crystallinity index and the radial width at half heights determined on oriented samples are more sensitive to the changes in the cellulose fine structure than those determined on powder diagrams.

In addition, the procedure (106) for pellet making ignores the fact that the cellulose crystallinity is not a stable equilibrium quantity. The procedure calls for Wiley milling of the sample to 20 mesh, an addition of a few drops of amyl acetate-based Duco cement, and compressing at 2500 p.s.i. for two to three minutes. All these processes are likely to affect the crystallinity of the cellulose sample and overshadow the changes under investigation.

APPENDIX IX

INCREASE IN THE DEGREE OF CRYSTALLINITY DURING THE HYGROTHERMAL TREATMENT OF CELLULOSIC SUBSTANCES

Several investigators have shown that the hygrothermal treatment results in an increase in the degree of crystallinity of cellulose regardless of the source or the previous history of the cellulosic sample (84-87, 110). In the present study it is observed that the hygrothermal treatment of the green wood as well as of the holowood at any degree of delignification also results in an increase in the crystallinity index. A similar observation is made on heating of the holowood at 105°C. and 9.7% moisture content for two hours. These results are summarized in Table XXV. In addition, the radial width at half height decreases in each case. Hence, the heat treatment of holocellulose at the given moisture content results in an increase in the degree of order of the highly ordered fraction of cellulose.

TABLE XXV

THE EFFECT OF HEAT TREATMENTS ON THE CRYSTALLINITY OF WOOD CELLULOSE AND HOLOCELLULOSE

Sample	Number of Samples Tested	Crystallinity Index		Radial Width at Half Height	
		Before Heating	After Heating	Before Heating	After Heating
Tangential green wood sections	16	60.23	60.79	13.04	12.59
Radial green wood sections	8	66.43	67.73	13.01	12.63
Tangential holowood sections	10	56.69	59.70	12.83	11.83
Radial holowood sections	9	53.00	60.35	12.64	11.74
Air dried holowood	2	75.32	78.30[a]	12.50	11.81[a]

[a]Heated at 105°C. at 9.7% moisture content for two hours.

Stevens (97) observed that the equilibrium moisture content of the beech-wood dried to 13% moisture content at 70°C. is lower at 30% R.H. and at 75% R.H. than that of the similar samples dried at 25°C. The results of the present x-ray study indicate that the decrease in the equilibrium moisture content is due to the crystallization taking place during the wet heating.

Merchant (187) observed that the prolonged drying of the solvent exchange dried bleached, Mitscherlich sulfite, spruce pulp at temperatures above 60°C. resulted in decreased B.E.T. area, which he attributed to changes in the fiber structural units caused by thermal effects influencing hydrogen bonding. Stone (75) observed a similar decrease in the B.E.T. area for solvent exchange dried bleached sulfite pulp especially in the small pore range and attributed it to the thermally induced motion at the microfibrillar level. According to the present study, the packing density of cellulose increases during heating at a given moisture content. Using a cellulose powder diagram, Stone did not observe an increase in the crystallinity index. This technique, however, is not as sensitive to the crystallinity changes as the technique used in the present study.

APPENDIX X

WATER-HOLDING CAPACITY AND THE CRYSTALLINITY

It is suggested in the literature (185) that the water retention value (WRV) is a more sensitive indicator of the conversion of cellulose I to cellulose II than the conventional dry state x-ray diffraction analysis. The increase in the water-holding capacity of pulps, characteristic of cellulose II, can be detected earlier than the changes in the crystalline pattern. This, of course, is true since the irreversible recrystallization effects are avoided by the application of the WRV-method.

The results of the present study, however, indicate that extreme care must be exercised in interpreting the meaning of the WRV. During water washing of pulps, the centrifugal water retention value increases indicating swelling and the crystallinity index increases indicating consolidation. This is an opposite phenomenon to that cited above. These results suggest that the combination of WRV-method and of the x-ray techniques are necessary to obtain reliable information about the changes in the cellulose fine structure.

APPENDIX XI

EXPANSION OF TRACHEID WALLS AND PREFERENTIAL DEFIBERING ALONG RADIAL WALLS

The concept that the microfibrils can slip along each other's surfaces more easily in the tangential walls than in the radial walls can offer an explanation why the tangential walls expand or shrink more than the radial walls as the moisture content of wood or holowood section is changed. The intermicrofibrillar bonding at the microfibril crossing resists both the expansion and the contraction of the tracheid walls. The microfibrils in the tracheid tangential walls, having fewer crossings and being separated by swellable cellulose and hemicellulose layers, are capable of sliding along each other's surfaces more readily than those in the radial walls which have more crystalline bridgings between the neighboring microfibrils.

A similar argument can be offered to explain the preferential defibering along the radial walls versus that along the tangential walls observed by Thompson and Hankey (186). The structure of the adjacent radial walls is disrupted by pits and by ray parenchyma crossings. Hence, as the walls expand, more severe local stress concentrations develop on the microfibrillar level in the adjacent radial walls than on the more uniform and more plastic tangential walls resulting in one by one breaking of the bonds. If the bonding is through the parent tracheid wall, the effect is even stronger, since the parent wall is already very severely stretched and cannot deform with equal ease as the daughter cell wall.

APPENDIX XII

TABLE XXVII

WEIGHT LOSS DURING PULPING OPERATIONS

Sample	Saturated Weight After Pulping, g.	Calculated Ovendry Weight of Wood, g.	Ovendry Weight After Treatment, g.	Accumulated Weight Loss, %
Green wood, G2 (5.558 g.)				
L	4.154	1.360	1.397	-2.7
W	4.005	1.312	1.292	1.5
2H	4.443	1.456	1.418	2.6
8H	4.362	1.429	1.288	9.9
Preheated wood, PH2 (6.142 g.)				
L	4.978	1.614	1.641	-1.7
W	4.637	1.504	1.436	4.5
2H	4.607	1.494	1.390	7.0
8H	4.723	1.532	1.364	11.0
Green wood, G5 (6.544 g.)				
L	5.213	1.683	1.730	-2.8
W	5.160	1.666	1.564	6.1
2H	4.947	1.597	1.397	12.5
8H	4.940	1.595	1.318	17.4
Preheated wood, PH5 (6.917 g.)				
L	5.747	1.830	1.867	-2.0
W	5.645	1.808	1.720	4.9
2H	5.241	1.678	1.486	11.4
8H	5.001	1.601	1.382	13.7
Green wood, G10 (6.422 g.)				
L	4.920	1.566	1.571	-0.3
W	5.061	1.610	1.427	11.6
2H	5.096	1.622	1.387	14.5
8H	5.105	1.624	1.305	19.6

TABLE XXVII (Continued)

WEIGHT LOSS DURING PULPING OPERATIONS

Sample	Saturated Weight After Pulping, g.	Calculated Ovendry Weight of Wood, g.	Ovendry Weight After Treatment, g.	Accumulated Weight Loss, %
Preheated wood, PH10 (6.152 g.)				
L	4.852	1.541	1.573	-2.1
W	5.029	1.598	1.487	7.5
2H	4.841	1.538	1.335	13.2
8H	4.641	1.474	1.218	17.3
Green wood, G15 (6.443 g.)				
L	4.954	1.593	1.537	3.5
W	5.156	1.658	1.403	15.4
2H	5.122	1.647	1.354	17.8
8H	4.817	1.545	1.206	21.9
Preheated wood, PH15 (6.842 g.)				
L	5.434	1.712	1.631	4.7
W	5.562	1.740	1.490	14.4
2H	5.453	1.705	1.376	19.3
8H	5.391	1.685	1.303	22.6
Green wood, G20 (6.519 g.)				
L	4.949	1.587	1.587	0.0
W	5.434	1.742	1.510	13.3
2H	4.879	1.564	1.315	15.9
8H	5.071	1.626	1.273	21.7
Preheated wood, PH20 (6.359 g.)				
L	4.822	1.542	1.437	6.8
W	4.972	1.590	1.367	14.0
2H	5.106	1.633	1.303	20.2
8H	4.981	1.593	1.229	22.9

TABLE XXVII (Continued)

WEIGHT LOSS DURING PULPING OPERATIONS

Sample	Saturated Weight After Pulping, g.	Calculated Ovendry Weight of Wood, g.	Ovendry Weight After Treatment, g.	Accumulated Weight Loss, %
Green wood, G30 (6.428 g.)				
L	5.363	1.630	1.487	8.8
W	4.917	1.495	1.191	20.3
2H	5.348	1.626	1.241	23.7
8H	5.514	1.676	1.198	28.5
Preheated wood, PH30 (6.474 g.)				
L	5.112	1.564	1.411	9.8
W	4.879	1.493	1.212	18.8
2H	4.917	1.505	1.133	24.7
8H	4.964	1.519	1.094	28.0
Preheated wood, PH40 (6.000 g.)				
L	5.497	1.743	1.509	13.4
W	4.558	1.445	1.125	22.2
2H	4.303	1.364	1.010	26.0
8H	4.573	1.450	1.000	31.0
Preheated wood, PH50 (5.892 g.)				
L	4.543	1.417	1.199	15.4
W	4.698	1.466	1.112	24.2
2H	4.841	1.510	1.078	28.6
8H	4.796	1.496	0.990	33.8
Green wood, G60 (6.385 g.)				
L	4.190	1.642	1.473	10.3
W	5.047	1.597	1.269	20.5
2H	5.081	1.610		
8H	4.861	1.538	1.004	34.7

TABLE XXVII (Continued)

WEIGHT LOSS DURING PULPING OPERATIONS

Sample	Saturated Weight After Pulping, g.	Calculated Ovendry Weight of Wood, g.	Ovendry Weight After Treatment, g.	Accumulated Weight Loss, %
Preheated wood, PH60 (6.660 g.)				
L	5.206	1.615	1.342	16.9
W	5.395	1.673	1.294	28.6
2H	5.126	1.590	1.021	35.8
8H	5.706	1.770	1.121	36.7
Green wood, G90 (6.434 g.)				
L	6.325	1.996	1.599	19.9
W	6.885	2.173	1.573	32.6
8H	7.179	2.266	1.360	40.0
Preheated wood, G90 (7.080 g.)				
L	7.733	2.395	1.929	19.5
W	7.625	2.361	1.463	32.4
8H	7.505	2.324	1.359	41.5
Preheated wood, PH106 (6.378 g.)				
L	6.932	2.127	1.652	22.3
W	6.636	2.036	1.320	35.2
8H	7.229	2.218	1.261	43.2
Green wood, G120 (5.624 g.)				
L	4.968	1.400	1.122	19.8
W	4.726	1.336	0.829	41.1
2H	4.488	1.408	0.829	41.1
8H	4.705	1.480	0.841	43.2

TABLE XXVIII

CENTRIFUGAL WATER RETENTION OF PULPS

Sample		Wet Weight After Centrifugation, g. In Holopulping Liquor	After Water Washing	After Hygrothermal Treatment	Ovendry Weight, g.
G29	1	--	1.675	1.469	0.417
	2	--	2.611	2.464	0.740
	3	--	2.503	2.380	0.693
	4	--	2.833	2.504	0.764
	5	--	--	3.440	1.052
	6	--	--	3.830	1.166
G44	1	1.566	1.657	1.580	0.439
	2	2.126	2.124	2.176	0.663
	3	1.910	1.950	1.935	0.588
	4	2.196	2.290	2.150	0.641
G54	1	1.310	1.503	1.232	0.348
	2	2.007	2.141	2.100	0.583
	3	1.662	1.862	1.582	0.447
	4	1.709	1.941	1.745	0.476
G65	1	--	1.531	1.516	0.360
	2	--	1.815	1.694	0.410
	3	--	2.005	1.954	0.464
	4	--	1.394	1.297	0.315
	5	--	1.362	1.235	0.302
	6	--	1.425	1.243	0.302
	7	--	1.697	1.596	0.387
	8	--	1.630	1.429	0.355
G80	1	1.800	2.195	1.924	0.525
	2	1.572	1.807	1.585	0.446
	3	--	--	1.751	0.465
	4	--	--	1.485	0.395
G89	1	2.059	2.485	2.059	0.540
	2	2.417	2.911	2.600	0.660
	3	--	--	2.611	0.662
	4	--	--	2.824	0.699
	5	--	--	2.808	0.708
	6	--	--	2.794	0.713

TABLE XXVIII (Continued)

CENTRIFUGAL WATER RETENTION OF PULPS

Sample		Wet Weight After Centrifugation, g. In Holopulping Liquor	After Water Washing	After Hygrothermal Treatment	Ovendry Weight, g.
G110	1	1.441	1.877	1.477	0.370
	2	1.042	1.443	1.122	0.277
	3	--	--	2.418	0.581
	4	--	--	2.354	0.556
	5	--	--	2.285	0.552
	6	--	--	2.393	0.573
G116	1	1.158	1.447	1.243 (8)[a]	0.297
	2	1.839	2.387	1.980 (8)	0.500
	3	1.443	1.953	1.505 (24)	0.386
	4	1.288	1.667	1.261 (24)	0.317
	5	1.570	2.072	2.147 (2)	0.412
	6	1.296	1.733	1.615 (2)	0.333
	7	1.603	2.203	1.987 (4)	0.440
	8	1.900	2.478	2.422 (4)	0.534
	9	1.401	1.819	1.968 (1)	0.386
	10	1.739	2.229	2.419 (1)	0.483
G127	1	--	1.331	1.155	0.260
	2	--	1.800	1.503	0.354
	3	--	1.890	1.636	0.371
	4	--	1.323	1.101	0.252
G120	1	0.842	1.120	0.973	0.212
	2	0.855	1.196	1.030	0.210
	3	0.836	1.135	0.956	0.204
	4	0.822	1.222	1.017	0.213
	5	0.847	1.224	1.043	0.221
	6	0.967	1.195	1.204	0.246
	7	0.975	1.351	1.154	0.255
	8	1.073	1.490	1.266	0.280
	9	--	1.075	--	0.220
	10	--	1.227	--	0.248
	11	--	1.184	--	0.241
PH18	1	1.354	1.367	1.324	0.389
	2	1.224	1.289	1.209	0.382
	3	1.945	2.018	1.904	0.565
	4	1.410	1.496	1.378	0.404

[a]Hours of heating, all others are heated for 8 hours.

TABLE XXVIII (Continued)

CENTRIFUGAL WATER RETENTION OF PULPS

Sample		Wet Weight After Centrifugation, g. In Holopulping Liquor	After Water Washing	After Hygrothermal Treatment	Ovendry Weight, g.
PH29	1	--	1.836	1.497	0.445
	2	--	2.029	1.612	0.490
	3	--	1.832	1.452	0.442
	4	--	2.019	1.706	0.519
	5	--	1.719	1.562	0.434
	6	--	2.416	2.157	0.635
PH41	1	1.888	2.130	1.941	0.531
	2	1.592	1.826	1.608	0.441
	3	1.877	2.042	1.950	0.533
	4	1.572	1.802	1.692	0.455
PH50	1	1.861	1.987	1.911	0.528
	2	1.781	2.056	1.873	0.520
PH54	1	--	2.940	2.768	0.655
	2	--	2.686	2.342	0.552
	3	--	3.376	3.189	0.753
	4	--	3.273	3.052	0.724
PH71	1	1.712	1.774	1.490	0.446
	2	1.856	2.066	1.676	0.495
	3	--	--	2.111	0.500
	4	--	--	1.403	0.329
	5	--	--	1.602	0.399
	6	--	--	1.373	0.330
PH83	1	1.216	1.584	1.317	0.311
	2	1.588	2.006	1.625	0.404
	3	--	--	2.135	0.535
	4	--	--	1.720	0.427
	5	--	--	1.701	0.418
	6	--	--	2.035	0.501
PH103	1	1.594	1.983	1.606	0.392
	2	1.591	1.948	1.523	0.382
	3	--	--	2.233	0.521
	4	--	--	2.540	0.577
	5	--	--	1.834	0.390
	6	--	--	1.766	0.369

GLOSSARY FOR TABLES XXIX-XXXII

T_{002} = transmittance at 18.5 degrees

T_{am} = transmittance at 22.8 degrees

BaT_0 = transmittance at 18.5 degrees due to background

I = intensity

CrI = crystallinity index

T = tangentially cut section

R = radially cut section

EW = earlywood

LW = latewood

G = the test section consisted of whole growth ring thickness

Ho = delignified for indicated number of days

L = exposure made while the test section was pulping liquor saturated

W = exposure made after water washing while the block was still waterlogged

H = exposure made after hygrothermal treatment while the sample was still waterlogged

Pad = test sample consisted of pulp pad with random tracheid alignment in the plane of the pad

TABLE XXIX

CRYSTALLINITY INDEX

Sample		Transmittance T_{002}	Transmittance T_{am}	Corrected Intensity I_{002}	Corrected Intensity I_{am}	CrI
TEW	1	27.5	53.0	376	146	61.17
		27.5	53.0	376	146	61.17
	2	21.5	45.0	448	190	57.59
		22.0	45.5	442	187	57.69
	3	26.5	53.0	388	146	62.37
		25.8	52.5	411	148	63.99
	4	25.8	51.5	411	154	62.53
		25.2	51.0	403	158	60.79
TEW	H1	20.2	46.0	470	181	61.49
		20.8	47.5	461	177	61.61
	H2	21.8	48.5	448	172	61.61
		22.7	50.0	437	163	62.70
	H3	19.7	46.0	479	186	61.17
		20.8	45.5	463	189	59.18
	H4	30.4	57.0	347	128	63.11
		30.5	59.5	343	116	66.18
TEW	1	23.0	55.0	437	142	67.51
		22.5	54.5	444	144	67.57
	2	24.0	54.0	427	147	65.57
		20.8	53.0	468	153	67.31
	3	25.0	54.5	413	1447	65.13
		23.5	55.5	430	139	67.67
	4	30.2	59.0	352	125	64.67
		28.0	59.5	375	120	68.00
TLW	H1	27.5	59.0	381	122	67.98
		33.5	63.5	320	101	68.13
	H2	38.5	67.0	277	87	68.59
		30.0	63.5	357	103	71.15
	H3	20.5	51.5	471	161	65.82
		24.5	52.5	418	152	63.64
	H4	20.2	51.5	477	161	66.25
		23.0	52.5	438	154	64.84

TABLE XXIX (Continued)

CRYSTALLINITY INDEX

Sample		Transmittance T_{002}	Transmittance T_{am}	Corrected Intensity I_{002}	Corrected Intensity I_{am}	CrI
TG	1	38.5	62.5	278	111	60.07
		38.0	63.0	283	108	61.84
	2	47.5	65.5	212	96	54.72
		49.0	68.5	204	84	58.82
	3	48.0	67.5	210	89	57.62
		48.5	67.5	207	89	57.00
	4	44.0	64.0	237	104	56.54
		45.0	64.2	230	103	55.22
	5	49.0	66.5	203	93	54.19
		47.2	64.0	214	104	51.40
	6	49.8	67.5	198	88	55.56
		50.8	69.2	181	83	56.54
	7	46.0	66.0	223	94	56.95
		46.0	65.5	223	96	57.85
	8	46.0	65.0	223	99	55.61
		45.0	65.0	230	99	56.96
TG	H1	36.5	60.0	295	120	59.32
		39.0	61.5	274	114	58.39
	H2	41.0	62.0	259	112	56.76
		40.8	63.0	261	107	59.00
	H3	42.0	61.3	255	114	55.29
		40.0	61.5	268	114	57.46
	H4	39.2	62.0	273	112	58.97
		40.0	61.0	267	116	56.55
	H5	26.0	53.5	332	148	55.42
		26.5	52.5	326	151	53.68
	H6	40.2	61.0	266	114	57.14
		38.2	60.0	281	120	57.30
	H7	41.2	62.5	255	110	56.86
		39.7	60.0	270	117	56.67
	H8	40.0	62.0	266	112	57.89
		38.5	60.0	278	117	57.91
THol	L	32.5	52.0	335	162	51.64
		32.5	51.5	335	162	51.34
	W	27.0	45.5	379	184	51.45
		28.5	45.5	361	184	49.03
	H	26.7	48.5	382	166	56.54
		28.0	50.0	366	157	57.10

TABLE XXIX (Continued)

CRYSTALLINITY INDEX

Sample		Transmittance T_{002}	Transmittance T_{am}	Corrected Intensity I_{002}	Corrected Intensity I_{am}	CrI
Tho4	L	32.0	53.0	340	156	54.12
		30.5	52.0	354	161	54.52
	W	43.0	60.5	230	101	56.09
		45.7	64.5	211	84	60.19
	H	21.7	46.7	443	176	60.29
		24.3	49.0	409	163	61.16
Tho11	L1	39.0	55.5	277	142	48.74
		38.0	54.5	287	147	48.78
	W1	44.0	65.5	222	83	62.61
		46.0	65.5	209	83	60.29
	H1	26.7	47.5	378	165	56.35
		27.0	48.0	375	163	56.53
	L2	39.0	55.0	277	145	47.65
		39.5	55.0	273	145	46.89
	W2	31.2	52.0	331	146	54.94
		32.0	52.0	324	146	54.94
	H2	26.0	47.5	390	169	56.67
		26.8	48.0	380	167	56.05
THo18	L	38.0	53.0	287	156	45.64
		37.0	54.0	293	150	48.81
	W	26.0	48.0	404	183	54.70
		27.0	47.5	391	185	52.69
	H	19.3	40.5	477	211	55.77
		19.0	39.2	481	220	54.26
THo29	L	32.0	47.5	340	183	46.18
		32.0	48.0	340	180	47.06
	W	23.3	43.5	416	193	53.61
		33.5	43.5	415	193	53.49
	H	20.2	41.5	458	204	55.46
		20.2	41.0	458	207	54.80
THo46	L	35.5	49.0	306	178	41.83
		35.2	49.5	307	174	43.32
	W	41.0	57.0	245	120	51.02
		42.0	56.5	239	122	48.95
THo62	L	34.0	53.0	321	154	52.02
		33.0	52.5	331	157	52.57
	W	37.0	59.0	277	109	60.65
		41.0	62.0	244	95	61.07

TABLE XXIX (Continued)

CRYSTALLINITY INDEX

Sample		Transmittance T_{002}	Transmittance T_{am}	Corrected Intensity I_{002}	Corrected Intensity I_{am}	CrI
Tho97	L	39.0	59.0	277	125	54.87
		43.0	61.5	247	112	54.66
	W	24.5	53.5	405	133	67.16
		29.0	55.5	353	122	65.44
	H	30.5	60.0	336	104	69.05
		36.0	63.5	285	88	69.12
THol20	L1	33.0	56.0	333	143	57.06
		33.5	56.5	328	141	57.01
	W1	46.0	64.5	212	89	58.02
		44.5	64.0	222	91	59.01
THol20	L2	31.0	56.0	353	156	55.81
		28.5	54.0	379	153	59.63
	W2	25.0	49.0	405	163	59.75
		25.5	50.0	398	161	59.55
	H2	24.5	49.5	409	161	60.64
		24.5	50.0	409	158	61.37
THol20	L3	25.0	47.0	420	193	54.05
		27.0	49.5	395	178	54.94
	W3	27.5	50.5	373	157	57.91
		27.0	49.5	379	163	56.99
	H3	41.0	64.5	247	87	64.78
		41.0	63.0	247	94	61.94
THol20	W4	30.5	50.5	340	157	53.82
		30.0	50.5	346	157	54.62
	H4	23.4	48.0	422	169	59.95
		23.0	47.0	427	175	59.02
THol20	L5	20.0	45.5	485	200	58.76
		18.7	40.8	507	229	54.83
	W5	22.0	43.0	430	189	56.05
		21.0	41.0	445	203	54.38
	H5	21.7	44.0	428	175	59.11
		22.3	44.5	418	172	58.85
RLWI	1	20.8	52.0	472	153	67.58
		24.0	52.5	420	148	64.76
	2	24.7	51.0	412	158	61.65
		21.2	51.0	454	158	65.20
	3	21.5	50.0	450	163	63.78
		19.3	49.5	485	166	65.77
	4	20.2	47.0	466	178	61.80
		16.2	45.5	539	187	64.94

TABLE XXIX (Continued)

CRYSTALLINITY INDEX

Sample		Transmittance T_{002}	Transmittance T_{am}	Corrected Intensity I_{002}	Corrected Intensity I_{am}	CrI
RLWI	1H	21.5	54.5	452	142	68.58
		27.0	56.0	383	130	66.06
	2H	22.6	53.0	437	146	66.59
		27.5	56.0	377	130	65.52
	3H	25.3	55.5	402	132	67.16
		26.0	52.5	395	150	62.03
	4H	18.7	47.7	478	157	67.15
		19.4	45.0	467	174	62.74
RLWII	1	48.0	73.0	214	69	67.76
		46.0	73.0	227	69	69.60
	2	28.5	62.0	379	116	69.39
		27.0	61.0	395	116	70.63
	3	27.5	59.0	376	130	65.43
		29.0	61.0	371	118	68.19
	4	34.0	64.5	322	104	67.70
		33.0	64.5	332	104	68.67
RLWII	H1	41.5	72.0	259	74	71.43
		40.0	70.0	270	81	70.00
	H2	28.5	61.0	379	120	68.34
		29.5	63.0	366	111	69.67
	H3	28.7	61.0	363	120	68.67
		30.0	62.0	362	91	74.86
	H4	32.3	63.5	336	109	67.56
		32.5	63.0	339	111	67.26
RHo1	L	24.5	42.0	418	212	49.28
		23.5	42.0	430	212	50.70
	W	22.2	44.0	422	177	58.06
		24.8	46.5	390	163	58.21
	H	15.0	40.0	547	205	62.52
		16.8	41.5	511	199	61.06
RHo4	L	31.0	51.5	346	156	54.91
		28.0	50.5	378	157	58.47
	W	16.5	36.5	516	227	56.01
		16.8	38.0	511	216	57.73
	H	18.5	42.0	478	192	59.83
		18.0	42.5	489	188	61.55

TABLE XXIX (Continued)

CRYSTALLINITY INDEX

Sample		Transmittance T_{002}	Transmittance T_{am}	Corrected Intensity I_{002}	Corrected Intensity I_{am}	CrI
RHo16	L	41.5	52.5	252	150	40.48
		44.0	55.5	233	146	37.34
	W	30.8	49.0	323	147	54.49
		29.7	48.0	334	153	54.12
	H	24.8	44.0	389	174	55.27
		22.5	42.5	417	183	56.12
RHo29	L	33.0	48.5	325	172	47.08
		31.3	48.5	340	172	49.41
	W	19.8	40.0	459	204	55.56
		20.0	39.5	455	204	55.16
	H	23.5	48.0	404	150	62.87
		25.5	49.0	379	145	61.74
RHo46	L	42.0	55.0	250	136	45.35
		43.5	55.5	251	133	47.01
	W	37.5	50.5	259	137	47.10
		36.0	48.5	273	150	45.05
	W	34.0	51.5	291	157	46.05
		34.7	51.0	284	153	46.11
	H	37.0	49.0	265	141	46.78
		36.5	49.0	271	141	47.98
RHo62	L	45.0	54.0	228	141	38.16
		45.0	54.0	228	141	38.16
	W	36.5	47.5	268	154	42.54
		30.5	39.0	324	211	34.88
	H	37.0	53.0	256	108	57.81
		39.5	53.0	235	108	54.04
RHo97	L	66.5	73.0	105	56	46.67
		64.5	75.0	115	62	46.09
	W	23.0	45.0	408	167	59.07
		25.0	44.0	383	173	54.83
	H	21.0	49.0	432	136	68.52
		24.0	51.0	393	124	68.45

TABLE XXIX (Continued)

CRYSTALLINITY INDEX

Sample	Transmittance		Corrected Intensity		CrI
	T_{002}	T_{am}	I_{002}	I_{am}	
RHol20 Earlywood					
L	42.5	65.5	251	96	61.75
	42.0	63.0	255	106	58.43
W	47.0	59.0	196	102	47.96
	44.0	56.0	216	116	46.30
H	56.5	70.0	133	47	64.66
	56.0	71.0	131	43	67.18
RHol20 Transitionwood					
L	31.5	60.5	345	117	66.09
	30.3	59.5	356	122	65.73
W	39.0	57.0	254	111	56.30
	41.0	57.5	239	109	54.39
H	32.0	54.5	313	118	62.30
	32.0	55.0	311	116	62.70
RHol20 Latewood					
L	19.5	51.0	493	165	66.53
	19.5	51.0	493	165	66.53
W	31.0	51.0	327	142	56.57
	32.5	53.0	312	131	58.01
H	26.5	51.0	372	137	63.17
	27.0	51.0	366	137	62.57
Air Dry					
Ho I	31.0	70.5	365	93	74.52
	27.5	67.5	402	106	73.63
H Air Dry[a]					
Ho I	24.5	70.5	438	93	78.77
	23.0	68.5	457	102	77.68
Air Dry					
Ho II	25.0	66.5	432	110	74.54
	22.0	68.5	470	101	78.51
H Air Dry[a]					
Ho II	39.0	77.0	292	69	76.37
	35.5	78.8	321	63	80.37
Air Dry					
Ho Pad I	31.0	50.0	365	192	47.40
	30.5	48.7	368	198	46.20
Ho Pad II	30.0	49.5	373	193	48.26
	29.0	49.5	386	193	50.00

[a]Heated at 105°C. at 9.7% moisture content for two hours.

TABLE XXX

RADIAL WIDTH AT HALF HEIGHT

Sample		T_{002}	BaT_0	T at Half Height	Width at Half Height, scale units	Degrees
TEW	1	27.5	51.5	37.5	10.8/149.0	13.05
		27.5	51.5	37.5	10.7/149.0	12.93
	2	21.5	46.0	31.5	10.3/149.0	12.44
		22.0	46.0	32.0	10.6/149.0	12.81
	3	26.5	50.5	36.5	10.9/149.0	13.17
		25.8	51.0	36.2	11.3/149.0	13.65
	4	25.8	49.5	35.5	10.5/150.5	12.56
		25.2	49.0	35.0	10.4/150.5	12.44
TEW	H1	20.2	43.5	29.7	10.5/149.0	12.68
		20.8	45.0	30.0	10.0/149.0	12.08
	2	21.8	47.0	32.0	10.1/144.5	12.58
		22.7	48.0	33.0	10.6/144.5	13.20
	3	19.7	43.0	29.2	11.0/151.0	13.11
		20.8	44.5	30.5	10.9/151.0	12.99
	4	30.4	55.0	41.0	10.7/149.0	12.93
		30.5	56.0	41.2	10.0/149.0	12.08
TLW	1	23.0	59.5	37.0	10.7/148.0	13.01
		22.5	57.0	36.0	10.9/148.0	13.26
	2	24.0	58.0	37.0	10.5/148.5	12.73
		20.8	55.5	34.0	10.6/148.5	12.85
	3	25.0	58.5	38.5	11.3/149.0	13.65
		23.5	57.0	36.5	10.9/149.0	13.17
	4	30.2	62.0	43.7	11.0/147.5	13.42
		28.0	61.0	41.5	10.5/147.5	12.81
TLW	H1	27.5	60.0	40.5	10.4/147.0	12.73
		33.5	67.0	47.2	10.7/147.0	13.10
	2	38.5	70.5	52.5	10.4/147.0	12.73
		30.0	64.5	43.7	10.7/147.0	13.10
	3	20.5	53.5	33.2	10.4/147.5	12.69
		24.5	56.5	37.0	10.5/147.5	12.81
	4	20.2	53.0	33.0	10.5/148.5	12.73
		23.0	55.5	35.7	10.4/148.5	12.61
TG	1	38.5	65.0	49.5	10.0/142.0	12.68
		38.0	65.0	49.7	10.0/142.0	12.68
	2	47.5	70.0	58.0	11.0/148.0	13.38
		49.0	72.0	59.5	10.6/148.0	12.89
	3	48.0	71.5	58.7	11.0/149.5	13.24
		49.0	71.0	59.0	11.4/149.5	13.73
	4	44.0	67.5	54.7	10.6/151.5	12.59
		45.0	68.0	55.2	11.2/151.5	13.31
	5	49.0	70.5	58.5	10.8/149.5	12.99
		47.5	68.0	57.0	11.5/149.5	13.84

TABLE XXX (Continued)

RADIAL WIDTH AT HALF HEIGHT

Sample		T_{002}	BaT_0	T at Half Height	Width at Half Height, scale units	Degrees
TG (cont'd)	6	50.0	70.5	59.2	10.8/151.0	12.87
		51.0	73.0	61.0	10.8/151.0	12.87
	7	46.0	70.0	57.0	11.3/152.5	13.34
		46.0	70.0	57.0	11.0/152.5	12.98
	8	46.0	69.0	56.2	11.0/151.0	13.11
		45.0	69.0	55.5	11.0/151.0	13.11
TG	H1	36.5	63.5	48.2	10.6/150.0	12.72
		39.0	66.0	50.5	9.8/150.0	11.76
	2	41.0	66.0	52.0	10.7/149.5	12.88
		41.0	67.5	52.5	10.3/149.5	12.40
	3	42.0	66.0	52.5	10.2/150.5	12.20
		40.0	66.0	51.5	10.7/150.5	12.80
	4	40.0	64.5	51.0	10.1/151.5	12.00
		39.0	65.5	50.5	10.1/151.5	12.00
	5	26.0	52.5	37.0	10.1/149.5	12.16
		26.5	53.5	37.5	10.3/149.5	12.40
	6	32.0	58.5	43.2	10.4/150.5	12.44
		33.5	58.5	43.2	10.6/150.5	12.68
	7	39.5	64.5	51.0	10.4/150.5	12.44
		41.0	66.5	51.0	10.3/150.5	12.32
	8	40.0	65.0	51.0	10.0/150.0	12.00
		38.5	64.0	49.7	10.0/150.0	12.00
RLWI	1	20.8	56.0	33.5	11.3/149.5	13.61
		24.0	58.5	37.0	10.8/149.5	13.00
	2	24.7	56.0	37.0	11.2/144.5	13.95
		21.2	53.5	34.0	11.0/144.5	13.70
	3	21.5	55.5	34.7	11.4/149.0	13.77
		19.3	52.5	32.0	10.9/149.0	13.17
	4	20.2	52.0	32.7	11.0/150.5	13.16
		16.2	48.5	28.0	11.1/150.5	13.28
RLWI	H1	21.5	57.5	35.0	10.7/149.0	12.93
		27.0	61.0	40.5	10.7/149.0	12.93
	2	22.6	56.0	35.5	10.5/152.0	12.43
		27.5	60.0	40.5	10.7/152.0	12.67
	3	25.3	57.0	38.0	10.9/151.0	12.99
		26.0	57.5	38.5	11.1/151.0	13.23
	4	18.7	51.0	31.0	10.7/150.0	12.84
		19.4	50.0	31.2	11.0/150.0	13.20

TABLE XXX (Continued)

RADIAL WIDTH AT HALF HEIGHT

Sample		T_{002}	BaT_0	T at Half Height	Width at Half Height, scale units	Degrees
RLWII	1	48.0	75.5	60.0	10.2/146.0	12.58
		46.0	75.0	58.5	10.0/146.0	12.33
	2	28.5	67.0	43.5	10.6/148.5	12.85
		27.0	66.5	42.2	10.6/148.5	12.85
	3	27.5	64.0	42.0	10.9/151.5	12.95
		29.0	66.0	43.5	11.2/151.5	13.31
	4	33.0	68.0	47.2	10.3/150.0	12.36
		34.0	68.0	48.0	10.7/150.0	12.84
RLWII	H1	41.5	73.5	55.5	10.4/152.0	12.32
		40.0	72.5	53.5	10.1/152.0	11.96
	2	28.5	66.0	43.2	10.1/149.0	12.20
		29.5	67.5	44.5	10.0/149.0	12.08
	3	28.7	66.0	43.0	10.4/147.0	12.73
		30.0	66.5	44.5	10.3/147.0	12.61
	4	32.3	66.5	46.5	10.2/147.5	12.45
		32.5	67.0	46.5	10.2/147.5	12.45
THo1	L	32.5	54.5	42.0	10.7/148.5	12.97
		32.5	54.0	41.7	10.2/148.5	12.36
	W	27.0	48.0	36.0	10.8/146.5	13.27
		28.5	49.0	37.2	10.2/146.5	12.53
	H	26.7	51.5	37.0	10.0/149.5	12.04
		28.0	52.5	38.2	9.9/149.5	11.92
THo4	L	32.0	54.0	41.5	10.7/147.5	13.06
		30.5	53.0	40.2	10.9/147.5	13.30
	W	43.0	62.0	51.5	10.5/150.5	12.56
		45.7	67.0	55.2	10.7/150.5	12.80
	H	21.7	47.5	32.2	9.7/150.0	11.64
		24.3	49.5	34.7	10.2/150.0	12.24
THo11	1L	39.0	61.0	49.0	10.5/150.0	12.60
		38.0	59.5	47.2	10.8/150.0	12.96
	1W	44.0	68.0	54.7	10.5/151.0	12.52
		46.0	69.0	56.5	10.7/151.0	12.76
	1H	26.7	52.0	37.2	10.3/148.5	12.48
		27.0	52.5	37.5	10.7/148.5	12.97
THo11	2L	39.0	59.5	48.0	10.8/153.0	12.70
		39.5	59.5	48.5	11.2/153.0	13.18
	2W	31.2	57.5	42.2	11.0/146.0	13.56
		32.0	56.5	42.5	10.8/146.0	13.32
	2H	26.0	52.0	36.5	10.0/148.5	12.12
		26.8	51.5	37.0	9.6/148.5	11.64

TABLE XXX (Continued)

RADIAL WIDTH AT HALF HEIGHT

Sample		T_{002}	BaT_0	T at Half Height	Width at Half Height, scale units	Degrees
THo18	L	38.0	58.5	47.0	10.8/148.0	13.13
		37.0	58.5	46.5	10.5/148.0	12.77
	W	26.0	52.5	46.5	10.5/148.0	12.77
		27.0	52.0	37.2	10.4/148.5	12.61
	H	20.0	44.0	29.2	9.6/145.0	11.92
		24.0	47.0	32.7	9.4/145.0	11.67
THo29	L	32.0	53.5	41.2	9.8/146.5	12.04
		32.0	53.5	41.2	10.1/146.5	12.41
	W	23.3	47.0	33.2	10.5/148.0	12.77
		23.5	47.5	33.5	10.3/148.0	12.53
	H	20.2	45.0	30.2	10.4/147.0	12.73
		20.2	45.5	30.5	10.4/147.0	12.73
THo46	L	35.5	54.0	44.0	10.2/145.0	12.66
		35.2	53.5	43.5	10.0/145.0	12.42
	W	41.0	61.0	50.0	10.0/149.5	12.04
		42.0	61.0	50.7	10.2/149.5	12.28
THo62	L	34.0	57.5	44.0	10.4/146.5	12.78
		33.0	56.5	43.0	10.0/146.5	12.29
	W	37.0	61.0	47.5	9.9/149.5	11.92
		41.0	64.5	51.2	10.6/149.5	12.76
THo97	L	39.0	61.5	49.0	10.1/150.5	12.08
		43.0	65.0	54.0	10.8/150.5	12.92
	W	30.5	58.5	42.0	10.2/150.5	12.20
		36.0	64.5	48.0	10.1/150.5	12.08
	H	24.5	52.7	36.0	9.4/149.0	11.36
		29.0	57.0	40.5	9.6/149.0	11.60
THo120	1L	33.0	56.5	43.2	10.4/150.5	12.44
		33.5	56.5	43.5	10.4/150.5	12.44
	1W	46.0	63.5	54.0	11.5/146.0	14.18
		44.5	63.0	53.0	11.5/146.0	14.18
THo120	2L	31.0	57.0	42.0	10.0/151.0	11.92
		28.5	54.5	39.5	9.6/151.0	11.44
	2W	25.0	48.0	34.5	10.8/144.5	13.45
		25.5	48.5	35.0	10.6/144.5	13.20
	2H	24.5	48.5	34.5	9.0/144.5	11.21
		24.5	48.0	34.2	9.5/144.5	11.83

TABLE XXX (Continued)

RADIAL WIDTH AT HALF HEIGHT

Sample		T_{002}	BaT_0	T at Half Height	Width at Half Height, scale units	Degrees
THo120	3L	25.0	45.0	33.5	10.3/150.5	12.32
		27.0	48.0	36.0	10.6/150.5	12.68
	3W	27.5	51.5	37.5	10.7/151.5	12.71
		27.0	49.5	36.5	11.1/151.5	13.19
	3H	41.0	63.0	51.0	9.6/152.0	11.37
		41.0	62.0	50.5	9.8/152.0	11.61
THo120	4W	30.5	50.0	39.0	10.8/150.0	12.96
		30.0	49.0	38.2	11.0/150.0	13.20
	4H	23.4	46.0	33.0	9.9/151.0	11.80
		23.0	45.5	32.5	9.8/151.0	11.68
THo120	5L	25.7	53.0	36.7	10.3/146.0	12.70
		29.0	58.0	40.7	9.9/146.0	12.21
	5W	17.8	41.0	27.0	10.5/147.5	12.81
		20.3	45.0	30.2	10.8/147.5	13.18
	5H	21.7	43.0	30.5	9.6/150.0	11.52
		22.3	43.5	31.2	9.3/150.0	11.16
RHo1	L	24.5	45.0	33.1	10.9/147.0	13.35
		23.5	45.5	32.8	11.1/147.0	13.59
	W	22.2	46.0	32.1	11.3/147.0	13.84
		24.8	49.5	35.0	10.7/147.0	13.10
	H	15.0	42.0	25.0	10.2/146.0	12.56
		16.8	43.0	26.3	10.1/146.0	12.45
RHo4	L	31.0	53.5	40.5	10.7/148.0	13.01
		28.0	53.0	39.5	11.4/148.0	13.86
	W	16.5	38.5	25.2	11.0/148.0	13.38
		16.8	39.5	25.7	11.1/148.0	13.50
	H	18.5	43.0	28.5	10.1/148.0	12.28
		18.0	43.5	28.2	10.0/148.0	12.16
RHo16	L	41.5	57.0	48.5	10.9/149.5	13.12
		44.0	60.5	51.5	10.9/149.5	13.12
	W	30.8	54.0	40.7	10.3/146.0	12.70
		29.7	53.0	39.7	10.5/146.0	12.95
	H	24.8	50.5	35.3	10.2/145.5	12.62
		22.5	49.0	33.3	10.2/145.5	12.62
RHo29	L	33.0	55.5	42.7	10.1/147.0	12.37
		31.3	54.0	41.0	9.9/147.0	12.13
	W	19.8	46.0	30.2	10.5/147.5	12.81
		20.0	45.0	28.7	10.9/147.5	13.30
	H	23.5	53.0	35.2	10.0/146.0	12.33
		25.5	55.0	37.7	10.4/146.0	12.83

TABLE XXX (Continued)

RADIAL WIDTH AT HALF HEIGHT

Sample		T_{002}	BaT_0	T at Half Height	Width at Half Height, scale units	Degrees
RHo46	L	42.0	60.0	50.0	9.9/143.0	12.46
		43.5	61.5	52.0	10.0/143.0	12.59
	W	37.5	55.0	45.2	9.7/146.5	11.92
		36.0	54.0	44.0	9.1/146.5	11.54
	W	34.0	56.5	43.7	10.2/145.0	12.66
		34.7	56.5	44.0	9.9/145.0	12.29
	H	37.0	54.5	44.7	9.2/147.0	11.26
		36.5	54.0	44.2	9.8/147.0	12.00
RHo62	L	45.0	58.0	51.0	10.0/147.5	12.21
		45.0	57.0	50.5	9.7/147.5	11.83
	W	36.5	52.5	43.7	9.8/145.5	12.13
		30.5	44.0	36.7	10.4/145.5	12.87
	H	37.0	56.0	45.5	9.0/149.0	10.87
		39.5	57.0	47.0	8.8/149.0	10.63
RHo97	L	66.5	76.0	70.5	10.4/148.5	12.60
		64.5	75.0	69.5	11.0/148.5	13.32
	W	23.0	45.5	32.2	10.4/150.5	12.44
		25.0	47.5	34.5	10.6/150.5	12.68
	H	21.0	49.5	32.2	9.8/154.5	11.42
		24.0	53.5	35.7	9.7/154.5	11.30
RHo120 Earlywood						
	L	42.5	65.0	52.5	10.2/148.0	12.41
		42.0	64.0	51.7	10.5/148.0	12.77
	W	47.0	60.5	53.2	10.2/149.5	12.28
		44.0	58.0	50.5	10.1/149.5	12.16
	H	56.5	70.5	61.7	7.4/149.0	8.94
		56.0	70.5	61.7	6.7/149.0	8.09
RHo120 Transitionwood						
	L	31.5	61.0	43.7	10.0/148.0	12.16
		30.3	61.0	43.0	10.8/148.0	13.14
	W	39.0	58.5	47.5	9.2/146.5	11.30
		41.0	59.5	49.5	10.1/146.5	12.41
	H	32.0	55.0	42.0	9.1/149.0	10.92
		32.0	56.0	42.2	9.4/149.0	11.29
RHo120 Latewood						
	L	19.5	55.0	32.7	10.5/150.5	12.56
		19.5	54.0	32.5	11.1/150.5	13.28
	W	31.0	53.0	40.5	9.6/148.0	11.68
		32.5	55.5	42.5	9.7/148.0	11.80
	H	26.5	52.0	37.0	8.8/146.5	10.81
		27.0	52.0	37.5	8.9/146.5	10.94

TABLE XXX (Continued)

RADIAL WIDTH AT HALF HEIGHT

Sample	T_{002}	BaT_0	T at Half Height	Width at Half Height, scale units	Degrees
Air Dry					
Ho I	31.0	78.0	49.0	10.0/151.5	11.88
	27.5	75.5	47.5	11.3/151.5	13.43
Air Dry					
Ho I H[a]	24.5	77.5	43.5	10.1/148.0	12.28
	23.0	75.5	41.5	9.2/148.0	11.19
Air Dry					
Ho II	25.0	76.5	43.5	10.3/153.0	12.18
	22.0	73.5	40.0	10.6/153.0	12.47
Air Dry					
Ho II H[a]	39.0	84.5	57.5	10.4/152.5	12.28
	35.5	83.5	55.0	9.7/152.5	11.45
Air Dry					
Ho Pad I	31.0	57.5	42.0	13.2/147.0	16.16
	30.5	56.0	41.0	12.9/147.0	15.80
Ho Pad II	30.0	57.0	41.0	13.5/150.5	16.15
	29.0	56.0	40.0	12.4/150.5	14.83

[a]Heated at 105°C. at 9.7% moisture content for two hours.

TABLE XXXI

CIRCUMFERENTIAL WIDTH AT HALF HEIGHT

Sample		T_{002}	BaT_0	T at Half Height	Width at Half Height, scale units	Degrees
TEW	1	25.2	45.5	34.0	37.6/366.5	18.47
		23.5	45.5	33.0	37.5/366.5	18.42
	2	19.7	41.0	28.7	34.9/362.5	17.33
		19.7	42.0	28.5	35.2/362.5	17.78
	3	23.5	44.5	32.2	35.2/368.0	17.22
		23.0	45.5	32.2	35.3/368.0	17.27
	4	23.8	45.0	32.7	36.5/367.5	17.88
		23.2	45.5	32.7	35.4/367.5	17.34
TEW	H1	18.0	38.5	27.0	37.0/365.5	18.22
		19.0	39.5	27.5	36.0/365.5	17.73
	2	20.4	42.0	29.5	35.3/367.0	17.31
		20.5	42.0	29.0	34.0/367.0	16.68
	3	18.2	38.0	26.5	36.4/365.0	17.95
		18.8	40.0	27.5	37.0/365.0	18.25
	4	23.5	50.5	34.5	36.5/366.5	17.93
		27.0	51.0	37.0	34.3/366.5	16.85
TLW	1	23.0	67.5	38.7	31.8/362.0	15.81
		25.0	68.5	41.0	34.1/362.0	16.96
	2	22.2	67.5	39.0	33.7/367.5	16.51
		25.5	67.5	41.5	34.0/367.5	16.65
	3	25.5	66.5	41.0	34.0/365.5	16.74
		24.5	66.0	40.0	32.6/365.5	16.06
	4	32.3	71.5	48.2	34.0/364.5	16.79
		29.8	70.5	46.0	33.2/364.5	16.40
TLW	H1	37.5	79.0	54.5	32.3/363.0	16.02
		29.5	75.0	47.0	33.7/363.0	16.71
	2	32.7	77.0	50.0	32.1/367.0	15.74
		43.5	82.5	59.5	31.7/367.0	15.55
	3	26.0	68.5	42.0	33.3/367.0	16.33
		21.7	65.0	38.0	34.0/367.0	16.68
	4	24.3	66.5	40.5	33.3/368.5	16.27
		21.4	65.0	37.7	34.4/368.5	16.80
TG	1	33.0	58.0	43.7	29.9/365.0	14.75
		32.5	58.0	43.5	29.1/365.0	14.35
	2	47.0	72.5	58.5	32.1/362.5	15.94
		43.5	68.0	54.7	28.2/362.5	14.00
	3	46.0	71.0	57.0	33.0/360.5	16.48
		45.0	70.0	56.0	30.5/360.5	15.29
	4	53.0	84.5	66.7	31.2/361.0	15.56
		51.5	86.0	66.2	31.3/361.0	15.61
	5	57.5	87.0	70.5	29.7/364.0	14.69
		54.5	86.0	68.5	30.7/364.0	15.18

TABLE XXXI (Continued)

CIRCUMFERENTIAL WIDTH AT HALF HEIGHT

Sample		T_{002}	BaT_0	T at Half Height	Width at Half Height, scale units	Degrees
TG (cont'd)	6	56.0	86.5	69.5	31.7/361.5	15.78
		57.5	87.0	70.5	29.0/361.5	14.44
	7	52.5	84.0	66.5	33.6/365.0	16.57
		53.0	84.0	66.7	30.6/365.0	15.09
	8	53.0	83.0	66.5	32.4/363.0	16.07
		52.0	83.0	65.7	30.9/363.0	15.32
TG	H1	40.5	76.0	55.5	30.0/366.0	14.75
		43.5	78.5	58.5	31.3/366.0	15.49
	2	46.5	79.0	60.5	31.5/366.0	15.49
		46.5	80.0	61.0	32.4/366.0	15.93
	3	46.5	78.0	60.0	33.0/366.0	16.23
		44.0	78.0	58.7	33.8/366.0	16.62
	4	46.0	81.0	61.2	32.5/362.5	16.14
		44.5	80.5	60.0	30.3/362.5	15.05
	5	28.5	64.5	43.0	31.4/368.0	15.36
		32.5	65.0	46.0	33.7/368.0	16.48
	6	36.5	70.0	50.5	31.2/361.0	15.86
		37.7	69.0	51.2	31.9/361.0	15.91
	7	42.0	79.0	60.2	30.6/358.5	15.36
		46.5	79.5	60.2	31.5/358.5	15.82
	8	43.0	73.5	56.2	30.7/355.0	15.57
		42.0	74.0	55.7	31.2/355.0	15.82
RLWI	1	24.0	66.0	40.0	30.6/365.5	15.07
		19.5	64.5	36.5	29.6/365.5	14.56
	2	25.0	66.0	40.5	30.2/363.0	14.98
		23.7	65.5	39.5	30.0/363.0	14.88
	3	20.5	64.5	36.5	32.0/363.5	15.85
		22.7	66.5	38.5	30.7/363.5	15.20
	4	23.0	64.0	38.2	30.2/364.5	14.91
		18.0	61.5	33.7	30.0/364.5	14.82
RLWI	H1	37.5	94.5	59.5	29.4/362.0	14.62
		27.5	88.0	49.0	28.6/362.0	14.22
	2	34.0	83.5	53.2	27.8/358.5	13.96
		28.4	81.5	48.5	28.5/358.5	14.31
	3	32.0	78.0	50.0	30.0/361.5	14.94
		31.2	78.5	49.7	32.7/362.0	15.29
	4	22.5	68.5	40.0	32.5/362.0	16.16
		22.0	71.5	39.7	28.5/362.0	14.87

TABLE XXXI (Continued)

CIRCUMFERENTIAL WIDTH AT HALF HEIGHT

Sample		T_{002}	BaT_0	T at Half Height	Width at Half Height, scale units	Degrees
RLWII	1	44.5	76.5	58.5	29.0/361.0	14.46
		46.5	76.0	59.7	28.7/361.0	14.31
	2	26.7	67.0	42.2	30.0/363.5	14.86
		26.7	67.0	42.2	28.1/363.5	13.92
	3	27.0	67.5	42.7	28.8/364.0	14.24
		25.7	61.5	39.7	27.3/364.0	13.50
	4	31.0	66.5	45.2	29.2/364.5	14.42
		30.5	65.5	44.7	28.2/364.5	13.93
RLWII	H1	39.0	72.0	53.0	28.7/364.5	14.17
		41.0	73.5	55.0	26.8/364.5	13.24
	2	30.5	71.0	46.7	29.7/366.0	14.61
		28.2	69.5	44.2	29.1/366.0	14.31
	3	30.0	66.5	43.0	27.4/362.5	13.60
		30.5	66.0	45.0	29.0/362.5	14.40
	4	31.5	65.0	45.0	27.8/365.5	13.69
		31.3	64.0	44.7	27.0/365.5	13.30
THo1	L	36.0	65.0	48.5	35.4/368.5	17.29
		38.0	65.0	50.0	36.0/368.5	17.56
	W	29.5	57.5	41.2	37.1/364.0	18.35
		29.5	56.0	40.5	37.0/364.0	18.30
	H	27.0	52.5	37.5	37.4/365.0	18.44
		26.3	52.0	37.0	35.3/365.0	17.80
THo4	L	33.3	59.5	44.5	36.1/362.0	17.95
		34.0	59.5	45.0	38.2/362.0	18.99
	W	42.0	63.0	51.2	36.5/365.0	18.00
		40.5	61.0	50.0	39.9/365.0	19.68
	H	22.2	47.0	32.2	36.7/366.5	18.01
		21.0	45.5	31.2	39.4/366.5	19.35
THo11	L	45.5	71.5	57.0	31.3/365.5	15.42
		43.5	72.0	56.0	30.0/365.5	14.77
	W	36.5	69.0	50.2	34.2/366.0	16.82
		35.0	68.0	49.0	33.0/366.0	16.23
	H	31.0	63.5	44.2	30.9/365.5	15.22
		31.0	64.0	44.5	30.8/365.5	15.17
THo11	1L	43.5	69.5	55.0	33.2/364.0	16.42
		41.5	70.0	54.0	31.2/364.0	15.49
	1W	19.5	49.0	30.2	32.0/363.0	15.87
		17.0	43.5	27.5	34.2/363.0	16.96
	1H	32.5	65.5	46.0	33.2/367.5	16.26
		30.0	64.5	44.0	31.8/367.5	15.58

TABLE XXXI (Continued)

CIRCUMFERENTIAL WIDTH AT HALF HEIGHT

Sample		T_{002}	BaT_0	T at Half Height	Width at Half Height, scale units	Degrees
THo18	L	42.5	71.5	55.2	33.3/365.0	16.42
		42.0	70.5	54.2	32.0/365.0	15.78
	W	30.5	65.0	44.5	32.8/361.0	16.36
		30.0	66.0	44.5	33.3/361.0	16.60
	H	20.0	53.0	32.7	33.7/367.0	16.53
		23.0	54.0	35.2	33.6/367.0	16.48
THo29	L	36.0	65.0	48.5	32.5/363.0	16.12
		36.5	66.0	49.2	33.3/363.0	16.51
	W	26.7	59.0	39.7	32.8/361.5	16.33
		26.0	59.0	39.2	33.3/361.5	16.58
	H	22.7	56.5	36.0	33.8/367.5	16.56
		22.5	57.5	36.0	33.6/367.5	16.46
THo46	L	58.0	76.5	66.5	32.0/363.0	15.87
		59.0	77.5	67.5	31.0/363.0	15.37
	W	40.5	62.5	50.5	43.0/362.5	16.88
		39.5	64.0	50.2	35.9/362.5	17.83
THo62	L	37.0	66.5	49.7	35.1/363.0	17.41
		36.5	67.0	49.5	36.0/363.0	17.85
	W	45.0	73.5	59.5	38.3/361.5	19.07
		40.5	71.5	53.7	37.0/361.5	18.43
THo97	L	40.0	63.5	50.5	32.7/362.5	16.24
		36.5	60.0	47.0	31.6/362.5	15.69
	W	23.5	47.0	33.2	35.5/362.0	17.65
		20.2	44.5	30.2	37.1/362.0	18.82
	H	36.5	63.5	48.2	37.1/365.5	18.27
		28.7	59.5	41.2	35.2/365.5	17.34
THo120	1L	34.2	62.0	46.0	35.5/360.0	17.75
		33.5	60.5	45.0	36.1/360.0	18.05
	1W	40.5	57.0	48.0	41.0/365.5	20.20
		42.0	57.5	49.0	39.1/365.5	19.26
THo120	2L	29.0	55.5	40.0	36.0/362.5	17.88
		26.7	55.0	38.2	35.7/362.5	17.73
	2W	24.5	49.0	34.5	35.0/367.0	17.17
		25.0	49.5	35.0	36.0/367.0	17.66
	2H	26.5	46.5	35.0	36.6/367.5	17.93
		26.5	48.0	35.7	34.7/367.5	17.00

TABLE XXXI (Continued)

CIRCUMFERENTIAL WIDTH AT HALF HEIGHT

Sample		T_{002}	BaT_0	T at Half Height	Width at Half Height, scale units	Degrees
THol20	3L	24.0	45.0	33.0	37.0/364.0	18.30
		26.5	47.0	35.2	37.8/364.0	18.70
	3W	25.5	50.0	35.7	37.8/366.5	18.57
		25.5	52.5	36.7	35.0/366.5	17.19
	3H	43.5	65.0	53.2	37.0/361.0	18.45
		43.7	67.0	54.2	38.5/361.0	19.20
THol20	4W	29.5	48.0	37.7	38.0/366.5	18.66
		28.5	46.5	36.5	39.1/366.5	19.20
	4H	25.0	46.5	34.0	36.1/366.0	17.75
		24.5	48.0	34.2	35.2/366.0	17.31
THol20	5L	23.0	53.0	35.0	32.0/363.5	15.85
		25.7	56.5	38.2	33.0/363.5	16.34
	5W	19.6	40.0	28.2	36.1/365.0	17.80
		18.5	38.5	27.0	36.6/365.0	18.05
	5H	19.0	38.5	27.2	38.0/365.5	18.71
		19.0	39.5	27.5	36.4/365.5	17.93
RHol	W	21.5	45.5	31.0	30.7/364.0	15.18
		22.8	48.0	32.5	29.7/364.0	14.69
	H	24.3	46.5	33.5	31.5/369.5	15.35
		22.0	46.5	32.0	30.5/369.5	14.86
RHo4	L	25.7	51.0	36.2	31.2/370.5	15.16
		30.0	51.0	39.0	33.7/370.5	16.37
	W	15.5	38.5	24.7	33.2/365.5	16.35
		15.7	38.5	25.0	34.1/365.5	16.79
	H	16.5	41.0	26.2	31.7/366.0	15.59
		16.5	41.5	26.2	31.5/366.0	15.49
RHol6	L	54.0	67.5	60.2	32.0/362.5	15.89
		48.5	62.0	54.7	31.0/362.5	15.39
	W	30.5	59.0	42.5	32.0/364.0	15.82
		30.8	59.5	43.0	31.9/364.0	15.78
	H	22.5	57.0	36.0	31.0/366.0	15.25
		24.5	57.5	37.5	32.2/366.0	15.84
RHo29	L	33.0	62.0	45.0	29.4/365.5	14.48
		34.0	63.5	46.2	28.6/365.5	14.09
	W	20.5	53.5	33.2	32.3/365.5	15.86
		20.3	53.5	33.2	31.5/365.5	15.51
	H	27.0	64.0	41.5	28.4/364.5	14.03
		25.8	63.5	39.7	28.2/364.5	13.93

TABLE XXXI (Continued)

CIRCUMFERENTIAL WIDTH AT HALF HEIGHT

Sample		T_{002}	BaT_0	T at Half Height	Width at Half Height, scale units	Degrees
RHo46	L	45.0	68.5	55.5	28.9/363.5	14.31
		44.0	67.0	54.0	28.3/363.5	14.01
	W	35.5	61.5	47.0	32.1/367.5	15.72
		34.0	61.0	45.7	32.0/367.5	15.67
	H	36.0	57.0	45.0	30.3/367.5	14.84
		37.0	58.5	46.5	33.0/367.5	16.16
RHo62	L	46.5	62.0	53.7	30.3/365.5	14.92
		47.0	62.0	54.0	31.0/365.5	15.27
	W	46.0	60.5	52.7	36.4/367.5	17.83
		31.0	49.0	39.0	33.0/367.5	16.16
	H	33.0	52.5	41.5	30.0/367.0	14.71
		33.0	53.0	42.0	32.6/367.0	15.99
RHo97	L	69.5	82.0	75.5	28.2/364.0	13.95
		72.0	82.0	77.0	29.0/364.0	14.34
	W	21.3	50.5	33.0	35.0/365.0	17.26
		19.0	48.0	30.2	34.1/365.0	16.82
	H	23.5	51.0	34.7	31.8/364.5	15.70
		26.0	53.0	37.0	32.2/364.5	15.90
RHo120 Earlywood						
	L	42.0	65.0	52.2	30.1/361.0	15.01
		41.5	63.5	51.5	30.1/361.0	15.01
	W	40.0	55.0	47.0	35.6/361.5	17.73
		43.5	57.0	50.0	33.6/361.5	16.73
	H	53.0	65.0	58.7	31.5/365.5	15.51
		52.0	67.0	59.0	32.0/365.5	15.76
RHo120 Transitionwood						
	L	31.0	63.5	44.2	29.3/361.0	14.61
		30.0	63.5	43.5	29.2/361.0	14.56
	W	38.0	57.5	47.0	34.2/363.5	16.94
		37.0	57.0	46.0	36.6/363.5	18.12
	H	29.5	53.5	39.7	36.6/366.5	17.98
		30.5	54.0	40.7	35.2/366.5	17.29
RHo120 Latewood						
	L	20.0	57.0	34.0	30.6/365.5	15.07
		19.0	55.5	32.7	31.2/365.5	15.37
	W	30.0	54.0	40.2	35.6/363.0	17.65
		31.0	57.0	42.0	34.5/363.0	17.11
	H	26.5	50.5	36.5	34.2/364.0	16.91
		26.0	50.5	36.0	35.0/364.0	17.31

TABLE XXXI (Continued)

CIRCUMFERENTIAL WIDTH AT HALF HEIGHT

Sample	T_{002}	BaT_0	T at Half Height	Width at Half Height, scale units	Degrees
Air Dry					
Ho I	26.0	77.0	44.7	35.3/365.5	17.38
	27.5	78.5	46.2	34.0/365.5	16.74
Air Dry					
Ho I H[a]	21.5	76.5	40.5	32.6/368.0	15.95
	22.5	77.5	42.0	33.2/368.0	16.24
Air Dry					
Ho II	19.8	75.5	38.7	34.6/366.0	17.02
	22.8	78.0	42.0	33.0/366.0	16.23
Air Dry					
Ho II H[a]	32.0	80.0	50.5	35.6/365.0	17.56
	34.0	82.0	52.7	34.0/365.0	16.77

[a]Heated at 105°C. and 9.7% moisture content for two hours.

TABLE XXXII

CIRCUMFERENTIAL 2T WIDTH

Sample		Maximum I	Maximum II	Average
TEW I	I 1	70/366.5	72/366.5	34.87
	2	75/362.5	71/362.5	36.25
	3	73/368.0	72/368.0	35.46
	4	76/367.5	71/367.5	36.00
TEW I H	I 1	74/365.5	74/365.5	36.45
	2	70/367.0	73/367.0	35.06
	3	76/365.0	77/365.0	37.73
	4	73/366.5	76/366.5	36.59
TLW I	1	74/362.0	71/362.0	36.05
	2	74/367.5	72/367.5	35.75
	3	72/365.5	72/365.5	35.46
	4	69/364.5	69/364.5	34.07
TLW I H	1	66/363.0	70/363.0	33.48
	2	65/367.0	68/367.0	32.62
	3	71/367.0	74/367.0	35.55
	4	72/364.5	74/364.5	36.05
TG	1	62/365.0	62/365.0	30.58
	2	58/362.5	60/362.5	29.30
	3	59/360.5	60/360.5	29.70
	4	58/361.0	59/361.0	29.16
	5	61/364.0	58/364.0	29.43
	6	61/361.5	61/361.5	30.37
	7	64/365.0	68/365.0	32.54
	8	63/363.0	63/363.0	31.29
TG H	1	62/366.0	60/366.0	30.01
	2	66/366.0	65/366.0	32.22
	3	63/366.0	65/366.0	31.48
	4	63/362.5	63/362.5	31.28
	5	68/368.0	66/368.0	32.78
	6	62/361.0	62/361.0	30.91
	7	59/358.5	64/358.5	30.87
	8	57/355.0	59/355.0	29.41
RLW I	1	63/365.5	63/365.5	31.03
	2	63/363.0	63/363.0	31.25
	3	67/365.5	67/365.5	32.99
	4	65/364.5	65/364.5	32.09

TABLE XXXII (Continued)

CIRCUMFERENTIAL 2T WIDTH

Sample		Maximum I	Maximum II	Average
RLW I H	1	61/361.5	62/361.5	30.62
	2	61/358.5	60/358.5	30.38
	3	63/361.5	65/361.5	31.86
	4	67/362.0	67/362.0	33.32
RLW II	1	58/361.0	60/361.0	29.41
	2	61/363.5	60/363.5	29.92
	3	63/364.0	63/364.0	31.16
	4	61/364.5	61/364.5	30.13
RLW II H	1	59/364.5	55/364.5	28.15
	2	61/366.0	61/366.0	30.01
	3	60/362.5	60/362.5	29.79
	4	60/365.5	59/365.5	29.30
THo1	L	71/368.5	70/368.5	36.14
	W	75/364.0	74/364.0	36.85
	H	76/365.0	74/365.0	36.99
THo4	L	73/362.0	76/362.0	37.04
	W	76/365.0	77/365.0	37.73
	H	78/366.5	78/366.5	38.30
THo11	L1	59/365.5	60/365.5	29.30
	2	60/364.0	63/364.0	30.42
	W1	65/366.0	69/366.0	33.19
	2	62/364.0	62/364.0	30.65
	H1	62/365.5	62/365.5	30.53
	2	68/367.5	67/367.5	33.07
THo18	L	65/365.0	66/365.0	32.31
	W	66/361.0	67/361.0	33.16
	H	67/364.0	70/364.0	33.88
THo29	L	62/363.0	64/363.0	31.25
	W	65/361.5	66/361.5	32.62
	H	66/367.5	67/367.5	32.58
THo46	L	61/363.0	60/363.0	30.01
	W	65/363.0	70/363.0	33.39
THo62	L	70/363.0	73/363.0	35.46
	W	71/361.5	75/361.5	36.34
THo97	L	62/362.5	61/362.5	30.55
	W	68/362.0	71/362.0	34.56
	H	73/365.5	70/365.5	35.21

TABLE XXXII (Continued)

CIRCUMFERENTIAL 2T WIDTH

Sample		Maximum I	Maximum II	Average
THo120	L1	69/360.0	70/360.0	34.75
	W1	72/365.5	77/365.5	36.68
THo120	L2	70/362.5	69/362.5	34.51
	W2	74/367.0	72/367.0	35.80
	H2	69/367.5	69/367.5	33.80
THo120	L3	70/364.0	70/364.0	34.61
	W3	73/366.5	72/366.5	35.60
	H3	72/361.0	72/361.0	35.89
THo120	W4	72/366.5	74/366.5	35.86
	H4	72/366.0	74/366.0	35.91
THo120	L5	68/364.5	70/364.5	34.32
	W5	70/365.0	73/365.0	35.26
	H5	71/365.0	71/365.0	34.47
RHo1	W	62/364.0	62/364.0	30.65
	H	60/369.5	60/369.5	29.23
RHo4	L	63/370.5	65/370.5	31.09
	W	64/365.5	68/365.5	32.51
	H	64/366.0	65/366.0	31.72
RHo16	L	60/362.5	64/362.5	30.78
	W	64/369.0	68/369.0	32.20
	H	63/366.0	63/366.0	30.98
RHo29	L	57/365.5	58/365.5	28.31
	W	63/365.5	63/365.5	31.03
	H	60/364.5	60/364.5	29.63
RHo46	L	59/363.5	58/363.5	28.96
	W	64/364.0	64/364.0	31.64
	H	60/367.5	61/367.5	29.63
RHo62	L	61/365.5	63/365.5	30.53
	W	70/367.5	69/367.5	34.04
	H	61/367.0	66/367.0	31.14
RHo97	L	59/364.0	58/364.0	28.93
	W	68/365.0	66/365.0	33.05
	H	65/364.5	62/364.5	31.36

TABLE XXXII (Continued)

CIRCUMFERENTIAL 2T WIDTH

Sample		Maximum I	Maximum II	Average
RHo120	L EW	57/361.0	59/361.0	28.93
	W	66/361.5	71/361.5	34.11
	H	68/365.5	68/365.5	33.48
RHo120	L TW	61/361.0	61/361.0	30.42
	W	68/363.5	66/363.5	33.17
	H	68/366.5	67/366.5	33.18
RHo120	L LW	62/365.5	58/365.5	29.55
	W	63/363.0	67/363.0	32.24
	H	67/364.0	66/364.0	32.89
Air Dry Ho I		72/365.5	72/365.5	35.46
Heated Air Dry Ho I		69/368.0	71/368.0	34.24
Air Dry Ho II		75/365.0	77/365.0	37.48
Heated Air Dry Ho II		71/366.0	75/366.0	35.90

TABLE XXXIII

EFFECT OF IONIC TREATMENT ON THE CENTRIFUGAL WATER RETENTION VALUE

Sample	Wet Weight After Washing, g.	Ionic Medium 0.1N Weight	Wet Weight from the Ionic Medium	Wet Weight After Rewashing	Ovendry Weight, g.
1	0.715	KCl	0.662	0.742	0.163
2	0.786	KCl	0.696	0.901	0.180
3	1.209	KCl 10[a]	0.832	1.099	0.224
4	1.461	KCl 40	1.022	1.342	0.268
5	1.494	KCl 100	1.091	1.374	0.293
6	1.194	KCl	0.831	0.929	0.226
7	1.450	KCl	1.005	1.275	0.284
8	1.383	KCl	0.950	1.222	0.269
9	1.599	NaCl	1.086	1.471	0.297
10	1.540	NaCl	1.033	1.388	0.281
11	1.566	$BaCl_2$	1.039	1.082	0.304
12	1.581	$BaCl_2$	1.044	1.139	0.316
13	1.462	$Ba(C_2H_3O_2)_2$	0.918	0.965	0.276
14	1.547	$Ba(C_2H_3O_2)_2$	1.068	1.152	0.322
15	1.453	$FeCl_3$ 10	0.952	0.882	0.275
16	1.275	$FeCl_3$ 40	0.869	0.816	0.250
17	1.241	$FeCl_3$ 100	0.809	0.776	0.240
18	1.438	$FeCl_3$	0.990	0.929	0.280
19	1.012	$FeCl_3$	0.682	0.641	0.197
20	1.126	$FeCl_3$	0.722	0.712	0.218
21	1.624	$FeCl_3$	1.155	1.115	0.338
22	1.622	$FeCl_3$	1.120	1.058	0.323

[a] Ionic treatment lasted the indicated number of minutes, all others were treated for twenty hours.

TABLE XXXIV

EFFECT OF EDTA ON THE CENTRIFUGAL WATER RETENTION VALUE OF IONICALLY TREATED PULPS

Sample		Rewashed Wet Weight, g.	Wet Weight in EDTA, 0.1N, g.	Wet Weight After the Subsequent Washing, g.	Ovendry Weight, g.
Pulping liquor	23	1.819	1.159	1.552	0.338
	24	1.689	1.106	1.478	0.321
NaCl	9	1.471	1.016	1.338	0.297
	10	1.388	0.966	1.262	0.281
KCl	7	1.275	0.957	1.295	0.284
	8	1.222	0.919	1.222	0.269
$BaCl_2$	11	1.082	1.024	1.394	0.304
	12	1.139	1.065	1.485	0.316
$Ba(C_2H_3O_2)_2$	13	0.965	0.917	1.277	0.276
	14	1.152	1.058	1.428	0.322
$FeCl_3$	21	1.115	1.089	1.351	0.338
	22	1.058	1.046	1.303	0.323

TABLE XXXV

EFFECT OF ACID AND ALKALINE TREATMENT
ON THE CENTRIFUGAL WATER RETENTION VALUE

Sample	Wet Weight After Washing, g.	Medium 0.1N	Wet Weight After Treatment, g.	Wet Weight After Rewashing, g.	Ovendry Weight, g.
25	1.968	HCl	0.919	1.004	0.297
26	1.903	HCl	1.180	1.245	0.381
27	1.825	CH_3COOH	1.191	1.254	0.365
28	1.408	CH_3COOH	0.946	0.969	0.284
29	1.774	KOH	1.244	1.571	0.360
30	1.663	KOH	1.164	1.459	0.334
31	1.652	NaOH	1.187	1.471	0.330
32	1.806	NaOH	1.239	1.563	0.353